iScience

Cell Press

Article

Catalytic Double Cyclization Process for Antitumor Agents against Breast Cancer Cell Lines

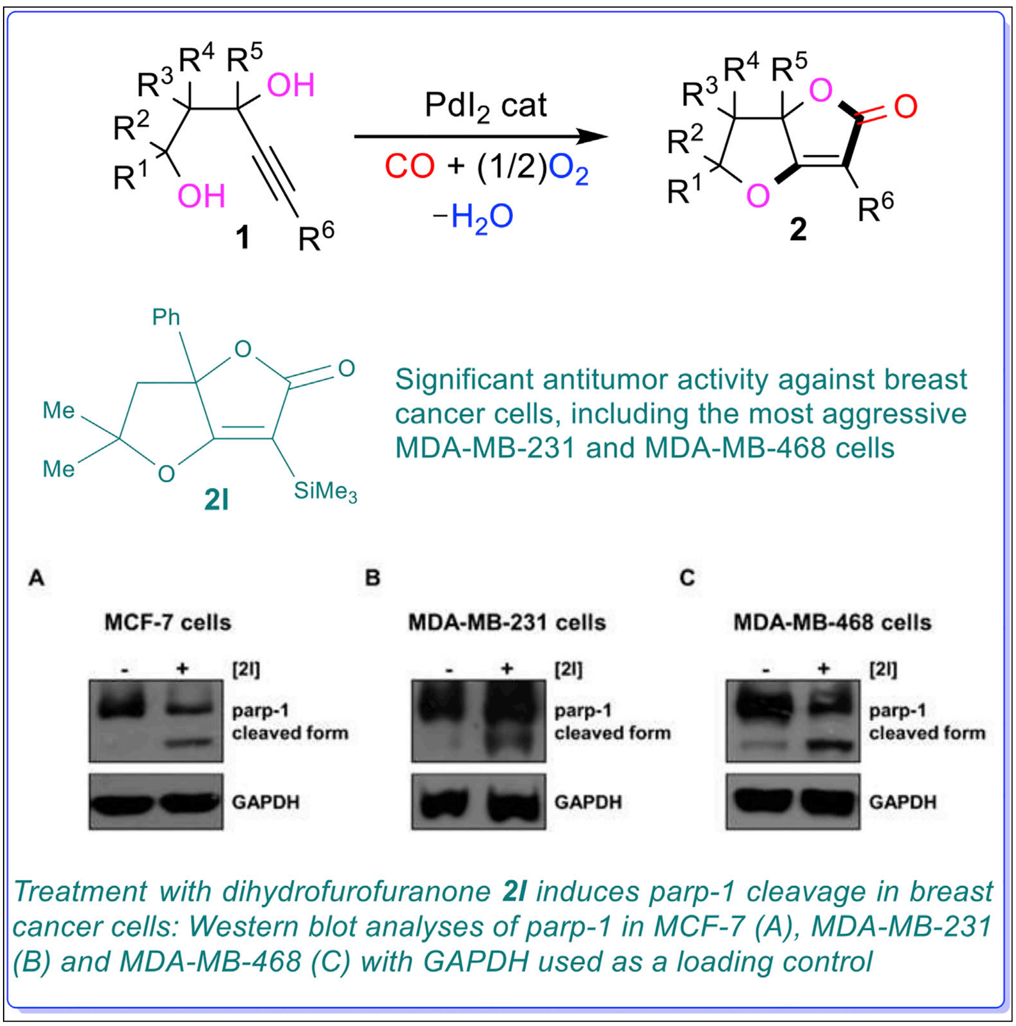

Raffaella Mancuso, Ida Ziccarelli, Adele Chimento, ..., Rosa Sirianni, Vincenzo Pezzi, Bartolo Gabriele

raffaella.mancuso@unical.it (R.M.)
bartolo.gabriele@unical.it (B.G.)

HIGHLIGHTS

Novel catalytic double cyclization method leading to bicyclic heterocycles in one step

Direct synthesis of antitumor agents from simple substrates (4-yne-1,3-diols and CO)

Identification of a new class of antitumor agents against breast cancer (BC) cells

Significant antitumor activity against the most aggressive triple-negative BC cells

Mancuso et al., iScience *3*, 279–288
May 25, 2018
https://doi.org/10.1016/j.isci.2018.04.022

iScience

CellPress

Article

Catalytic Double Cyclization Process for Antitumor Agents against Breast Cancer Cell Lines

Raffaella Mancuso,[1,*] Ida Ziccarelli,[1] Adele Chimento,[2] Nadia Marino,[3,5] Nicola Della Ca',[4] Rosa Sirianni,[2] Vincenzo Pezzi,[2] and Bartolo Gabriele[1,6,*]

SUMMARY

The development of efficient synthetic strategies for the discovery of novel antitumor molecules is a major goal in current research. In this context, we report here a catalytic double cyclization process leading to bicyclic heterocycles with significant antitumor activity on different human breast cancer (BC) cell lines. The products, 6,6*a*-dihydrofuro[3,2-*b*]furan-2(5*H*)-ones, were obtained in one step, starting from simple substrates (4-yne-1,3-diols, CO, and O_2), under the catalytic action of PdI_2 in conjunction with KI. These compounds have significant antiproliferative activity *in vitro* on human BC cell lines, both hormone receptor positive (MCF-7) and triple negative (triple-negative breast cancer [TNBC]; MDA-MB-231 and MDAMB-468), while exhibiting practically no effects on normal MCF-10A (human mammary epithelial) and 3T3-L1 (murine fibroblasts) cells. Thus, these compounds have the potential to expand the therapeutic options against BC, and in particular, against its most aggressive forms (TNBCs). Moreover, the present synthetic approach may provide an economic benefit for their production.

INTRODUCTION

Breast cancer (BC) is the leading cause of cancer death in women worldwide (Siegel et al., 2016, 2017), particularly in developed countries. Genetic factors, such as mutations of tumor suppressor genes BRCA1 and BRCA2; endocrine factors (such as estrogen exposure); as well as environmental and dietary factors may be involved in the onset of this disease. Several studies of gene expression profile have been performed to characterize BCs in different molecular subtypes, which may have a prognostic value (Voduc et al., 2010). An important classification can be made on the basis of specific receptor expression. Indeed, BCs are divided into hormone receptor (HR)-negative (HR−) and HR-positive (HR+) tumors. The latter group includes estrogen receptor (ER)-positive (ER+), progesterone receptor (PR)-positive (PR+), and human epidermal growth factor receptor 2 (HER2)-positive (HER2+) tumors, whereas HR− tumors include the so-called triple-negative breast cancers (TNBCs), which lack the expression of the three receptor types (Kirkpatrick, 2009). Although the survival rate at 5 years for treated patients with early-stage BC is extremely high, some subgroups of patients with advanced-stage BC may have recurrence within 10 years of treatment. The recurrence rate for HR+ tumors appears to be lower (recurrence rate is 8%) compared with that of the subtypes overexpressing HER2 or that have a triple-negative phenotype (recurrence rate is 15%–20%) (Haffty et al., 2006; Millar et al., 2009; Nguyen et al., 2008).

The selective ER modulator (SERM) tamoxifen and aromatase inhibitors (anastrazole, letrozole) are used for the treatment of tumors expressing steroid HRs, while trastuzumab (Herceptin), a monoclonal antibody that targets HER2, is used for the treatment of HER2+ tumors. TNBCs are particularly dangerous, because they are associated with an unfavorable prognosis (Bauer et al., 2007; Carey et al., 2007; Haffty et al., 2006) and because patients with TNBC derive no benefit from molecularly targeted regimens employing endocrine-based therapy or trastuzumab (Kirkpatrick, 2009). Classical chemotherapy aims to block cell proliferation, which, however, does not discriminate cancer cells from rapidly dividing normal cells within the organism. Therefore, new therapeutic approaches resulting from the discovery of new compounds with antitumor activity against TNBCs are still highly desirable.

In this work, we report an unprecedented catalytic double cyclization process leading to a new class of bicyclic heterocycles (dihydrofurofuranone derivatives) with significant antitumor activity *in vitro* against BC cell

[1]Laboratory of Industrial and Synthetic Organic Chemistry (LISOC), Department of Chemistry and Chemical Technologies, University of Calabria, Via Pietro Bucci 12/C, 87036 Arcavacata di Rende, Rende (CS), Italy

[2]Department of Pharmacy and Health and Nutritional Sciences, University of Calabria, 87036 Arcavacata di Rende, Rende (CS), Italy

[3]Department of Chemistry and Chemical Technologies, University of Calabria, Via Pietro Bucci 14/C, 87036 Arcavacata di Rende, Rende (CS), Italy

[4]Department of Life Sciences and Environmental Sustainability (SCVSA), University of Parma, Parco Area delle Scienze 11/A, 43124 Parma, Italy

[5]Present address: Department of Chemical Sciences, University of Padova, Via Marzolo 1, 35131 Padova, Italy

[6]Lead Contact

*Correspondence: raffaella.mancuso@unical.it (R.M.), bartolo.gabriele@unical.it (B.G.)

https://doi.org/10.1016/j.isci.2018.04.022

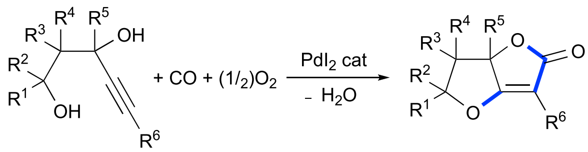

Scheme 1. PdI_2-Catalyzed Carbonylative Oxidative Double Cyclization of 4-Yne-1,3-diols Leading to Dihydrofurofuranones

lines, both HR+ (MCF-7) and TNBCs (MDA-MB-231 and MDAMB-468), while exhibiting practically no effects on normal MCF-10A (human mammary epithelial) and 3T3-L1 (murine fibroblasts) cells. These new compounds have therefore the potential to expand the therapeutic options against BC, in particular against its most aggressive forms (TNBCs).

RESULTS AND DISCUSSION

Palladium-Catalyzed Carbonylative Oxidative Double Cyclization of 4-Yne-1,2-diols Leading to Dihydrofurofuranone Derivatives

Catalytic cyclization processes have recently attracted great interest in the chemistry scientific community owing to the possibility to synthesize in one step high-value-added molecules starting from simple building blocks, by their ordered sequential activation by the catalytic center (Alcaide and Almendros, 2014; Debrouwer et al., 2015; Guo et al., 2011; Krause and Winter, 2011; Tanaka and Tajima, 2012; Valera and Saa, 2016; Vlaar et al., 2011; Ye and Ma, 2014). Among the raw starting materials, carbon monoxide represents a simple and largely available C-1 unit, and its catalytic activation may allow to directly introduce a carbonyl functional group into an organic substrate in a highly atom-economical and efficient manner. In fact, carbonylation reactions are currently known to play a major role in the direct synthesis of carbonyl compounds both in industry and in the production of fine chemicals (Beller, 2006; Friis et al., 2016; Gabriele et al., 2012; Gadge and Bhanage, 2014; Gehrtz et al., 2016; Kalck and Urrutigoïty, 2015; Kollár, 2008; Liu et al., 2011; Omae, 2011; Peng et al., 2017; Shen and Wu, 2017; Wu and Neumann, 2012; Wu et al., 2013a, 2013b, 2014; Wu, 2016; Wu and Beller, 2016).

In this work, we have developed an unprecedented carbonylative oxidative double cyclization process, which allows synthesizing bioactive, high-value-added bicyclic heterocycles (dihydrofurofuranone derivatives **2**) starting from readily available 4-yne-1,3-diols **1**; CO; and O_2 (Scheme 1). In this reaction, the alkynediol, carbon monoxide, and oxygen are sequentially activated through the catalytic action of a very simple system (consisting of PdI_2 in conjunction with an excess of KI) (Gabriele et al., 2014; Mancuso et al., 2014, 2015, 2016; Veltri et al., 2015, 2016a, 2016b, 2018), with the formation of two cycles and three new bonds (O-C, C-C, and C-O) in one single operation and in ordered sequence. It should be noted that, although an analogous process was reported for 4-ene-1,2-diols under different reaction conditions (Kapitán and Gracza, 2008), no previous example exists in the literature for the direct carbonylative double cyclization of 4-yne-1,3-diols leading to dihydrofurofuranones.

We started our investigation by studying the reaction between 3-methylnon-4-yne-1,3-diol **1a** and carbon monoxide using 2 mol % PdI_2 and 10 mol % KI, under 40 atm of a 4:1 mixture of CO and air in MeOH as the solvent (0.05 mmol of **1a** per mL of MeOH) at 100°C. After 15 hr reaction time, 3-butyl-6*a*-methyl-6,6*a*-dihydrofuro[3,2-*b*]furan-2(5*H*)-one **2a** was isolated in 30% yield following chromatographic purification (unidentified heavy by-products accounted for substrate total conversion). The yield of **2a** did not improve by changing the operative reaction conditions (data not shown); however, its formation confirmed the possibility to realize a previously unreported carbonylative double cyclization process starting from a 4-yne-1,3-diol in one step under catalytic conditions. The result was noteworthy, considering the different possible competitive pathways that could have been followed under carbonylation conditions by an alkynyldiol such as **1a** (formation of cyclic carbonates, maleic esters, monocyclic β- or γ-lactones, and so on) (Beller, 2006; Kollár, 2008; Gabriele et al., 2012; Wu et al., 2013a; Wu and Beller, 2016). The catalytic process may be interpreted as occurring through an ordered sequence of mechanistic stages, involving (1) 5-*exo-dig* cyclization, via intramolecular nucleophilic attack of the hydroxyl group at C-1 to the triple bond coordinated to PdI_2; (2) carbon monoxide insertion into the Pd-C bond of the ensuing vinylpalladium intermediate; (3) intramolecular trapping of the ensuing acylpalladium species by the hydroxyl at C-3, with further cyclization and nucleophilic displacement of palladium,

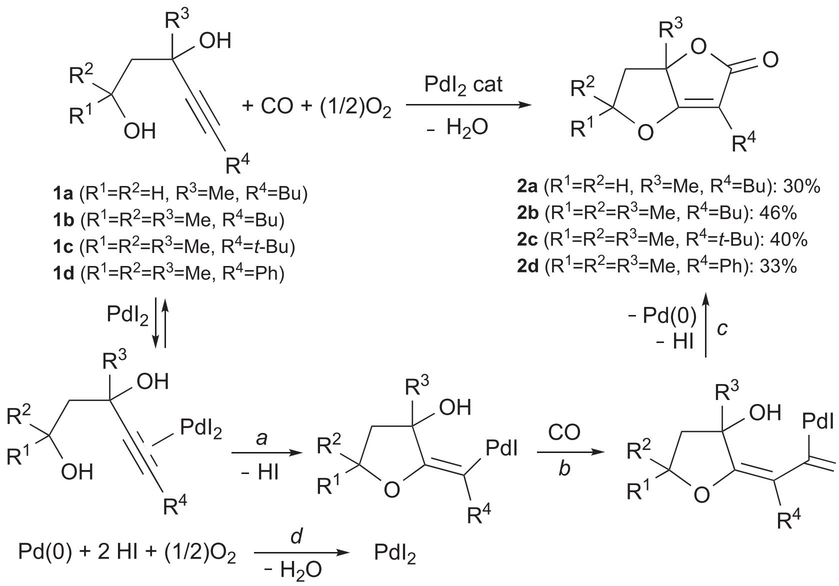

Scheme 2. Formation of Dihydrofurofuranones 2a–d by PdI_2-Catalyzed Carbonylative Oxidative Double Cyclization of 4-Yne-1,3-diols 1a–d

Anionic iodide ligands are omitted for clarity. See Transparent Methods for experimental details.

leading to the final bicyclic product and Pd(0); and (4) reoxidation of Pd(0) back to PdI_2 by oxygen in the presence of the 2 mol HI formally eliminated during the previous cyclization steps (Scheme 1; anionic iodide ligands are omitted for clarity).

We then tested the reactivity of a similar substrate, still bearing a butyl group on the triple bond, but with geminal methyl substituents at C-1. The reaction of 2,4-dimethyldec-5-yne-2,4-diol **1b** led to the corresponding dihydrofurofuranone **2b** in a higher isolated yield with respect to **2a**, most probably due to the effect exerted by the geminal alkyl groups, which is known to favor cyclization processes (Jung and Piizi, 2005; Sammes and Weller, 1995). A 40% yield of **2c** was obtained starting from alkynyldiol **1c**, bearing a sterically demanding *tert*-butyl group on the triple bond. On the other hand, 2,4-dimethyl-6-phenylhex-5-yne-2,4-diol **1d**, substituted with a phenyl group on the triple bond, afforded the corresponding dihydrofuranone **2d** in 33% yield (Scheme 2).

A significant increase in product yield was observed when the triple bond was substituted with a trimethylsilyl group. Thus, 3-methyl-5-(trimethylsilyl)pent-4-yne-1,3-diol **1e**, under conditions similar to those previously employed for **1a**, led to the dihydrofurofuranone **2e** in 72% yield after 3 hr reaction time (Figure 1). Other differently substituted substrates **1f–m**, still bearing the trimethylsilyl group (TMS) on the triple bond, behaved similarly, and afforded the corresponding dihydrofuranones **2f–m** in fair to excellent yields (58%–94%, Figure 1). The structure of dihydrofurofuranone **2g** was also confirmed by X-ray diffractometric analysis (for details see Figure S1, Table S1, Transparent Methods, and cif file for **2g**, Data S1).

In the case of alkynediols **1i–k**, the substrates employed were a mixture of 2*RS*,4*SR* and 2*RS*,4*RS* diastereomers. To assess the different performances of the two diastereomers in the double cyclization process, we tested them independently after chromatographic separation. The reactions of the single diastereomers could also allow isolating the corresponding diastereomeric products, considering that the process is stereospecific. The results obtained are shown in Table 1. As can be seen from Table 1, the 2*RS*,4*RS* diastereomer was the most productive isomer (in terms of yield obtained for the corresponding dihydrofurofuranone) in the case of **1i** and especially **1k**, whereas in the case of **1j** a slightly higher yield was observed starting from the 2*RS*,4*SR* diastereoisomer. The structure of (5*RS*,6*aRS*)-**2j** was unequivocally established by X-ray diffractometric analysis (for details, see Figure S2, Table S2, Transparent Methods, and cif file for 5*RS*,6*aRS*-**2j**, Data S2), which also permitted to corroborate (owing to the stereospecificity of the reaction) the 2*RS*,4*RS* stereochemistry of the starting material **1j**.

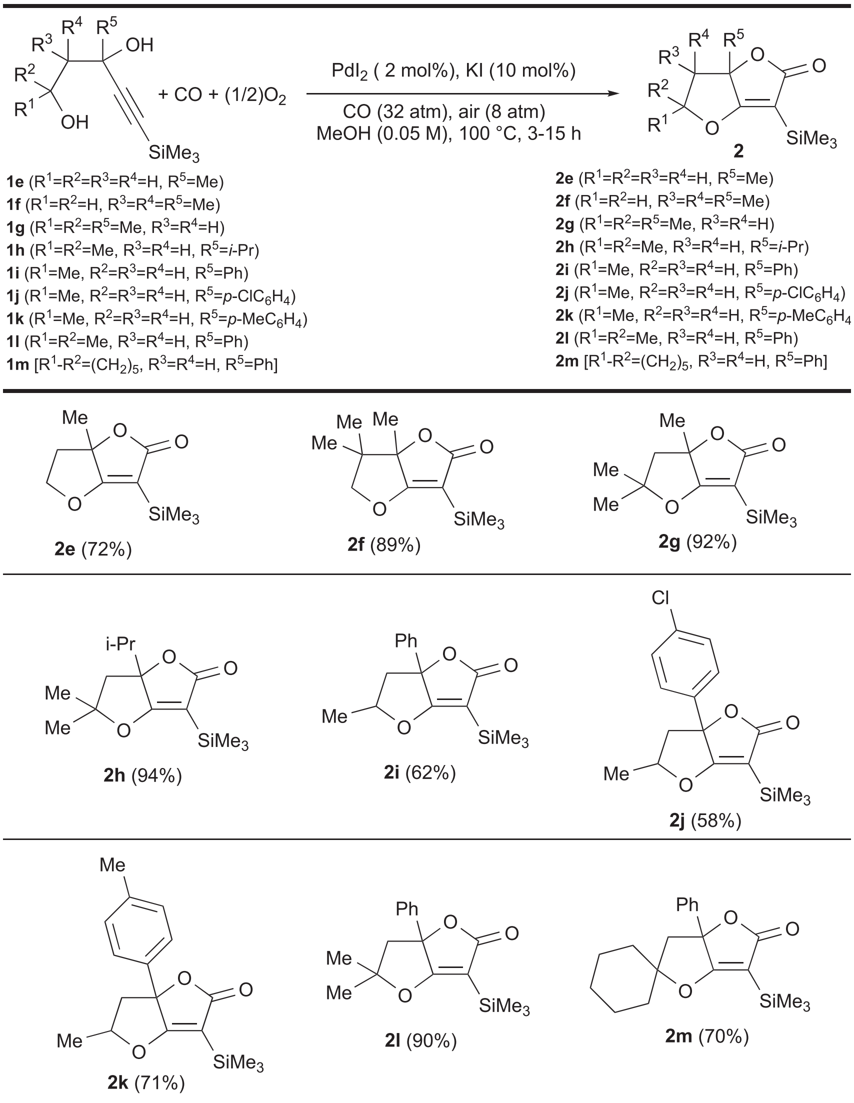

Figure 1. Synthesis of Dihydrofurofuranones 2 by PdI_2/KI-Catalyzed Carbonylative Oxidative Double Cyclization of 4-Yne-1,3-diols 1

Top: *Reaction conditions:* Alkynediol **1** (0.70 mmol), PdI_2 (1.39×10^{-2} mmol), KI (6.95×10^{-2} mmol), CO (32 atm), air (8 atm), MeOH (14 mL), 100°C, 3–15 hr. In parentheses, isolated yields based on starting **1**. See Transparent Methods for experimental details.

Bottom: Reaction time was 3 hr for **2e**, **2f**, **2g**, **2h**, **2l**, and **2m**.

Reaction time was 15 hr for **2i** and **2j**.

For **2i**, the (5*RS*,6a*SR*)/(5*RS*,6a*RS*) diastereomeric ratio (DR) was ca. 1.9, determined by ^{1}H NMR; starting **1i** was a mixture of (2*RS*,4*SR*)/(2*RS*,4*RS*) diastereomers (DR ca. 2.2, determined by ^{1}H NMR).

For **2j**, the (5*RS*,6a*SR*)/(5*RS*,6a*RS*) DR was ca. 1.8, determined by ^{1}H NMR; starting **1j** was a mixture of (2*RS*,4*SR*)/(2*RS*,4*RS*) diastereomers (DR ca. 1.4, determined by ^{1}H NMR).

Reaction time was 5 hr for **2k**.

For **2k**, the (5*RS*,6a*RS*)/(5*RS*,6a*SR*) DR was ca. 1.8, determined by ^{1}H NMR; starting **1k** was a mixture of (2*RS*,4*SR*)/(2*RS*,4*RS*) diastereomers (DR ca. 1.0, determined by ^{1}H NMR). See Transparent Methods for experimental details. NMR, nuclear magnetic resonance.

To further expand the synthetic scope of the reaction, we also attempted the desilylation of some representative silylated dihydrofurofuranones. Thus, crude products **2h**, **2l**, and **2m**, deriving from carbonylation of **1h**, **1l**, and **1m**, respectively, were treated, without further purification, with tetrabutylammonium fluoride (TBAF)•nH_2O in THF at room temperature for 2 hr. As shown in Scheme 3, the corresponding

Entry[a]	1	Time (h)	2	Yield of 2[b]
1	(2*RS*,4*SR*)-1i	8	(5*RS*,6a*SR*)-2i	52
2	(2*RS*,4*RS*)-1i	3	(5*RS*,6a*RS*)-2i	61
3	(2*RS*,4*SR*)-1j	15	(5*RS*,6a*SR*)-2j	68
4	(2*RS*,4*RS*)-1j	8	(5*RS*,6a*RS*)-2j	52
5	(2*RS*,4*SR*)-1k	5	(5*RS*,6a*SR*)-2k	40
6	(2*RS*,4*RS*)-1k	3	(5*RS*,6a*RS*)-2k	80

Table 1. Experiments with Single Diastereomers

[a]*Reaction conditions:* alkynediol **1** (0.25–0.5 mmol), PdI_2 (2 mol%), KI (10 mol%), CO (32 atm), air (8 atm), MeOH (5–10 mL), 100°C, 3–15 hr. See Transparent Methods for details.

[b]Isolated yields based on starting **1**.

desilylated furofuranone derivatives were obtained in good to high yields over the two steps (85%, 79%, and 61% based on starting **1h**, **1l**, and **1m**, respectively).

Antiproliferative Activity *In Vitro* of the Newly Synthesized Dihydrofurofuranones on MCF-7, MDA-MB-231, and MDA-MB-468 Human Breast Cancer Cell Lines

Some of the newly synthesized dihydrofurofuranones have shown significant antiproliferative activity *in vitro* on human breast adenocarcinoma cell lines, including the most dangerous triple-negative ones (MDA-MB-231 and MDAMB-468). Although several furanone derivatives were previously described to possess antitumor properties (for a recent example, see Wu et al., 2017), the possible anticancer activity of bicyclic dihydrofurofuranones such as **2** has not been reported so far. The effects on tumor cell viability of different concentrations (1, 5, 10, 20, 40 μM) of five 6,6*a*-diidrofuro[3,2-*b*]furan-2-(5*H*) derivatives (**2d**, **2e**, **2g**, **2l**, and **3l**) have been evaluated against MCF-7, MDAMB-231, and MDAMB-468 BC cell lines (Figure 2); normal breast epithelial cells MCF-10A; and immortalized fibroblasts 3T3-L1 (Figure 3). In particular, for **2d** a significant reduction in vitality of MCF-7 and MDA-MB231 was observed from 10 μM onward, whereas MDA-MB468 was slightly more sensitive and a significant reduction was obtained from the dose of 5 μM (Figure 2A). Compound **2g** decreased the cell viability of all three cell lines from the lowest dose of 1 μM (Figure 2B). Compound **2e** significantly affected the cell viability of TNBC cell lines from 5 μM, whereas it was effective from 10 μM on MCF-7 cells (Figure 2C). Product **2l** also decreased MCF-7 (1–40 μM), MDA-MB-231, and MDA-MB-468 (10–40 μM) cell viability (Figure 2D). Dihydrofurofuranone **3l** caused a modest but significant effect on MCF-7 (5–40 μM) and MDA-MB-231 (20–40 μM) cells, and was slightly more effective on MDA-MB-468, with the highest dose (40 μM) reaching almost a 40% inhibition (Figure 2E). These data indicate that among all tested cell lines MDA-MD-468 appears more sensitive to all

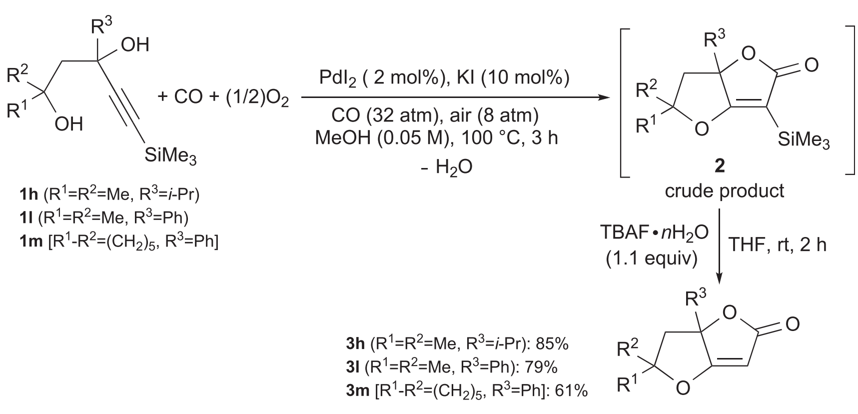

Scheme 3. Synthesis of Desilylated Dihydrofurofuranones 3h, 3l, and 3m by PdI_2-Catalyzed Carbonylative Double Cyclization of 4-Yne-1,3-diols 1h, 1l, and 1m, Respectively, Followed by TBAF-Induced Desilylation of the Crude Carbonylation Product

See Transparent Methods for experimental details.

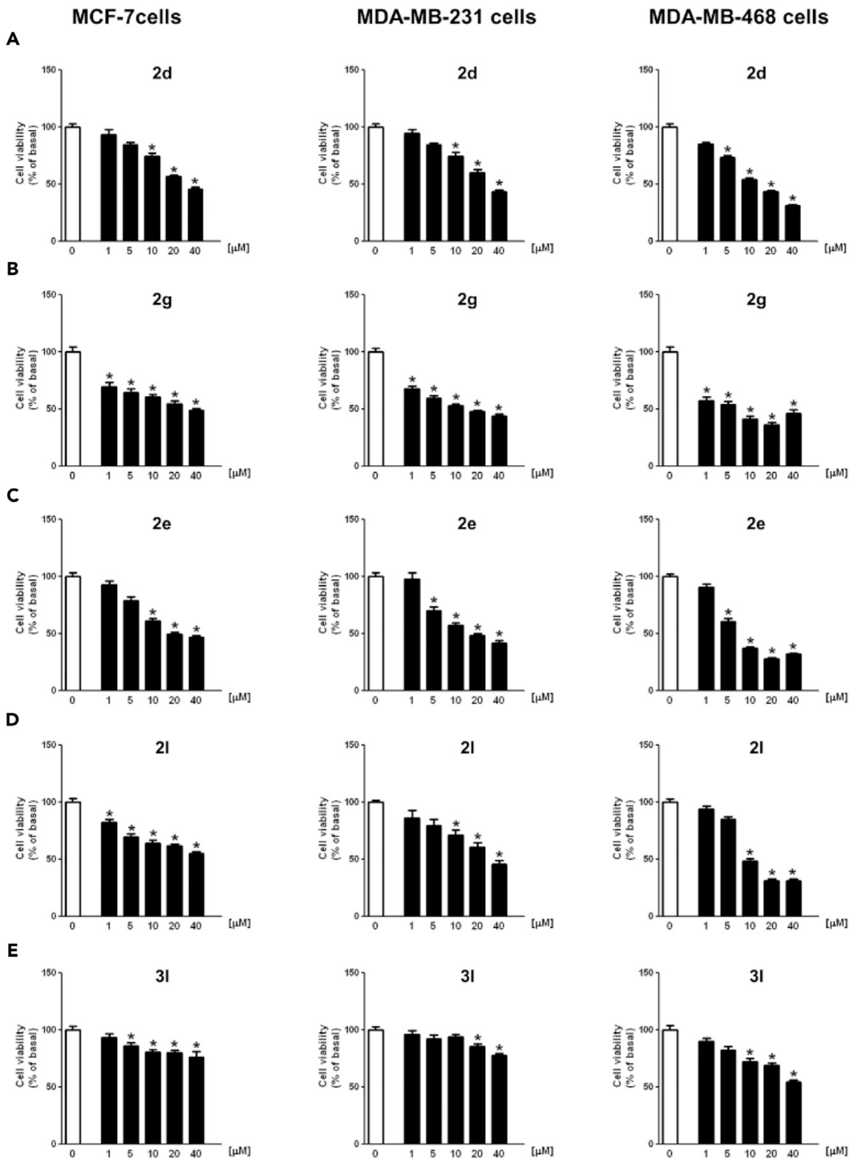

Figure 2. Dihydrofurofuranones 2d, 2e, 2g, 2l, and 3l Decrease Breast Cancer Cell Viability

(A–E) MCF-7, MDA-MB-231 and MDA-MB-468 cells were left untreated (0) or treated with different doses (1–40 μM) of **2d** (A), **2g** (B), **2e** (C), **2l** (D), and **3l** (E) for 72 hr. Cell viability was evaluated by MTT (MTT = 3-(4,5-dimethylthiazol-2-yl)-2, 5-diphenyltetrazolium bromide) assay. Results were expressed as mean ± SD of three independent experiments each performed in triplicate. Statistically significant differences are indicated (*$p < 0.05$ versus basal). See Transparent Methods for experimental details. SD, standard deviation.

compounds. This event could rely on a different pattern of gene expression present in these cells. A clear definition of target genes will help to explain such a difference.

To exclude the toxic effects of these compounds, experiments using normal breast epithelial cells MCF-10A and immortalized fibroblasts 3T3-L1 have been performed. As shown in Figure 3, the proliferative behavior of these cells is not affected by all doses of **2l** (Figure 3D) and **3l** (Figure 3E), whereas **2d** (Figure 3A), **2g** (Figure 3B), and **2e** (Figure 3C) caused a reduction of cell viability in both MCF-10A and 3T3-L1 cells. In particular, in MCF-10A cells, **2d** exerted a slight but statistically significant inhibitory effect at 20 and 40 μM (Figure 3A), whereas **2g** was effective starting from 5 μM (Figure 3B) and **2e** starting from 10 μM (Figure 3C). Moreover, in 3T3-L1, **2d** (Figure 3A) and **2e** (Figure 3C) decreased viability at 40 μM, whereas **2g** (Figure 3B) was effective from 20 μM.

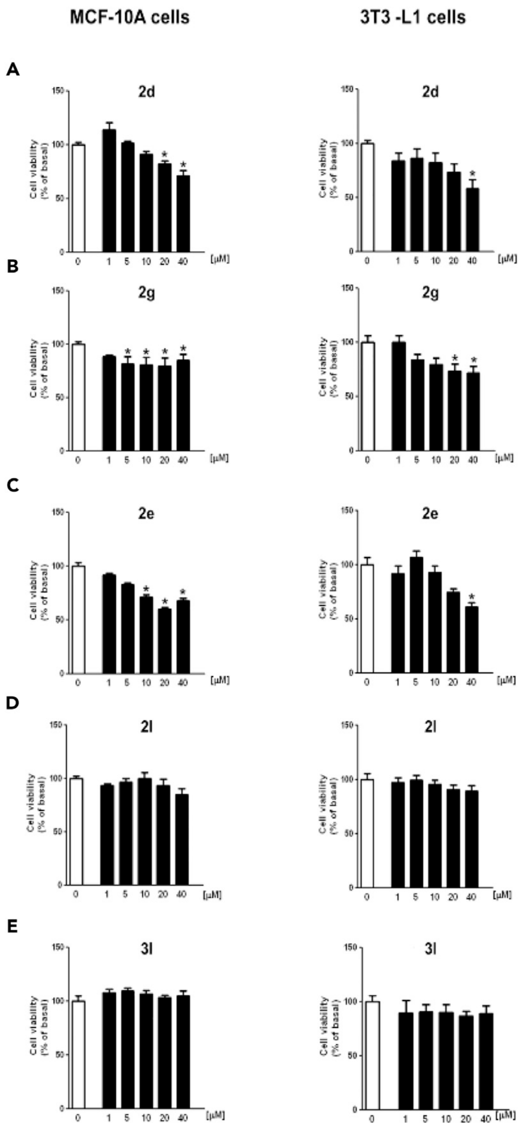

Figure 3. Effects of Dihydrofurofuranones 2d, 2e, 2g, 2l, and 3l on MCF-10A and 3T3-L1 Cell Viability

(A–E) MCF-10A and 3T3-L1 cells were left untreated (0) or treated with different doses (1–40 μM) of **2d** (A), **2g** (B), **2e** (C), **2l** (D), and **3l** (E) for 72 hr. Cell viability was evaluated by MTT (3-(4,5-dimethylthiazol-2-yl)-2,5-diphenyltetrazoliumbromide) assay. Results were expressed as mean ± SD of three independent experiments each performed in triplicate. Statistically significant differences are indicated (*p < 0.05 versus basal). See Transparent Methods for experimental details. SD, standard deviation.

Taken together, the results obtained indicate that, among all compounds, 5,5-dimethyl-6*a*-phenyl-3-(trimethylsilyl)-6,6*a*-dihydrofuro[3,2-*b*]furan-2(5*H*)-one **2l** is the one with the most significant inhibitory effects on the cell vitality of tumor cells, whereas it has little or no effect on the vitality of normal cells. This prompted us to investigate the molecular mechanism behind the **2l**-dependent decrease of BC cell viability. To this aim, we performed assays aimed to investigate if **2l** initiated an apoptotic mechanism in MCF-7 and MDA-MB-231 and MDA-MB-468 cells. Apoptosis is an energy-dependent process characterized by a number of hallmarks, such as membrane blebbing, nuclear chromatin condensation, cell shrinkage, internucleosomal DNA fragmentation, and protein cleavage (Bratton and Cohen, 2001). During apoptosis enzymes with cysteine protease activity designed as "caspases" (Chang and Yang, 2000) cleave several substrates including parp-1, a DNA nick sensor that catalyzes DNA repair (Duriez and Shah, 1997; Soldani and Scovassi, 2002). After cleavage, parp-1 loses the nick sensor function and is inactive toward DNA damage. Using western blot analysis, we showed that **2l** treatment induced parp-1 cleavage in all three cell lines (Figures 4A–4C).

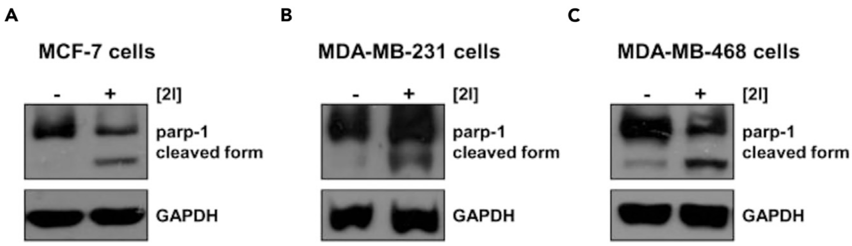

Figure 4. Treatment with Dihydrofurofuranone 2l Induces parp-1 Cleavage in Breast Cancer Cells

(A–C) Cells were left untreated (-) or treated with **2l** (20 μM) (+) for 48 hr. Western blot analyses of parp-1 in MCF-7 (A), MDA-MB-231 (B), and MDA-MB-468 (C) were performed on equal amounts of total proteins. GAPDH was used as a loading control. Blots are representative of three independent experiments with similar results. See Transparent Methods for experimental details.

In addition, we also investigated the effect of **2l** on the activation of other apoptotic markers, in particular the bcl-2 family members, playing pivotal roles in regulating the mitochondrial apoptotic pathway. As can be seen from Figure 5, the presence of **2l** decreased bcl-2 expression (Figure 5A) in all three BC cell lines. Cytosolic translocation of cytochrome *c* has been proposed to be an essential step

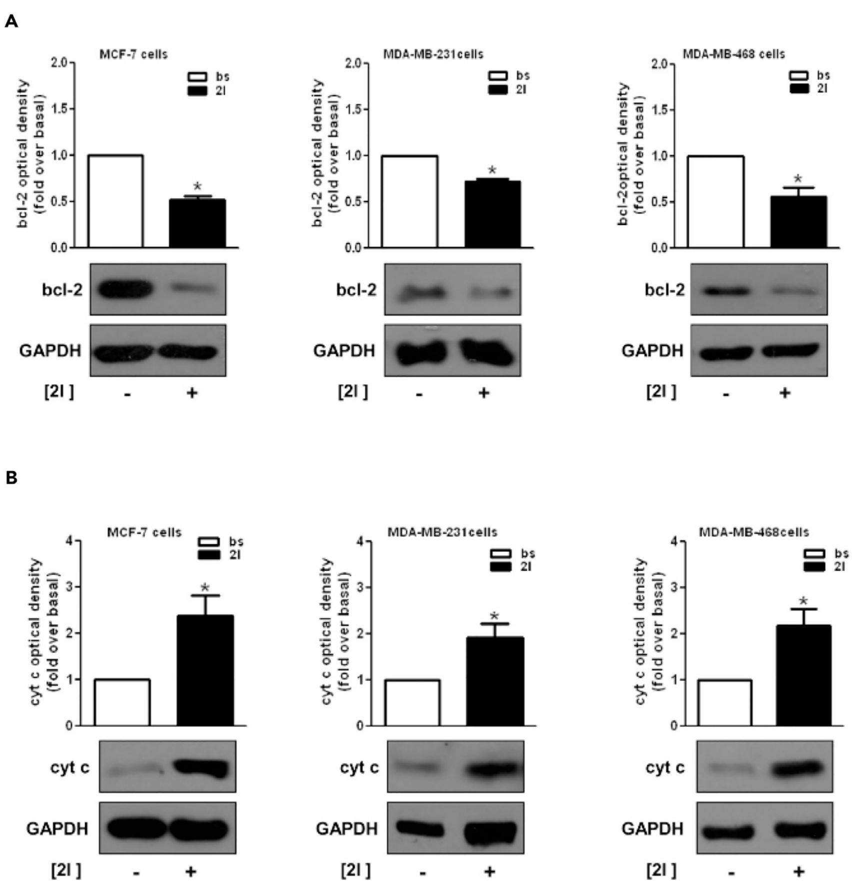

Figure 5. Treatment with Dihydrofurofuranone 2l Modulates the Expression of Apoptotic Markers in Breast Cancer Cells

(A and B) MCF-7, MDA-MB-231, and MDA-MB-468 breast cancer cells were left untreated (bs, −) or treated with **2l** (20 μM) (**2l**, +) for 48 hr. Western blot analyses of bcl-2 (A) and cytochrome *c* (cyt c) (B) were performed on equal amounts of total proteins. GAPDH was used as a loading control. Blots are representative of three independent experiments with similar results. (A and B, upper panels) Graphs represent means of normalized optical densities from three experiments, bars represent SD (*$p < 0.05$ versus untreated cells [−]). See Transparent Methods for experimental details. SD, standard deviation.

in the mitochondria-dependent apoptotic pathway. In fact, cytochrome *c* release from mitochondria into the cytosol triggers caspase activation (Kuida et al., 1998; Wang, 2001; Wilson, 1998). Therefore, we examined if cytochrome *c* was released into the cytosol after treatment with **2l**. Cytosolic protein fraction was isolated and analyzed by western blot analysis (Figure 5B). As reported in Figure 5B, cytochrome *c* levels increased in the cytosolic fraction of all three BC cell lines treated with **2l**.

Conclusions

In conclusion, we have reported a novel carbonylative double cyclization approach to biologically active 6,6*a*-dihydrofuro[3,2-*b*]furan-2(5*H*)-ones **2** starting from simple and readily available starting materials (4-yne-1,3-diols **1**, carbon monoxide, and oxygen). The process allows the formation of two cycles and three new bonds (O-C, C-C, and C-O) in one single operation and in ordered sequence. The dihydrofurofuranones thus synthesized have shown a significant antitumor activity against BC cell lines. In particular, 5,5-dimethyl-6*a*-phenyl-3-(trimethylsilyl)-6,6*a*-dihydrofuro[3,2-*b*]furan-2(5*H*)-one **2l** showed the most significant inhibitory effects on the cell vitality of tumor cells, whereas it had practically no effect on the vitality of normal cells. For **2l**, molecular events leading to cell death were further investigated, and the results evidenced that this molecule was able to activate an intrinsic apoptotic mechanism.

METHODS

All methods can be found in the accompanying Transparent Methods supplemental file.

SUPPLEMENTAL INFORMATION

Supplemental Information includes Transparent Methods, 74 figures, 2 tables, and 2 data files and can be found with this article online at https://doi.org/10.1016/j.isci.2018.04.022.

ACKNOWLEDGMENTS

We thank the University of Calabria for financial support.

AUTHOR CONTRIBUTIONS

Conceptualization, B.G., R.M, N.D.C., and V.P.; methodology, all authors; validation, R.M., I.Z., A.C., N.D.C., R.S.; investigation, I.Z., A.C., R.M., N.M.; writing, B.G. and V.P.; supervision, B.G.

DECLARATION OF INTERESTS

An Italian patent has been filed on July 13, 2017 (# 102017000078586), titled "Derivati 6,6*a*-diidrofuro[3,2-*b*] furan-2-(5*H*)onici, loro preparazione e uso nel trattamento dei tumori." Inventors: Bartolo Gabriele, Adele Chimento, Raffaella Mancuso, Vincenzo Pezzi, Ida Ziccarelli, Rosa Sirianni; Applicant: University of Calabria, Italy.

Received: February 20, 2018
Revised: March 23, 2018
Accepted: April 26, 2018
Published: May 25, 2018

REFERENCES

Alcaide, B., and Almendros, P. (2014). Gold-catalyzed cyclization reactions of allenol and alkynol derivatives. Acc. Chem. Res. *47*, 939–952.

Bauer, K.R., Brown, M., Cress, R.D., Parise, C.A., and Caggiano, V. (2007). Descriptive analysis of estrogen receptor (ER)-negative, progesterone receptor (PR)-negative, and HER2-negative invasive breast cancer, the so-called triple-negative phenotype. Cancer *109*, 1721–1728.

Beller, M., ed. (2006). Catalytic Carbonylation Reactions (Springer).

Bratton, S.B., and Cohen, G.M. (2001). Apoptotic death sensor: an organelle's alter ego? Trends Pharmacol. Sci. *22*, 306–315.

Carey, L.A., Dees, E.C., Sawyer, L., Gatti, L., Moore, D.T., Collichio, F., Ollila, D.W., Sartor, C.I., Graham, M.L., and Perou, C.M. (2007). The triple negative paradox: primary tumor chemosensitivity of breast cancer subtypes. Clin. Cancer Res. *13*, 2329.

Chang, H.Y., and Yang, X. (2000). Proteases for cell suicide: functions and regulation of caspases. Microbiol. Mol. Biol. Rev. *64*, 821–846.

Debrouwer, W., Heugebaert, T.S.A., Roman, B.I., and Stevens, C.V. (2015). Homogeneous gold-catalyzed cyclization reactions of alkynes with N- and S-nucleophiles. Adv. Synth. Catal. *357*, 2975–3006.

Duriez, P., and Shah, G.M. (1997). Cleavage of poly(ADP-ribose) polymerase: a sensitive parameter to study cell death. Biochem. Cell Biol. *75*, 337–349.

Friis, S.D., Lindhardt, A.T., and Skrydstrup, T. (2016). The development and application of two-chamber reactors and carbon monoxide precursors for safe carbonylation reactions. Acc. Chem. Res. *49*, 594–605.

Gabriele, B., Mancuso, R., and Salerno, G. (2012). Oxidative carbonylation as a powerful tool for the direct synthesis of carbonylated heterocycles. Eur. J. Org. Chem. 6825–6839.

Gabriele, B., Veltri, L., Mancuso, R., and Carfagna, C. (2014). Cascade reactions: a multicomponent approach to functionalized indane derivatives by a tandem palladium-catalyzed carbamoylation/carbocyclization process. Adv. Synth. Catal. *356*, 2547–2558.

Gadge, S.T., and Bhanage, B.M. (2014). Recent developments in palladium catalysed carbonylation reactions. RSC Adv. *4*, 10367–10389.

Gehrtz, P.H., Hirschbeck, V., Ciszek, B., and Fleischer, I. (2016). Carbonylations of alkenes in the total synthesis of natural compounds. Synthesis *48*, 1573–1576.

Guo, L.-N., Duan, X.-H., and Liang, Y.-M. (2011). Palladium-catalyzed cyclization of propargylic compounds. Acc. Chem. Res. *44*, 111–122.

Haffty, B.G., Yang, Q., Reiss, M., Kearney, T., Higgins, S.A., Weidhaas, J., Harris, L., Hait, W., and Toppmeyer, D. (2006). Locoregional relapse and distant metastasis in conservatively managed triple negative early-stage breast cancer. J. Clin. Oncol. *24*, 5652–5657.

Jung, M.E., and Piizi, G. (2005). *gem*-disubstituent effect: theoretical basis and synthetic applications. Chem. Rev. *105*, 1735–1766.

Kalck, P., and Urrutigoïty, M. (2015). Recent improvements in the alkoxycarbonylation reactions catalyzed by transition metal complexes. Inorg. Chim. Acta *431*, 110–121.

Kapitán, P., and Gracza, T. (2008). Asymmetric intramolecular Pd(II)-catalysed oxycarbonylation of alkene-1,3-diols. Arkivoc *viii*, 8–17.

Kirkpatrick, P. (2009). Anticancer drugs: targeting triple-negative breast cancer. Nat. Rev. Drug Discov. *8*, 21.

Kollár, L., ed. (2008). Modern Carbonylation Methods (Wiley-VCH).

Krause, N., and Winter, C. (2011). Gold-catalyzed nucleophilic cyclization of functionalized allenes: a powerful access to carbo- and heterocycles. Chem. Rev. *111*, 1994–2009.

Kuida, K., Haydar, T.F., Kuan, C.Y., Gu, Y., Taya, C., Karasuyama, H., Su, M.S., Rakic, P., and Flavell, R.A. (1998). Reduced apoptosis and cytochrome c-mediated caspase activation in mice lacking caspase 9. Cell *94*, 325–337.

Liu, Q., Zhang, H., and Lei, A. (2011). Oxidative carbonylation reactions: organometallic compounds (R-M) or hydrocarbons (R-H) as nucleophiles. Angew. Chem. Int. Ed. *50*, 10788–10799.

Mancuso, R., Ziccarelli, I., Armentano, D., Marino, N., Giofrè, S.V., and Gabriele, B. (2014). Divergent palladium iodide catalyzed multicomponent carbonylative approaches to functionalized isoindolinone and isobenzofuranimine derivatives. J. Org. Chem. *79*, 3506–3518.

Mancuso, R., Raut, D.S., Della Ca', N., Fini, F., Carfagna, C., and Gabriele, B. (2015). Catalytic oxidative carbonylation of amino moieties to ureas, oxamides, 2-oxazolidinones, and benzoxazolones. ChemSusChem *8*, 2204–2211.

Mancuso, R., Raut, D.S., Marino, N., De Luca, G., Gordano, C., Catalano, S., Barone, I., Andò, S., and Gabriele, B. (2016). A palladium-catalyzed carbonylation approach to eight-membered lactam derivatives with antitumor activity. Chem. Eur. J. *22*, 3053–3064.

Millar, E.K.A., Graham, P.H., O'Toole, S.A., McNeil, C.M., Browne, L., Morey, A.L., Eggleton, S., Beretov, J., Theocharous, C., Capp, A., et al. (2009). Prediction of local recurrence, distant metastases, and death after breast-conserving therapy in early-stage invasive breast cancer using a five-biomarker panel. J. Clin. Oncol. *27*, 4701–4708.

Nguyen, P.L., Taghian, A.G., Katz, M.S., Niemierko, A., Abi Raad, R.F., Boon, W.L., Bellon, J.R., Wong, J.S., Smith, B.L., and Harris, J.R. (2008). Breast cancer subtype approximated by estrogen receptor, progesterone receptor, and HER-2 is associated with local and distant recurrence after breast-conserving therapy. J. Clin. Oncol. *26*, 2373–2378.

Omae, I. (2011). Transition metal-catalyzed cyclocarbonylation in organic synthesis. Coord. Chem. Rev. *255*, 139–160.

Peng, J.-B., Qi, X., and Wu, X.-F. (2017). Recent achievements in carbonylation reactions: a personal account. Synlett *28*, 175–194.

Sammes, P.G., and Weller, D.J. (1995). Steric promotion of ring formation. Synthesis *1995*, 1205–1222.

Shen, C., and Wu, X.-F. (2017). Palladium-catalyzed carbonylative multicomponent reactions. Chem. Eur. J. *23*, 2973–2987.

Siegel, R.L., Miller, K.D., and Jemal, A. (2016). Cancer statistics, 2016. CA Cancer J. Clin. *66*, 7–30.

Siegel, R.L., Miller, K.D., and Jemal, A. (2017). Cancer statistics, 2017. CA Cancer J. Clin. *67*, 7–30.

Soldani, C., and Scovassi, A. (2002). Poly(ADP-ribose) polymerase-1 cleavage during apoptosis: an update. Apoptosis *7*, 321–328.

Tanaka, K., and Tajima, Y. (2012). Transition-metal-catalyzed cyclization of alkynal via ozametallacycle intermediates. Eur. J. Org. Chem. 3715–3725.

Valera, J.A., and Saa, C. (2016). Metal-catalyzed cyclizations to pyran and oxazine derivatives. Synthesis *48*, 3470–3478.

Veltri, L., Mancuso, R., Altomare, A., and Gabriele, B. (2015). Divergent multicomponent tandem palladium-catalyzed aminocarnonylation-cyclization approaches to functionalized imidazothiazinones and imidazothiazoles. ChemCatChem *7*, 2206–2213.

Veltri, L., Paladino, V., Plastina, P., and Gabriele, B. (2016a). A palladium iodide-catalyzed cyclocarbonylation approach to thiadiazafluorenones. J. Org. Chem. *81*, 6106–6111.

Veltri, L., Grasso, G., Rizzi, R., Mancuso, R., and Gabriele, B. (2016b). Palladium-catalyzed carbonylative multicomponent synthesis of functionalized benzimidazothiazoles. Asian J. Org. Chem. *5*, 560–567.

Veltri, L., Giofrè, S.V., Devo, P., Romeo, R., Dobbs, A.P., and Gabriele, B. (2018). A palladium iodide-catalyzed oxidative aminocarbonylation–heterocyclization approach to functionalized benzimidazoimidazoles. J. Org. Chem. *83*, 1680–1685.

Vlaar, T., Ruijter, E., and Orru, R.V.A. (2011). Recent advances in palladium-catalyzed cyclizations. Adv. Synth. Catal. *353*, 809–841.

Voduc, K.D., Cheang, M.C.U., Tyldesley, S., Gelmon, K., Nielsen, T.O., and Kennecke, H. (2010). Breast cancer subtypes and the risk of local and regional relapse. J. Clin. Oncol. *28*, 1684–1691.

Wang, X. (2001). The expanding role of mitochondria in apoptosis. Gene Dev. *15*, 2922–2933.

Wilson, M.R. (1998). Apoptosis: unmasking the executioner. Cell Death Differ. *5*, 646–652.

Wu, X.-F., and Neumann, H. (2012). Ruthenium and rhodium-catalyzed carbonylation reactions. ChemCatChem *4*, 447–458.

Wu, X.-F., Neumann, H., and Beller, M. (2013a). Synthesis of heterocycles via palladium-catalyzed carbonylations. Chem. Rev. *113*, 1–35.

Wu, X.-F., Neumann, H., and Beller, M. (2013b). Palladium-catalyzed oxidative carbonylation reactions. ChemSusChem *6*, 229–241.

Wu, L., Fang, X., Liu, Q., Jackstell, R., Beller, M., and Wu, X.-F. (2014). Palladium-catalyzed carbonylative transformation of C(sp^3)–X bonds. ACS Catal. *4*, 2977–2989.

Wu, X.-F. (2016). Palladium-catalyzed carbonylative transformation of aryl chlorides and aryl tosylates. RSC Adv. *6*, 83831–83837.

Wu, X.-F., and Beller, M., eds. (2016). In Transition Metal Catalyzed Carbonylative Synthesis of Heterocycles. Topics in Heterocyclic Chemistry, *Vol. 42* (Springer).

Wu, Y.-C., Luo, S.-H., Mei, W.-J., Cao, L., Wu, H.-Q., and Wang, Z.-Y. (2017). Synthesis and biological evaluation of 4-biphenylamino-5-halo-2(*5H*)-furanones as potential anticancer agents. Eur. J. Med. Chem. *139*, 84–94.

Ye, Y., and Ma, S. (2014). Palladium-catalyzed cyclization reactions of allenes in the presence of unsaturated carbon-carbon bonds. Acc. Chem. Res. *47*, 989–1000.

ISCI, Volume *3*

Supplemental Information

Catalytic Double Cyclization Process

for Antitumor Agents

against Breast Cancer Cell Lines

Raffaella Mancuso, Ida Ziccarelli, Adele Chimento, Nadia Marino, Nicola Della Ca', Rosa Sirianni, Vincenzo Pezzi, and Bartolo Gabriele

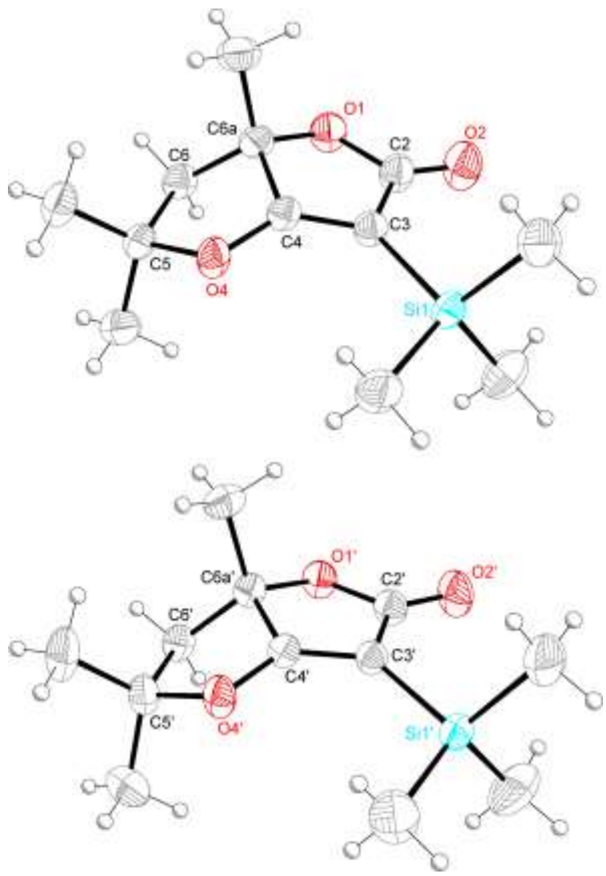

Figure S1. ORTEP drawing of the two crystallographically independent molecules in the asymmetric unit of crystals of **2g**. Thermal ellipsoids have been depicted at the 30% probability level. Note that only the (*6aS*) enantiomer is present in the asymmetric unit, while the (*6aR*) enantiomer is generated by symmetry, Related to **Figure 1**

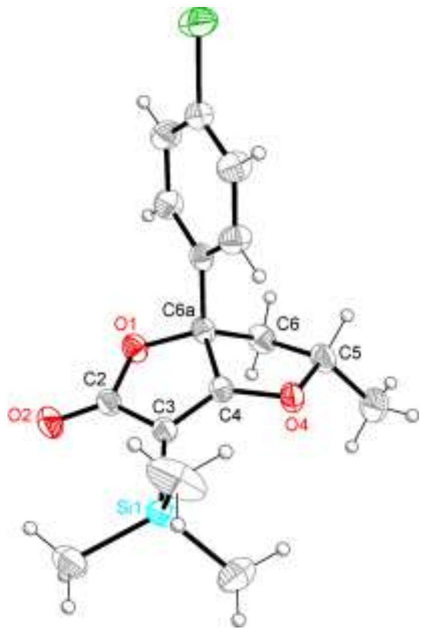

Figure S2. ORTEP drawing of the molecular structure of (5*RS*,6*aRS*)-**2j**. Thermal ellipsoids have been depicted at the 30% probability level. Note that only the (5*S*,*6aS*) enantiomer is present in the asymmetric unit of crystals of **2j**, while the (5*R*,*6aR*) enantiomer is generated by symmetry, Related to **Figure 1** and **Table 1**

Figure S3. ^{1}H-NMR ($CDCl_3$) of 2-(1-Hydroxycyclohexyl)-1-phenylethan-1-one, Related to **Figure 1**

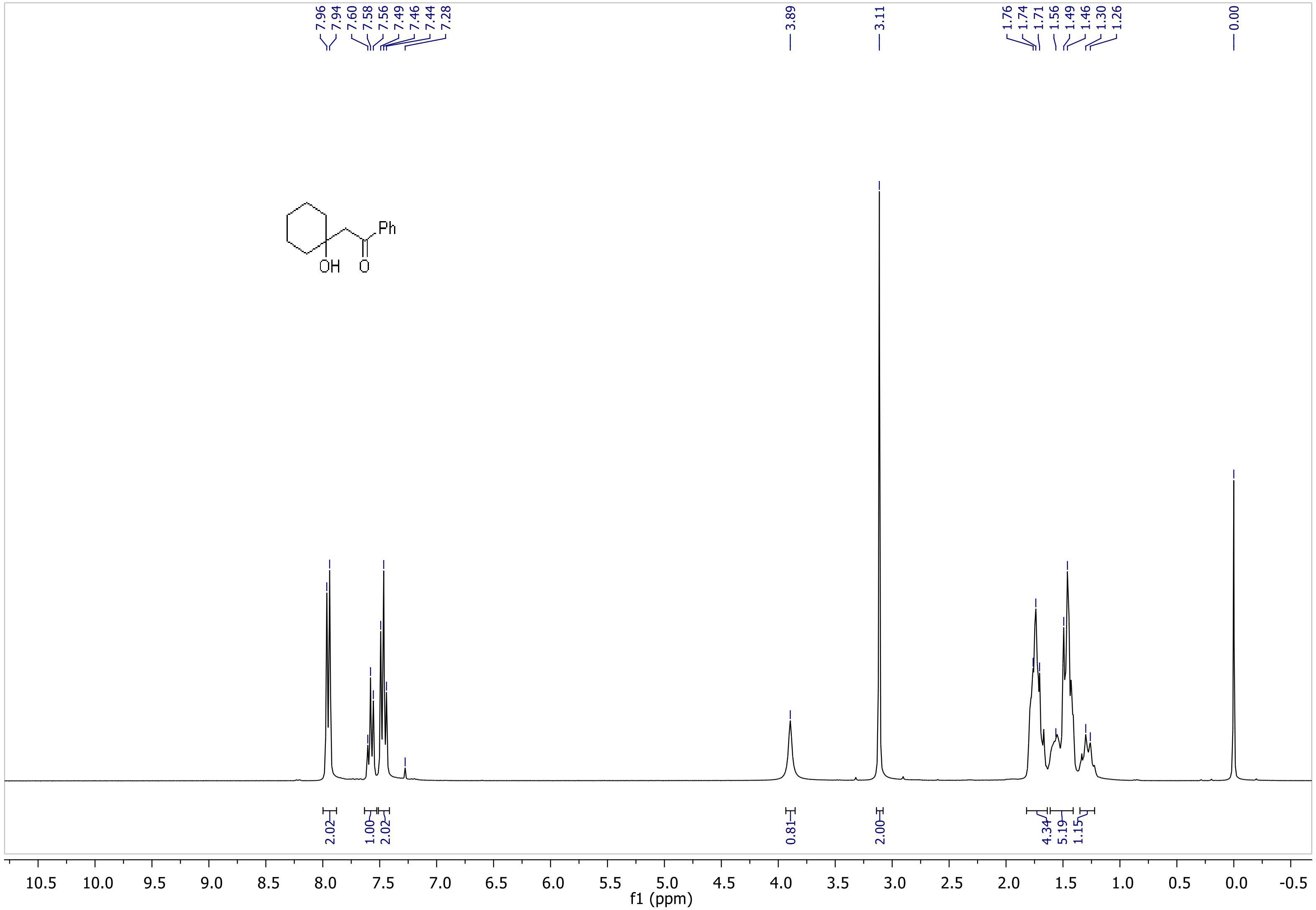

Figure S4. ^{13}C-NMR ($CDCl_3$) of 2-(1-Hydroxycyclohexyl)-1-phenylethan-1-one, Related to **Figure 1**

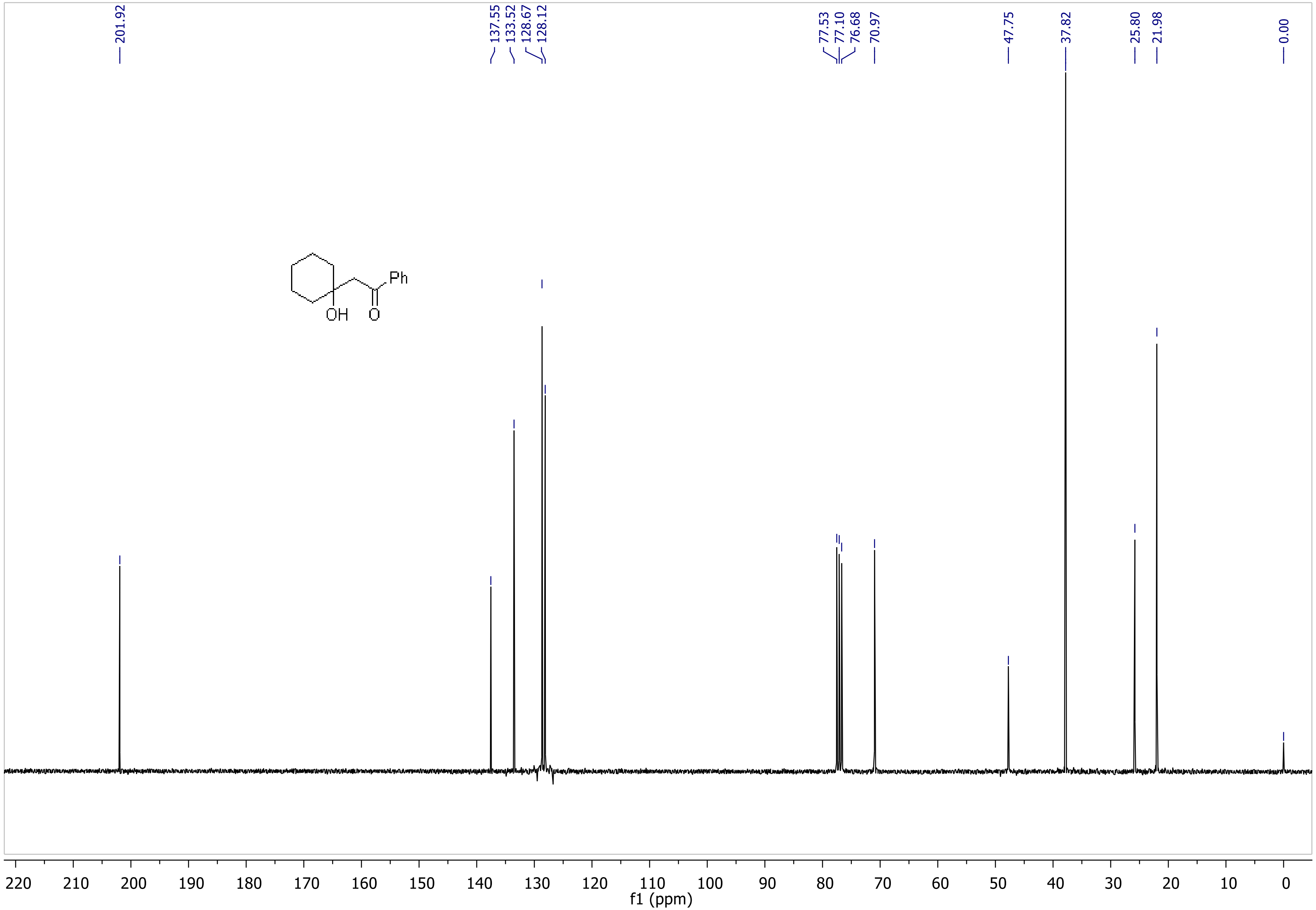

Figure S5. ^{1}H-NMR ($CDCl_3$) of **1a**, Related to **Scheme 2**

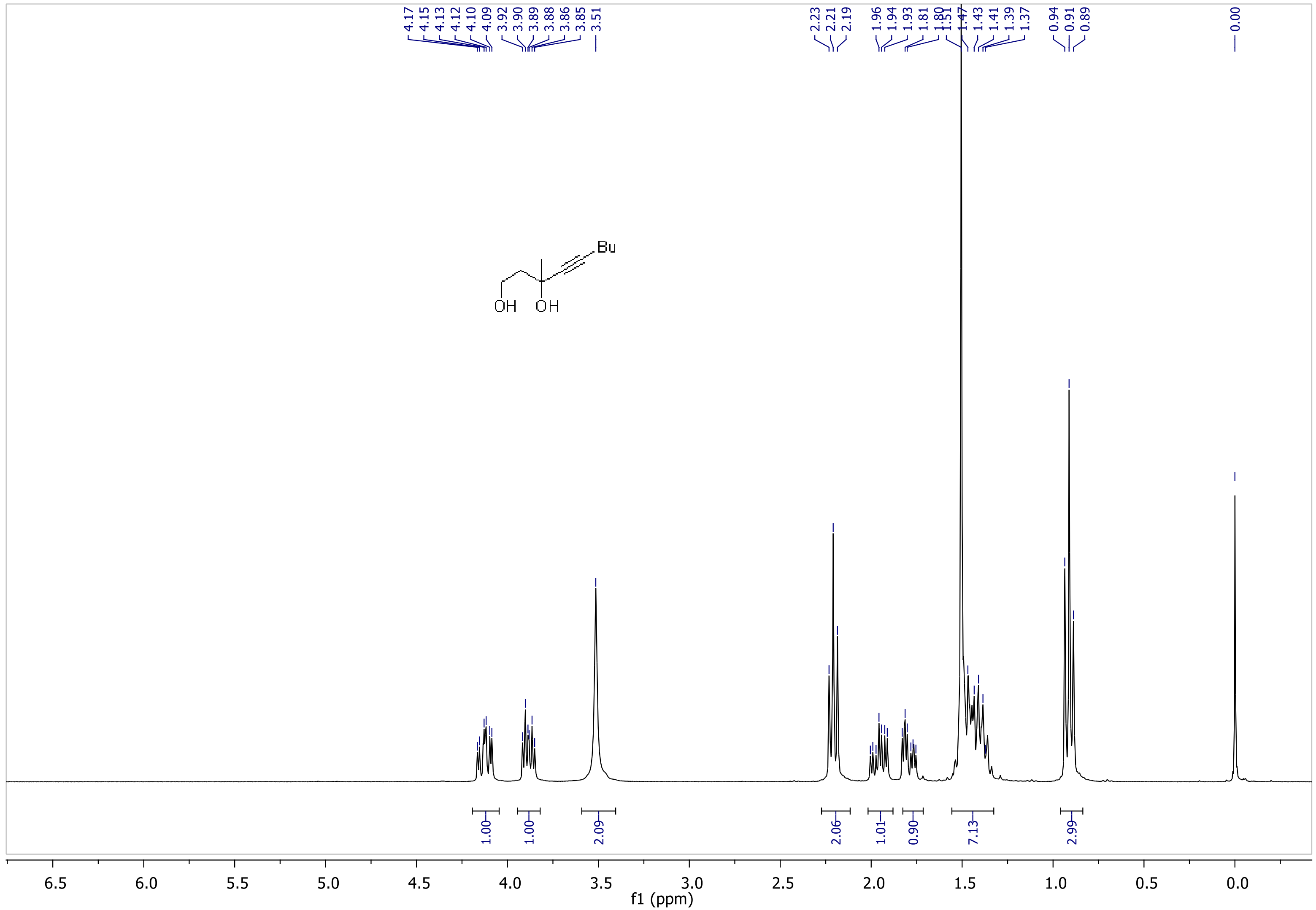

Figure S6. ^{13}C-NMR ($CDCl_3$) of **1a**, Related to **Scheme 2**

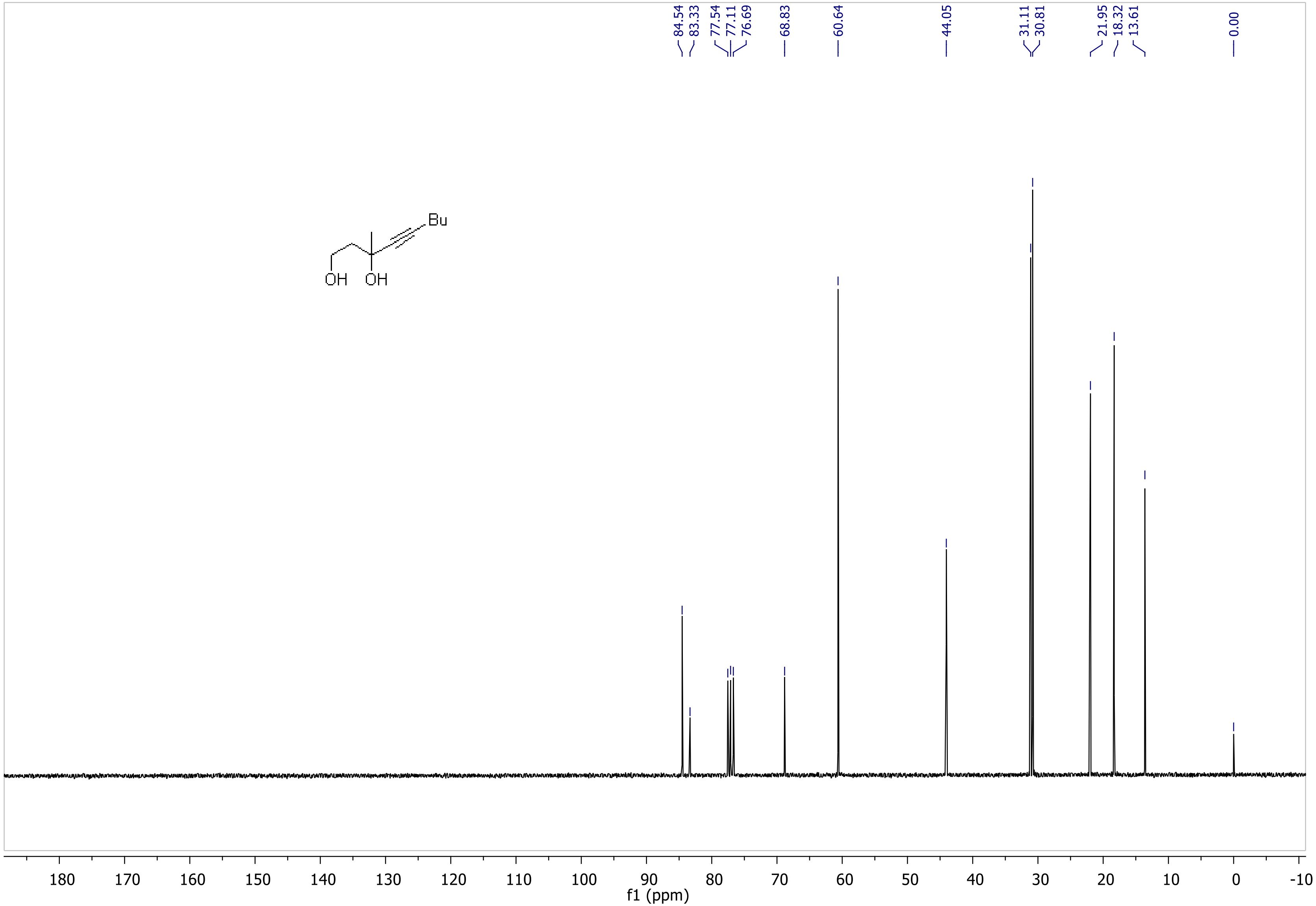

Figure S7. ^{1}H-NMR ($CDCl_3$) of **1b**, Related to **Scheme 2**

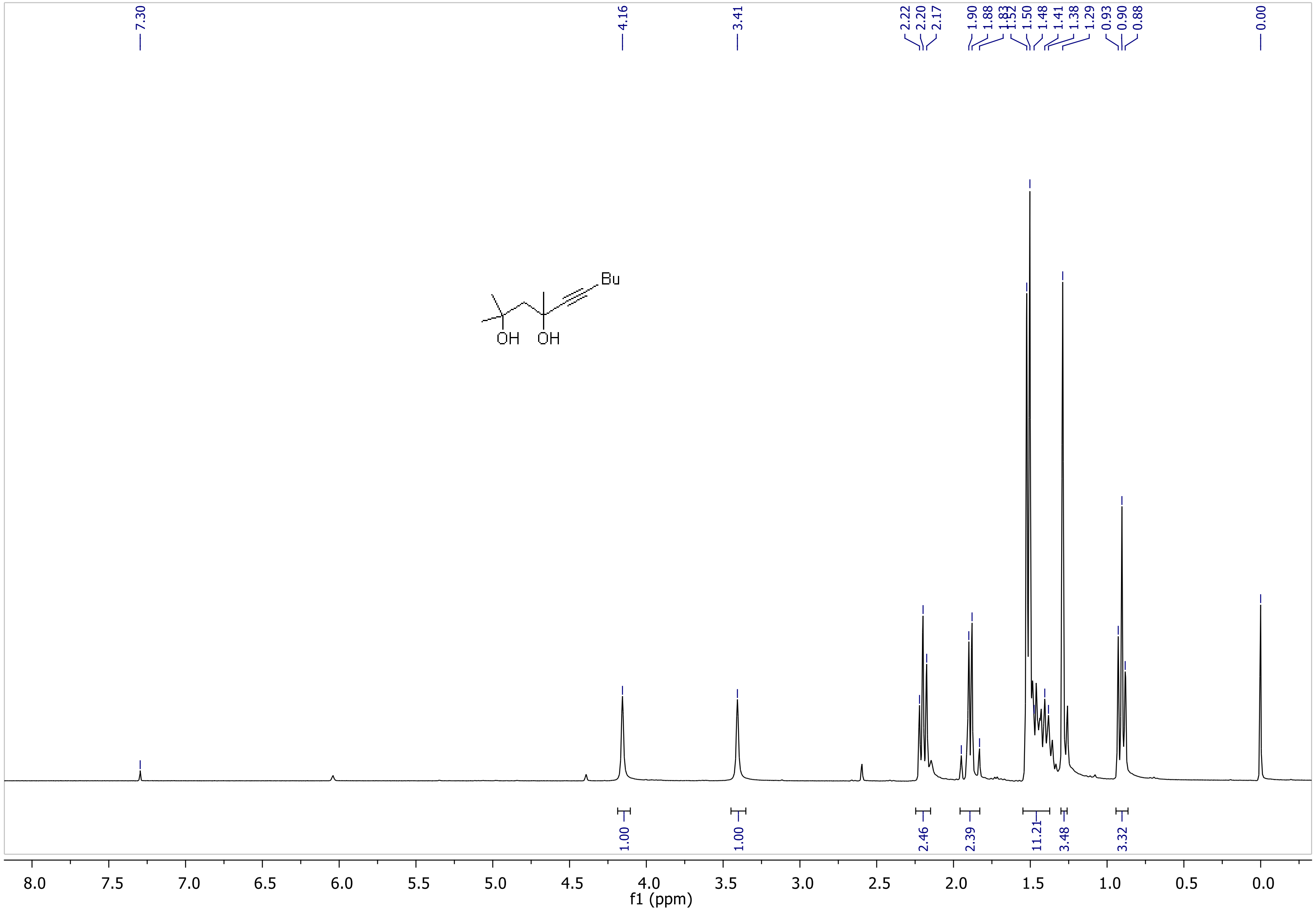

Figure S8. ^{13}C-NMR ($CDCl_3$) of **1b**, Related to **Scheme 2**

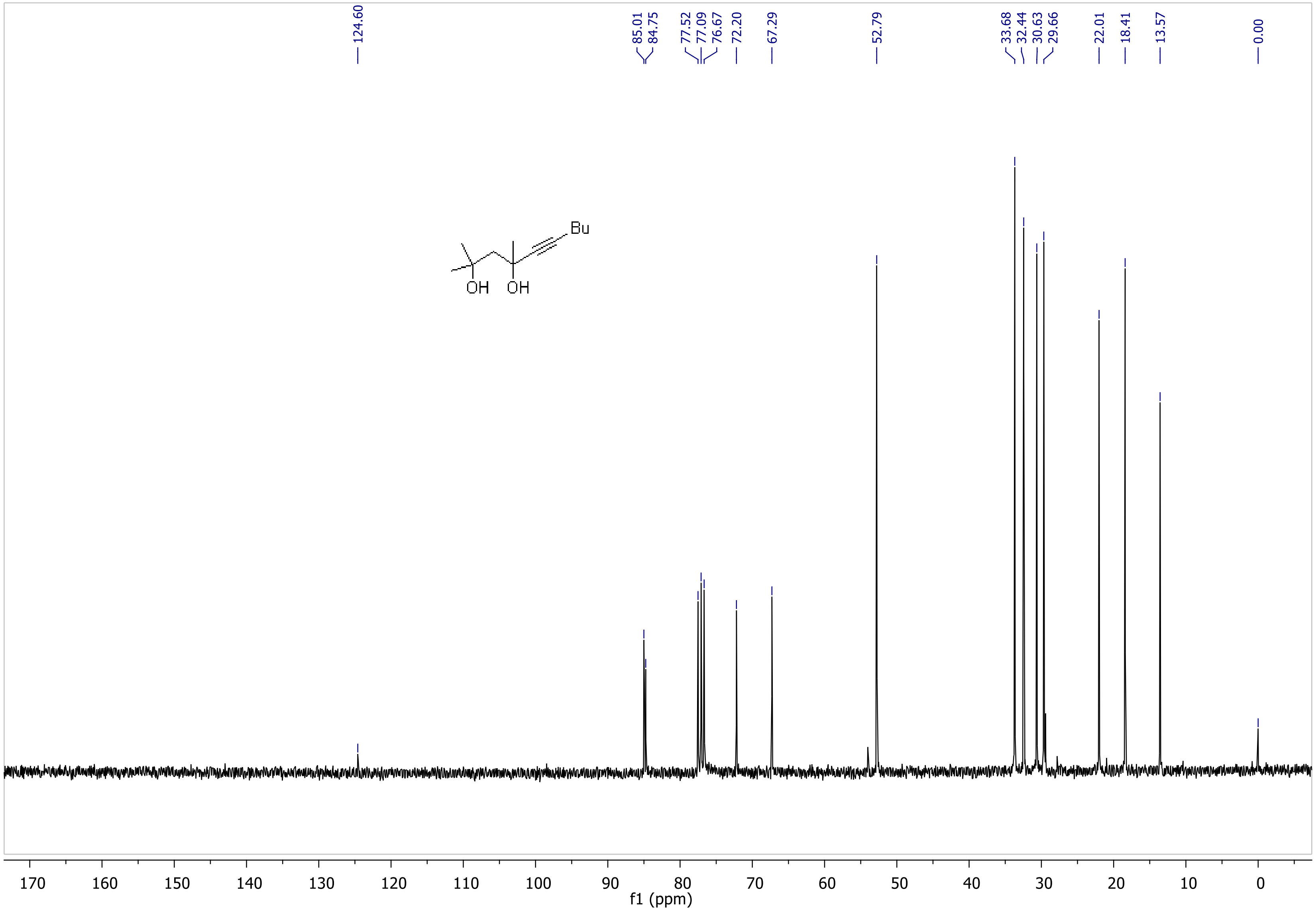

Figure S9. ^{1}H-NMR ($CDCl_3$) of **1c**, Related to **Scheme 2**

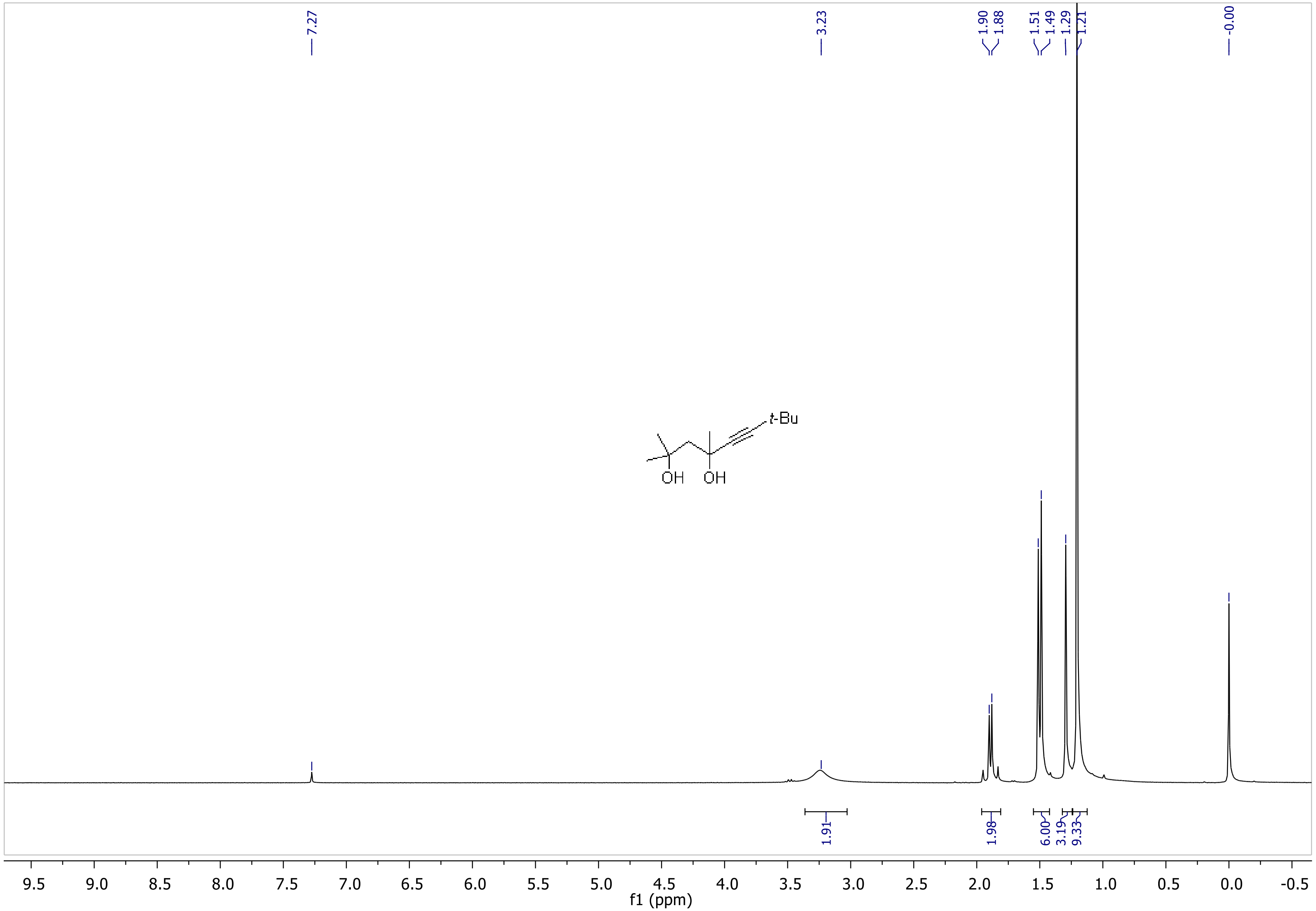

Figure S10. ^{13}C-NMR ($CDCl_3$) of **1c**, Related to **Scheme 2**

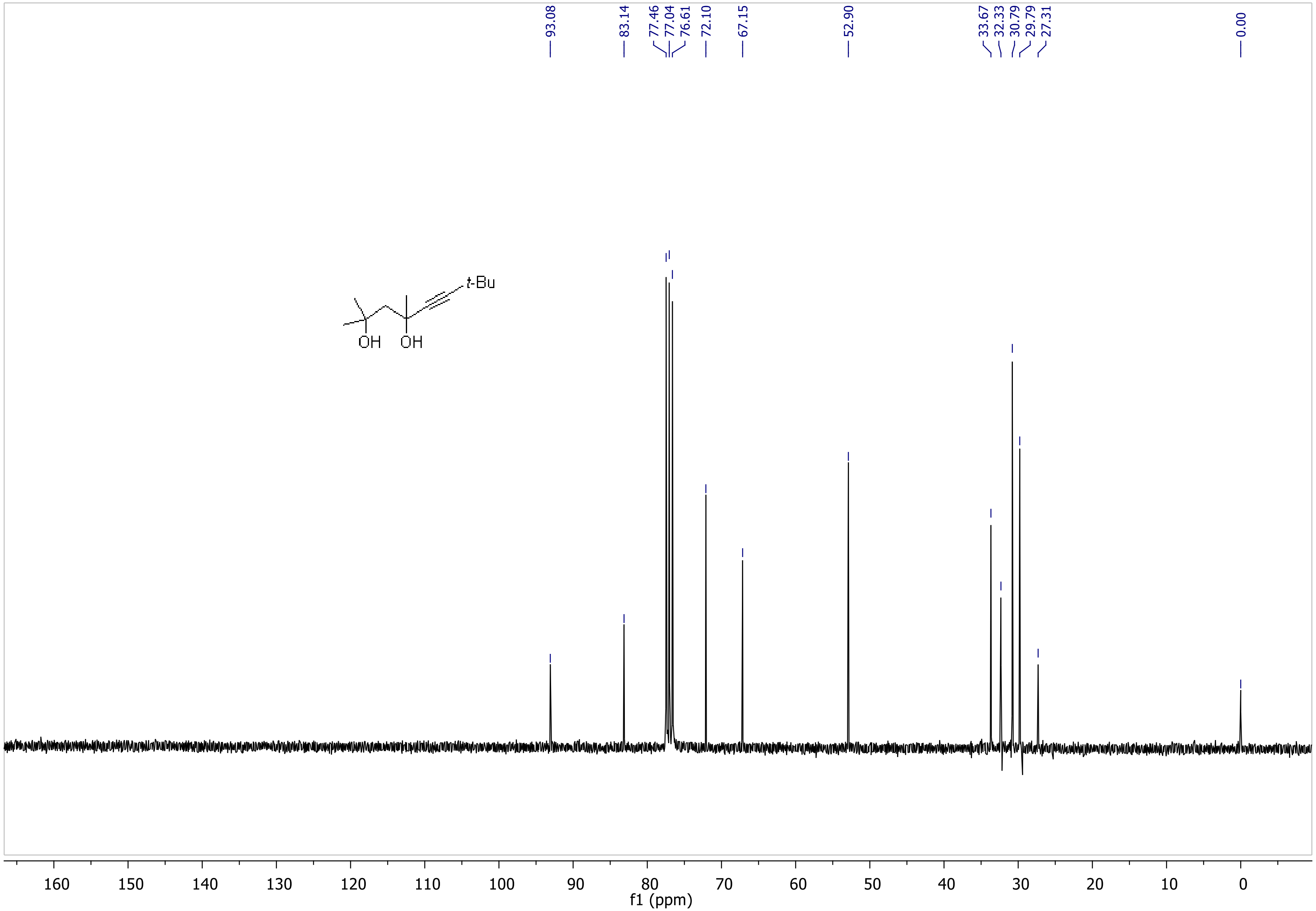

Figure S11. ^{1}H-NMR ($CDCl_3$) of **1d**, Related to **Scheme 2**

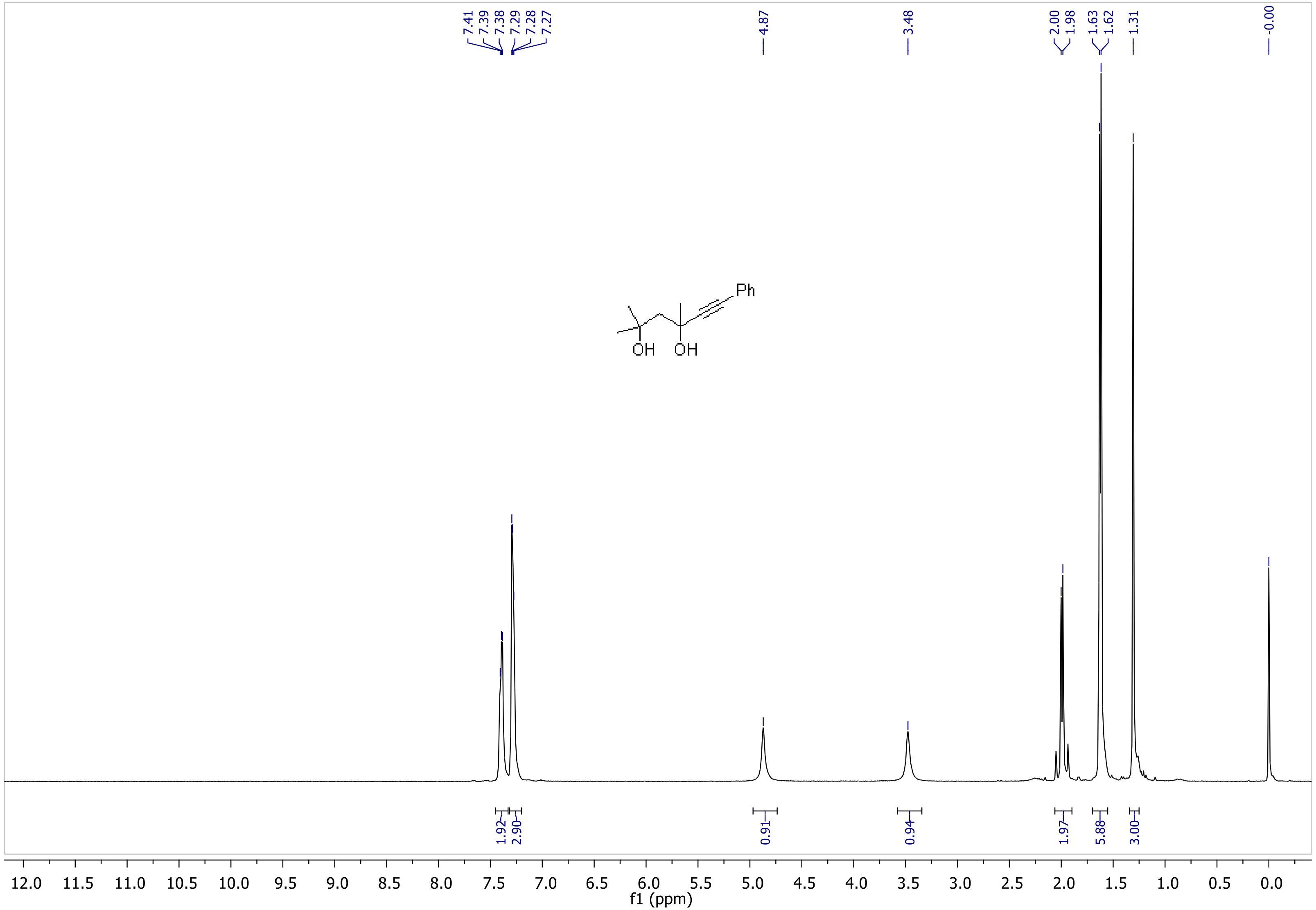

Figure S12. ^{13}C-NMR ($CDCl_3$) of **1d**, Related to **Scheme 2**

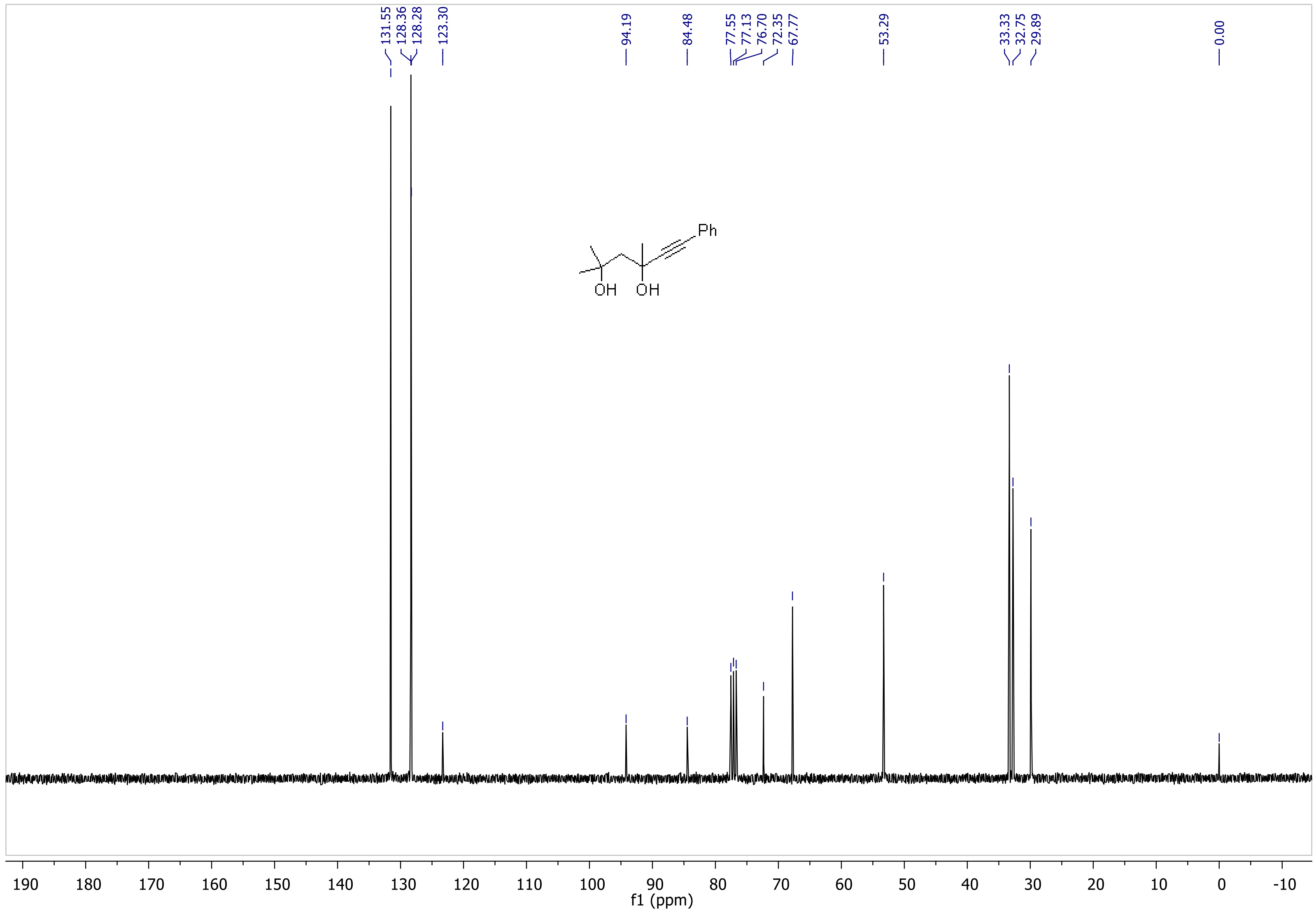

Figure S13. ^{1}H-NMR ($CDCl_3$) of **1e**, Related to **Figure 1**

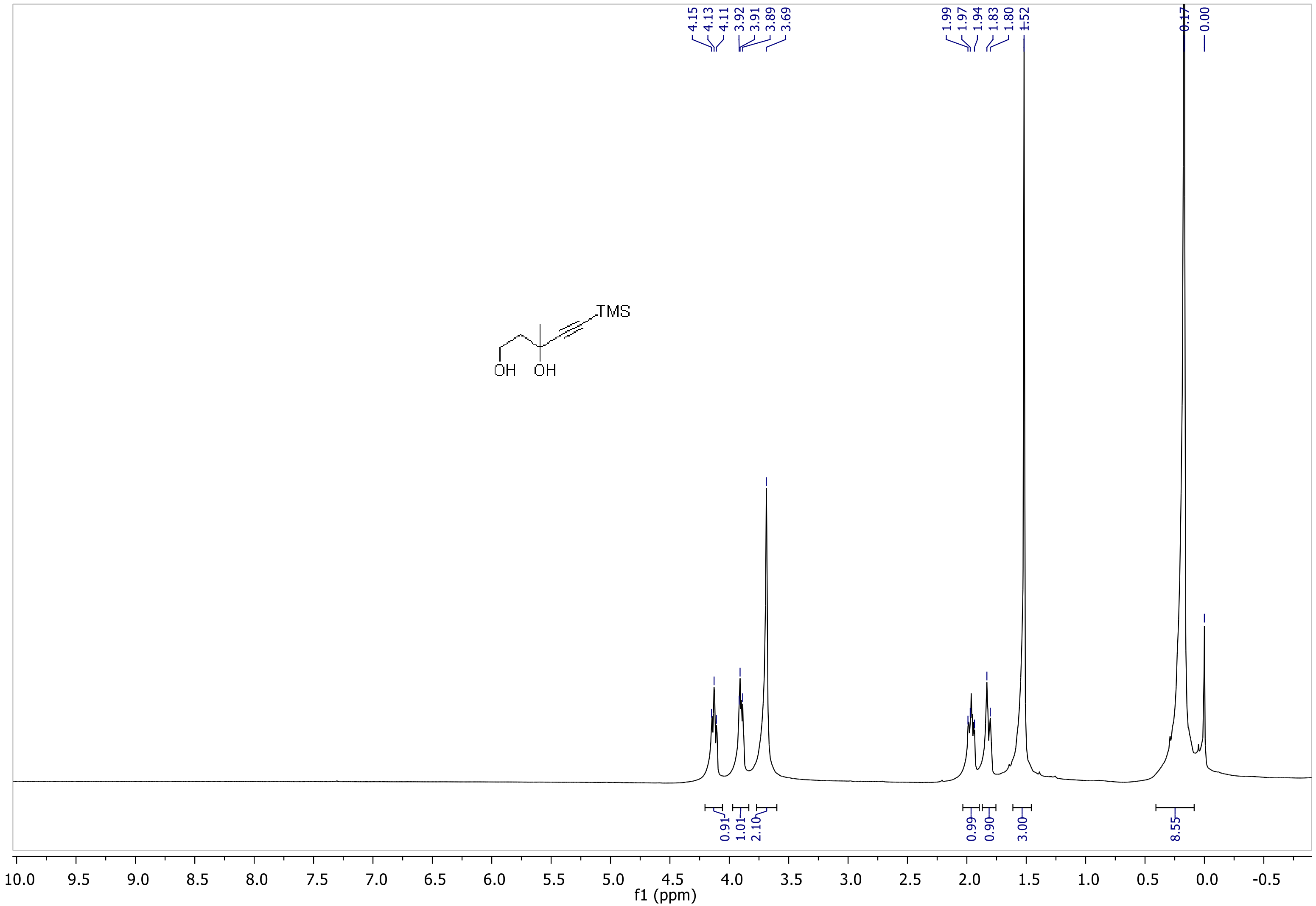

Figure S14. ^{13}C-NMR ($CDCl_3$) of **1e**, Related to **Figure 1**

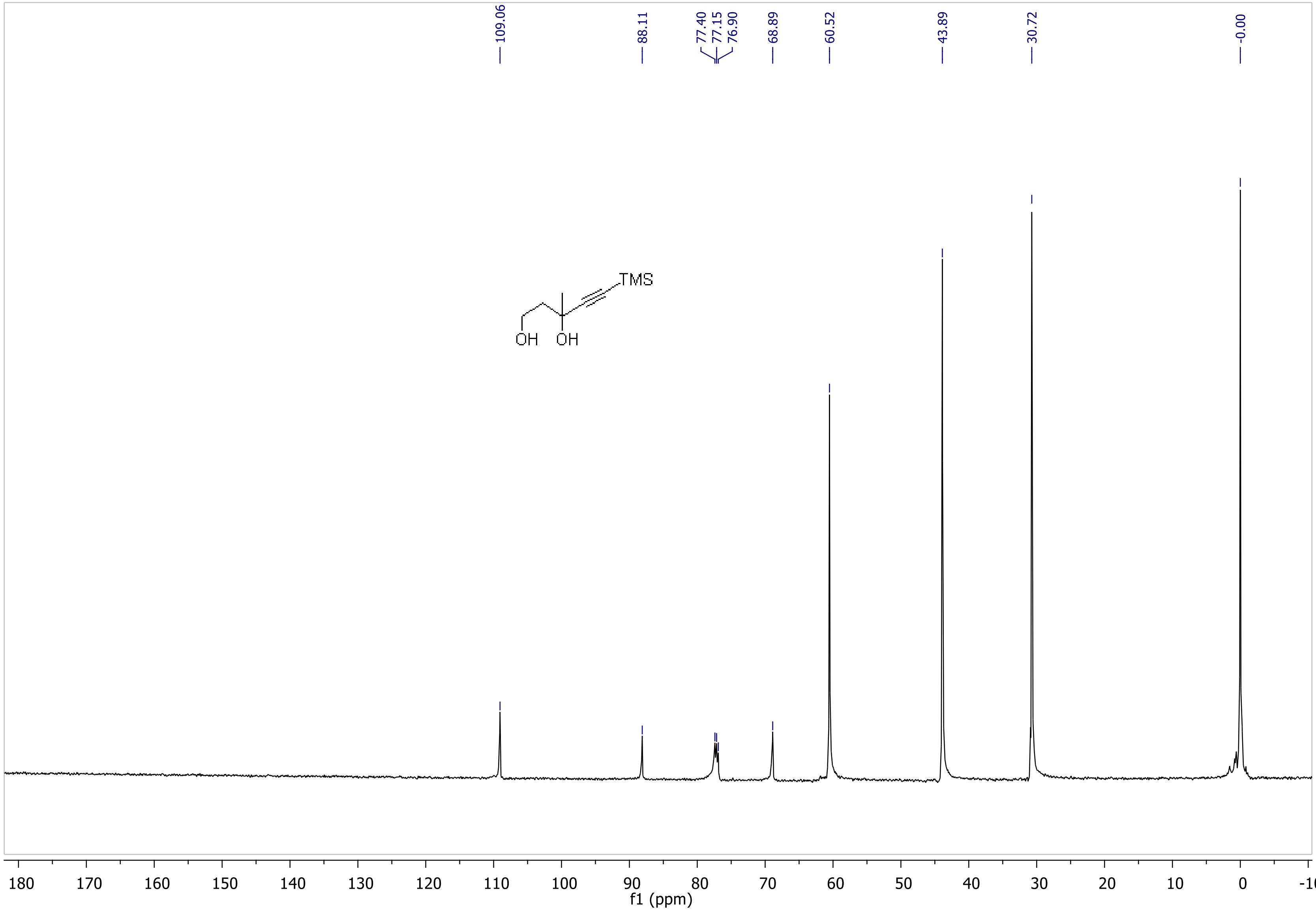

Figure S15. ^{1}H-NMR ($CDCl_3$) of **1f**, Related to **Figure 1**

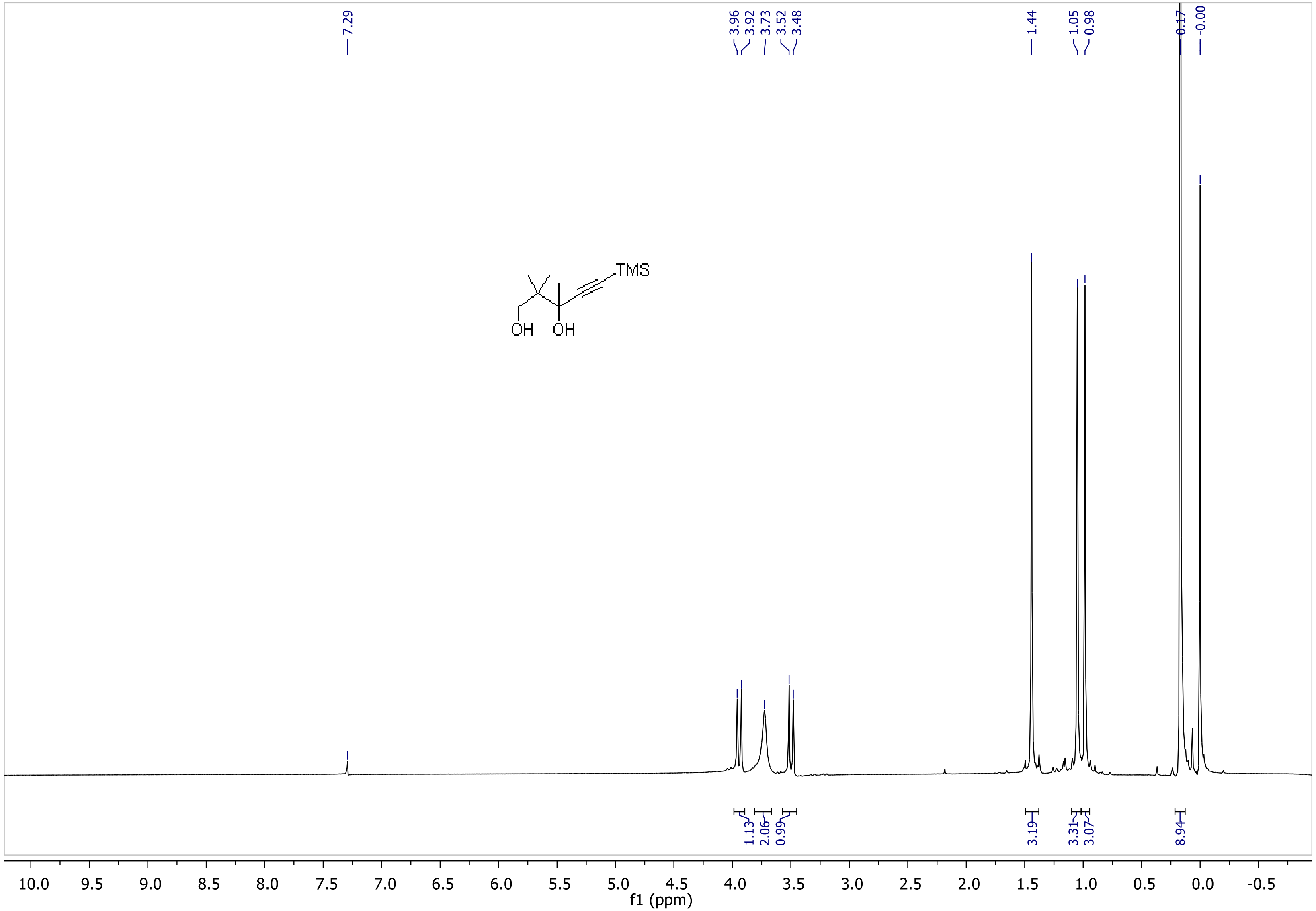

Figure S16. ^{13}C-NMR ($CDCl_3$) of **1f**, Related to **Figure 1**

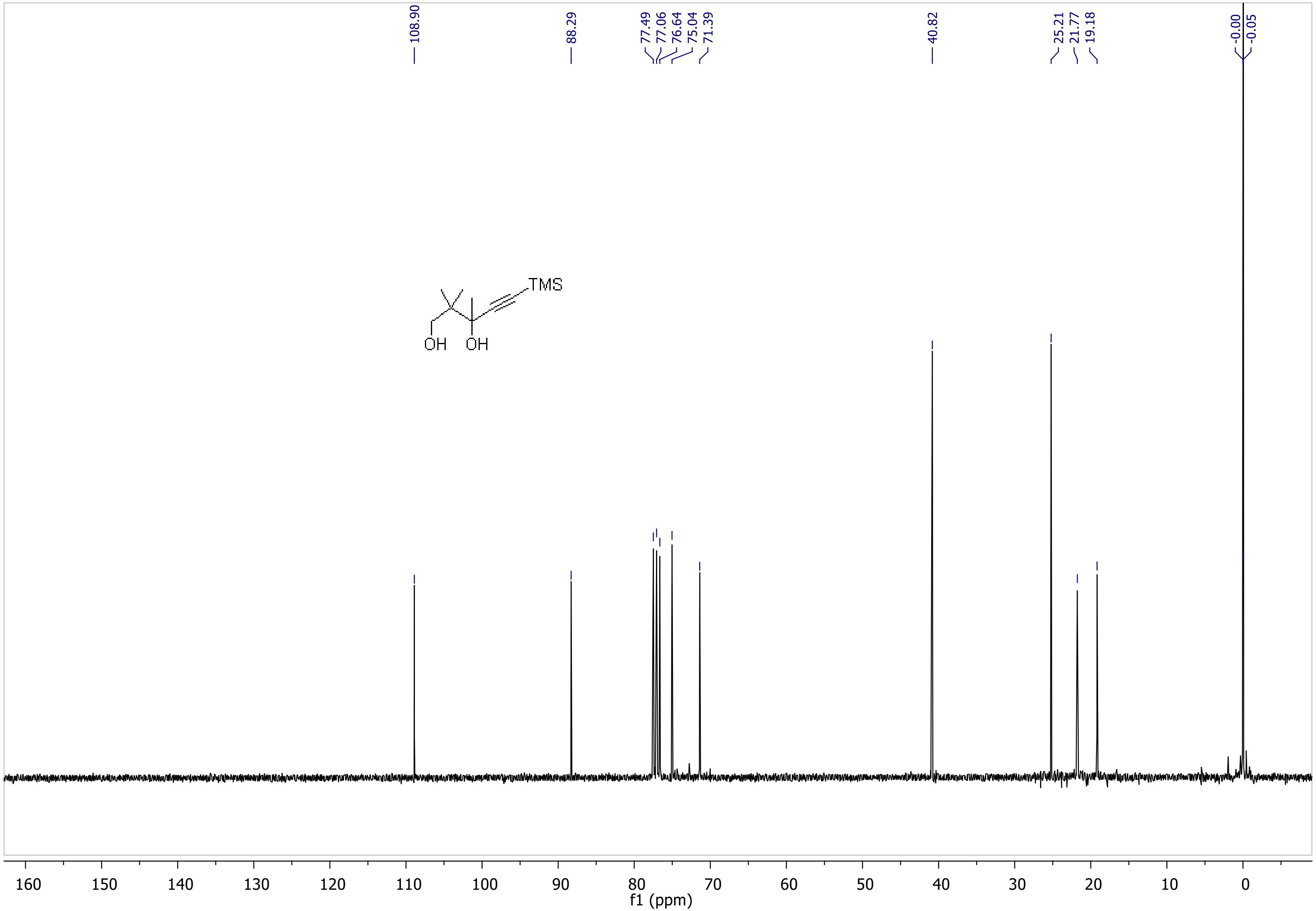

Figure S17. ^{1}H-NMR ($CDCl_3$) of **1g**, Related to **Figure 1**

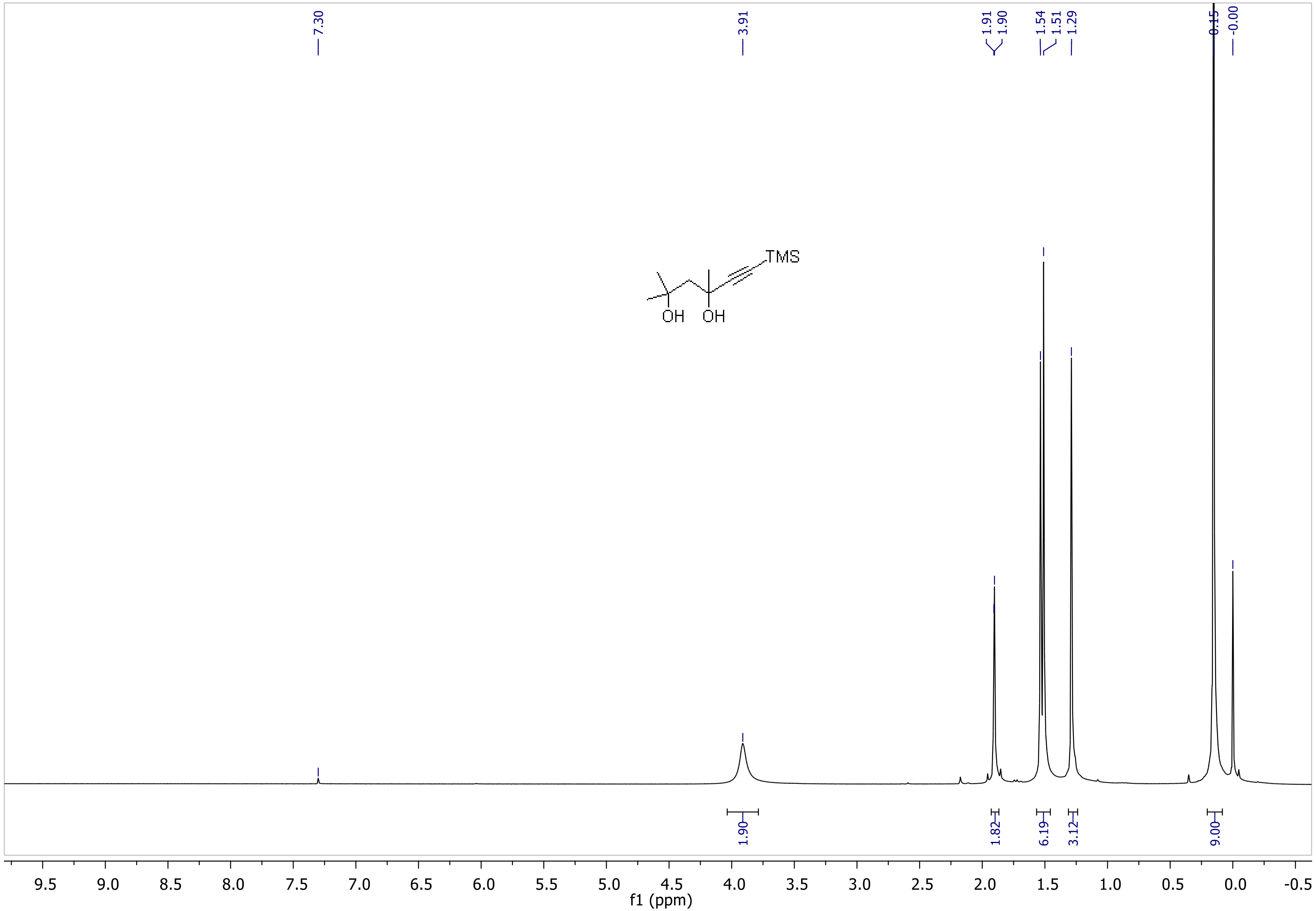

Figure S18. ^{1}C-NMR ($CDCl_3$) of **1g**, Related to **Figure 1**

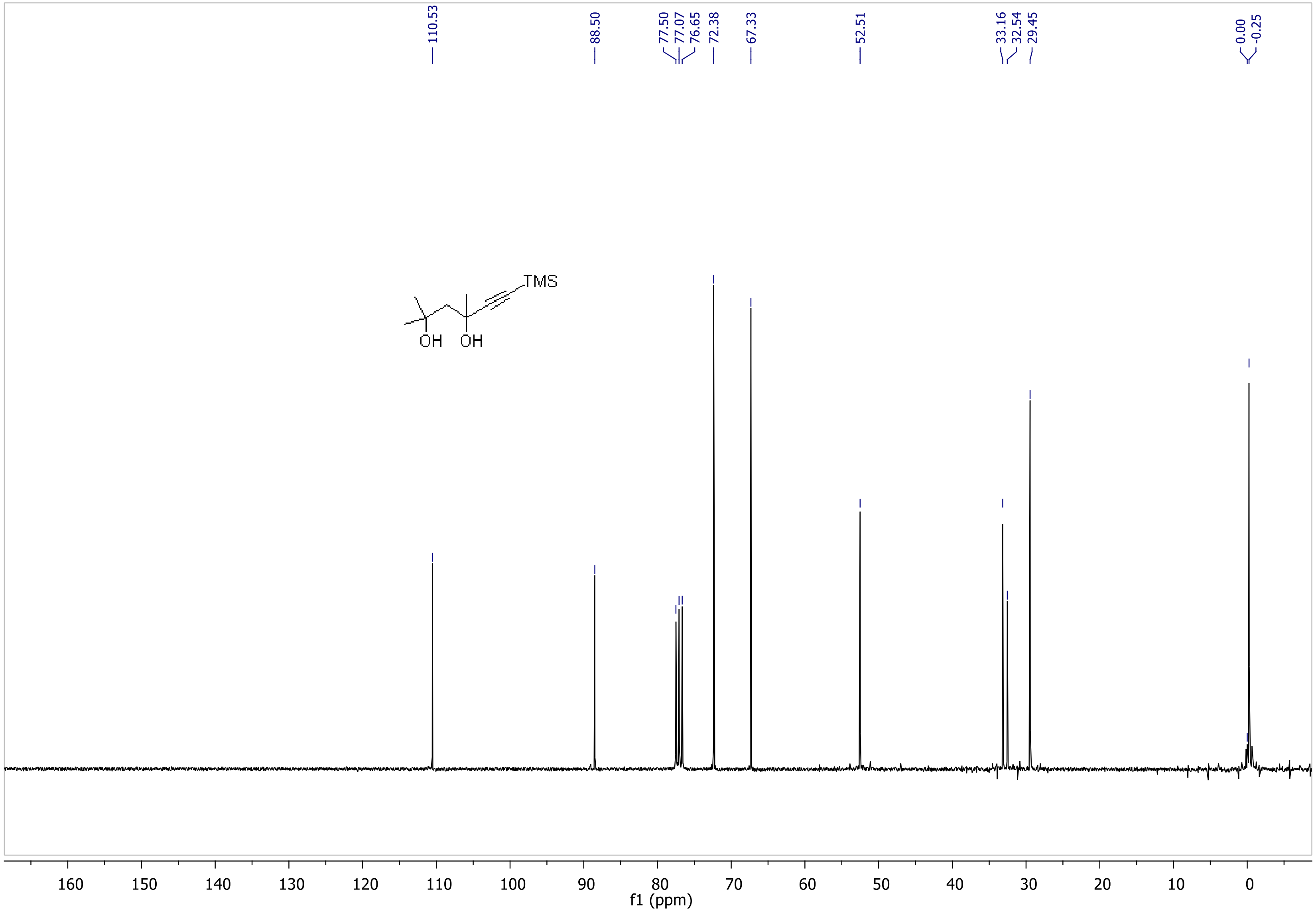

Figure S19. ^{1}H-NMR ($CDCl_3$) of **1h**, Related to **Figure 1** and **Scheme 3**

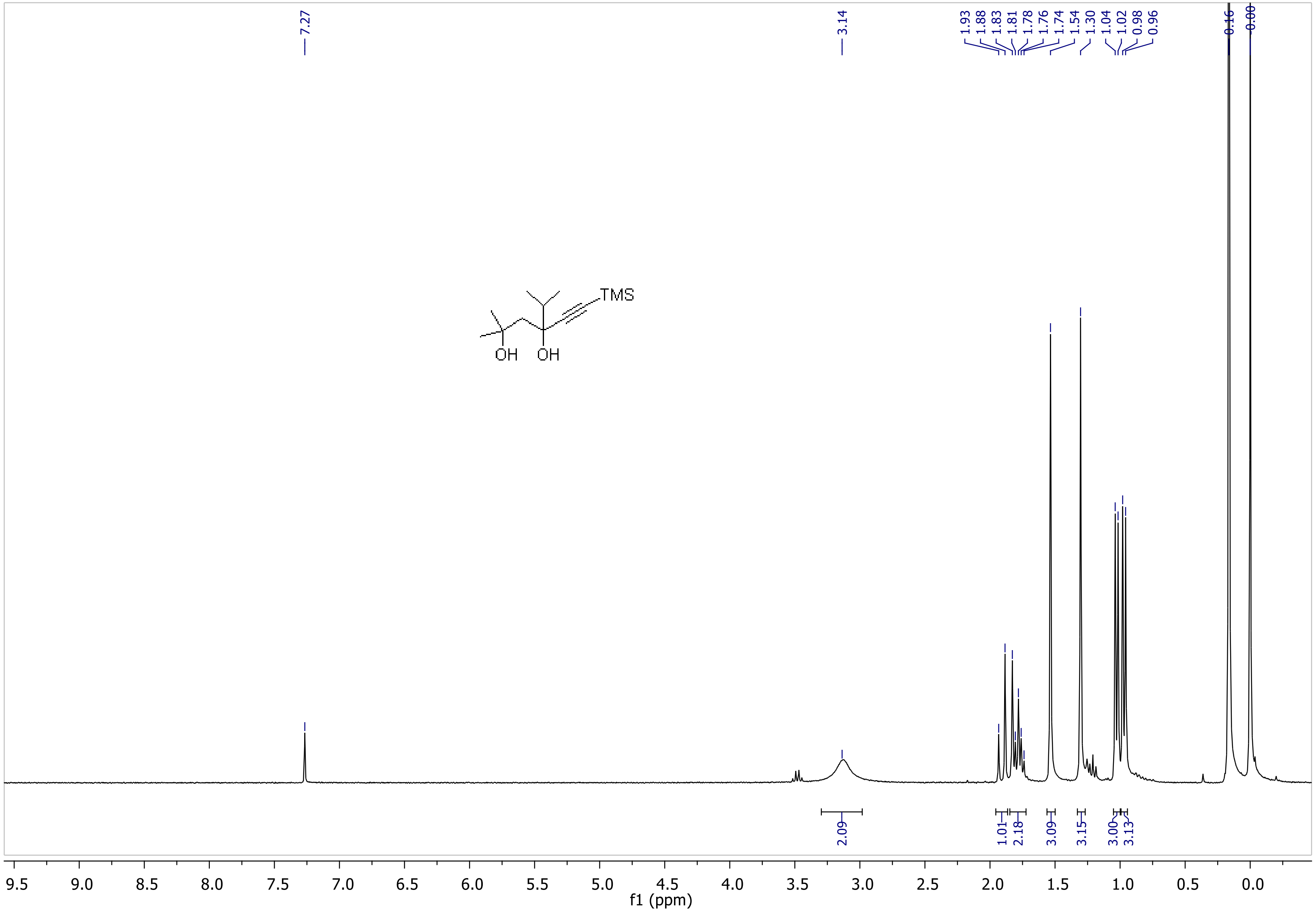

Figure S20. ^{13}C-NMR ($CDCl_3$) of **1h**, Related to **Figure 1** and **Scheme 3**

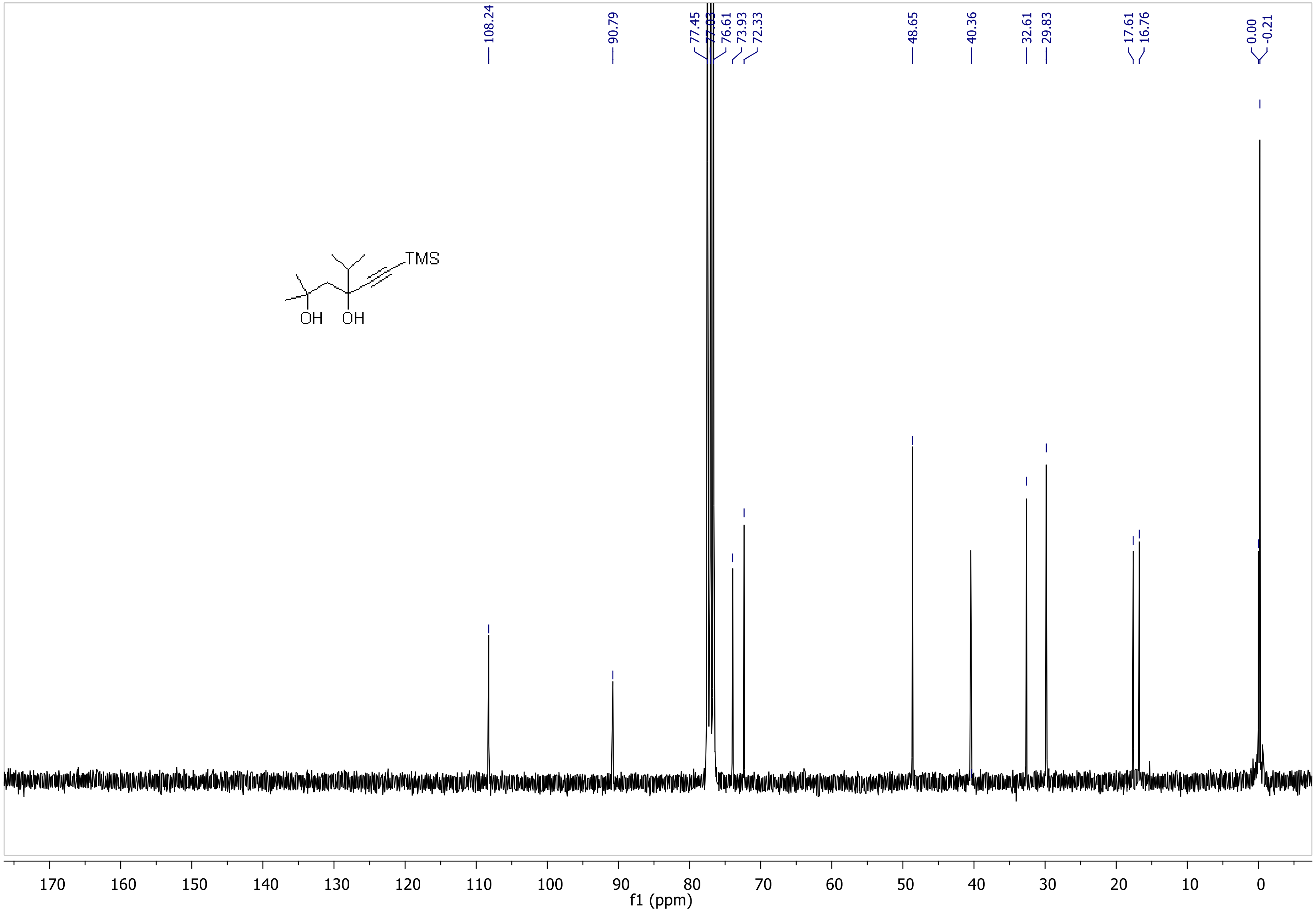

Figure S21. ^{1}H-NMR ($CDCl_3$) of (2*RS*,4*SR*)-**1i**, Related to **Figure 1** and **Table 1**

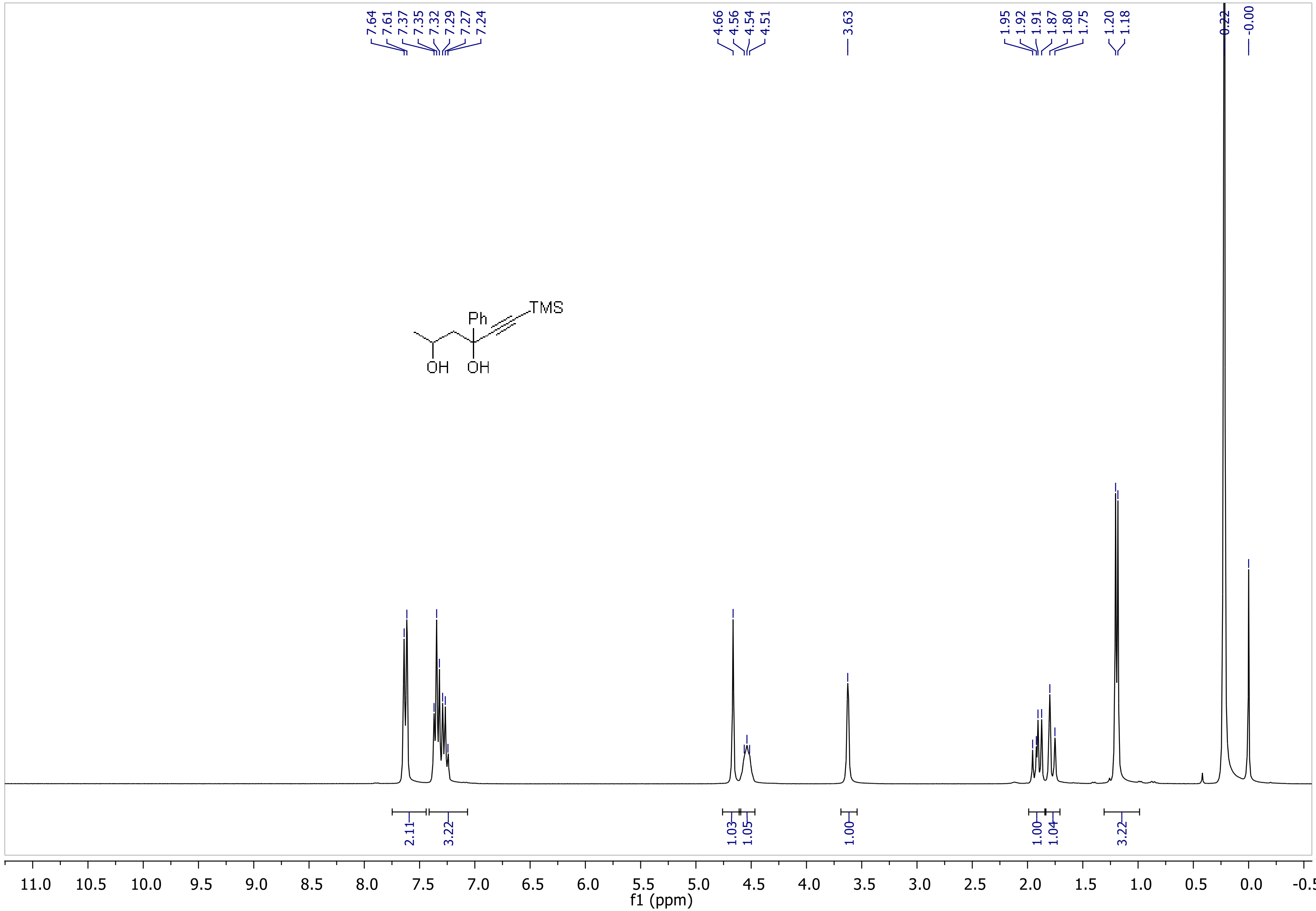

Figure S22. ^{13}C-NMR ($CDCl_3$) of (2*RS*,4*SR*)-**1i**, Related to **Figure 1** and **Table 1**

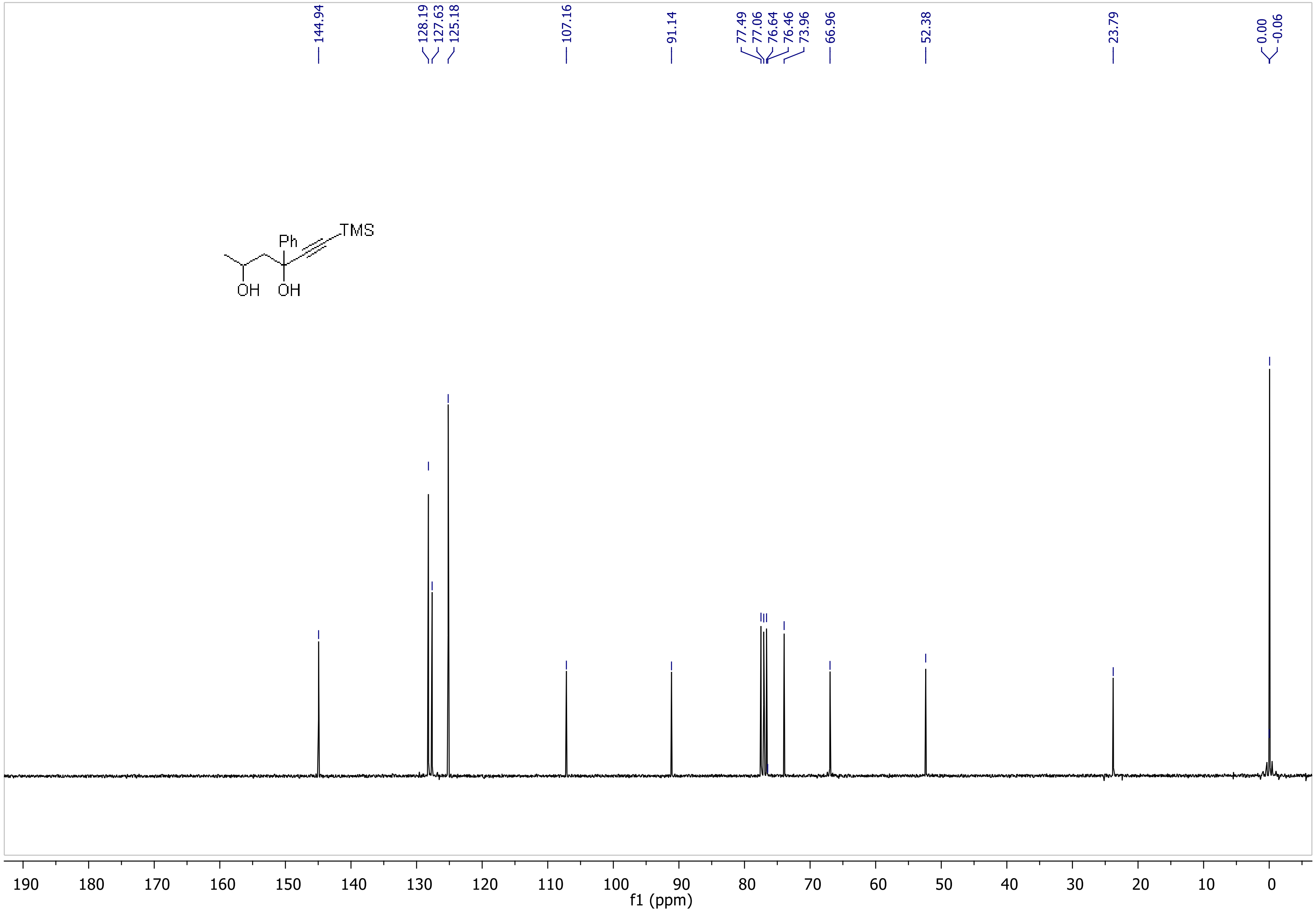

Figure S23. ^{1}H-NMR ($CDCl_3$) of (2*RS*,4*RS*)-**1i**, Related to **Figure 1** and **Table 1**

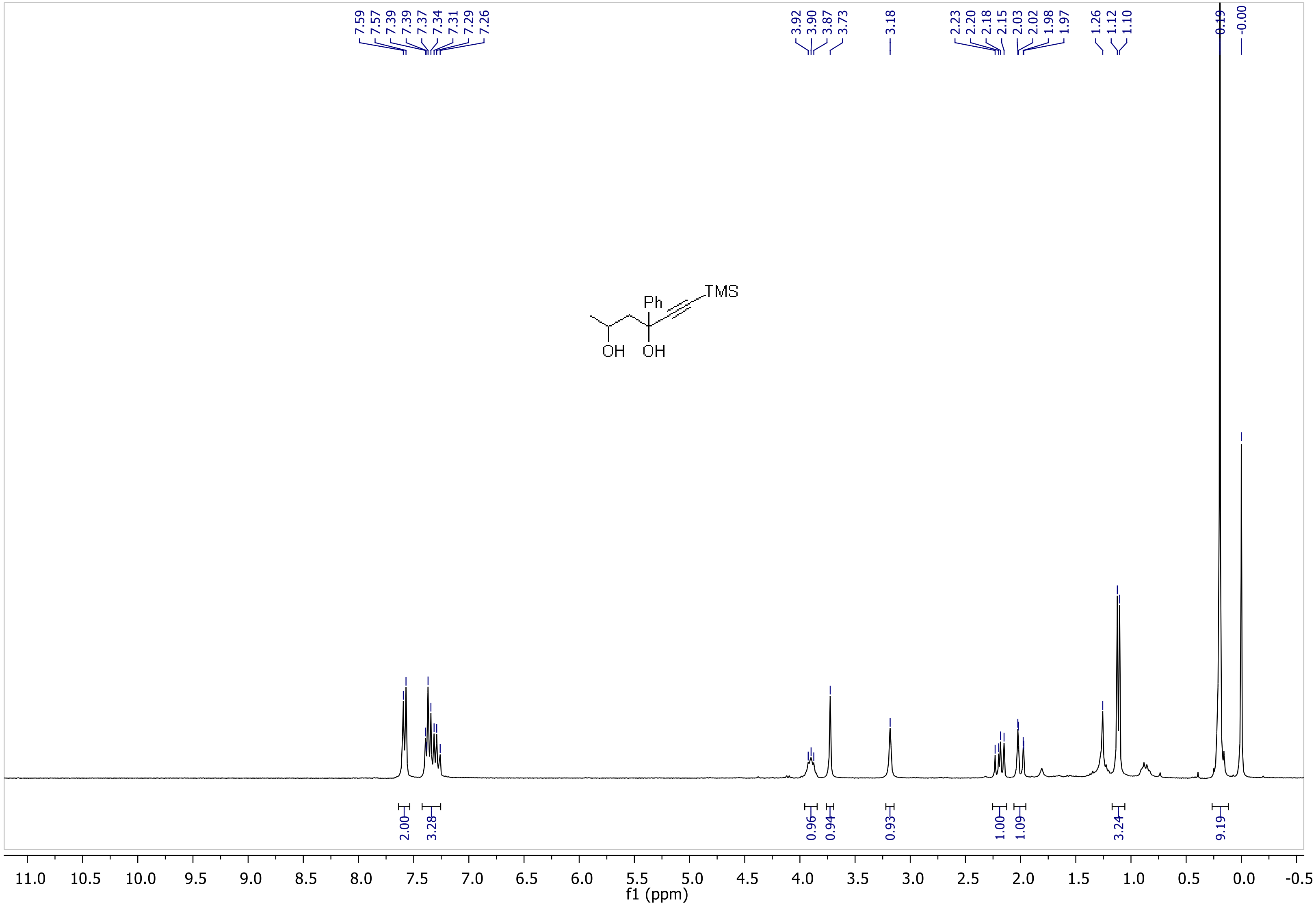

Figure S24. ^{13}C-NMR ($CDCl_3$) of (2*RS*,4*RS*)-**1i**, Related to **Figure 1** and **Table 1**

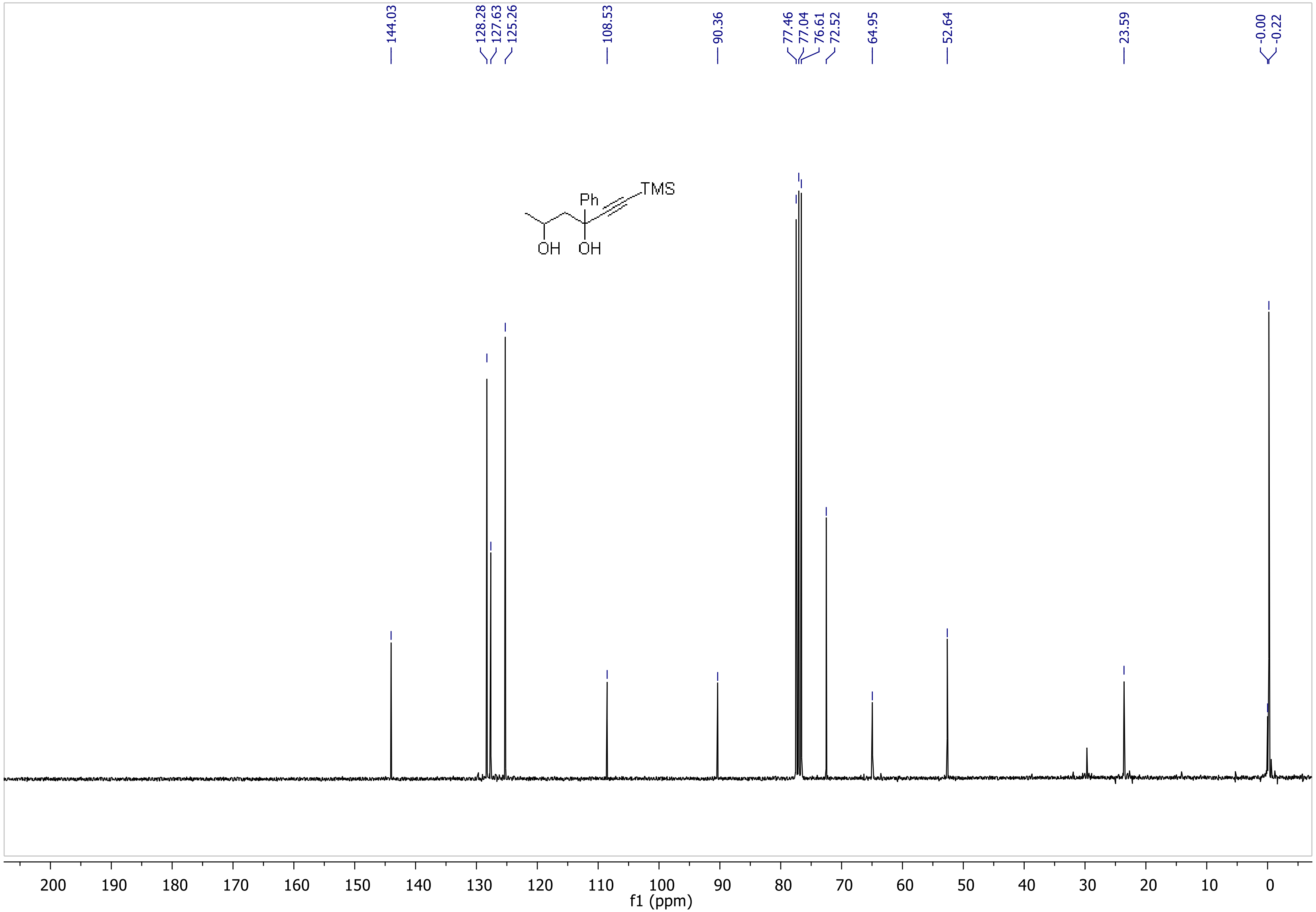

Figure S25. ^{1}H-NMR ($CDCl_3$) of (2*RS*,4*SR*)-**1j**, Related to **Figure 1** and **Table 1**

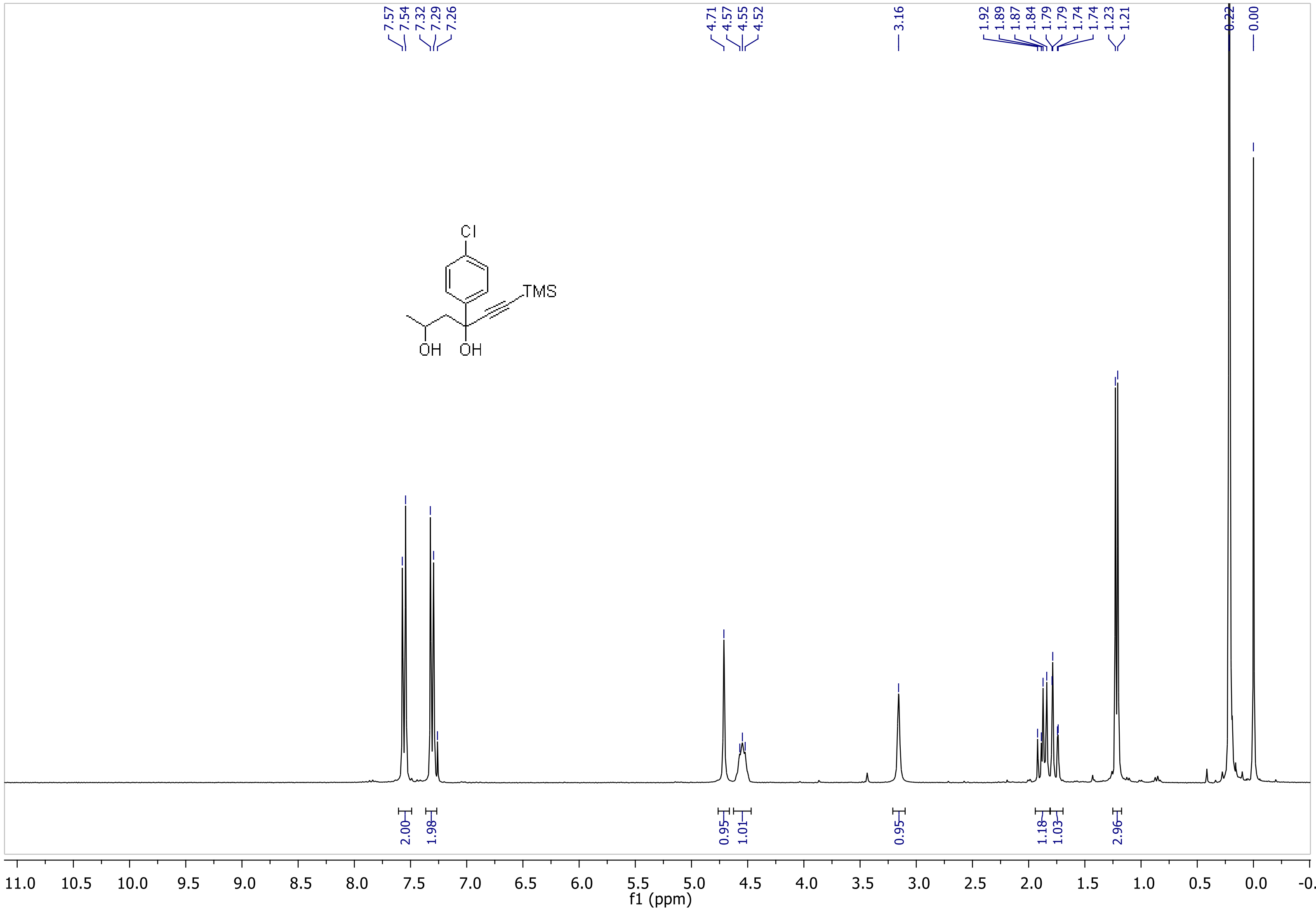

Figure S26. ^{13}C-NMR ($CDCl_3$) of (2*RS*,4*SR*)-**1j**, Related to **Figure 1** and **Table 1**

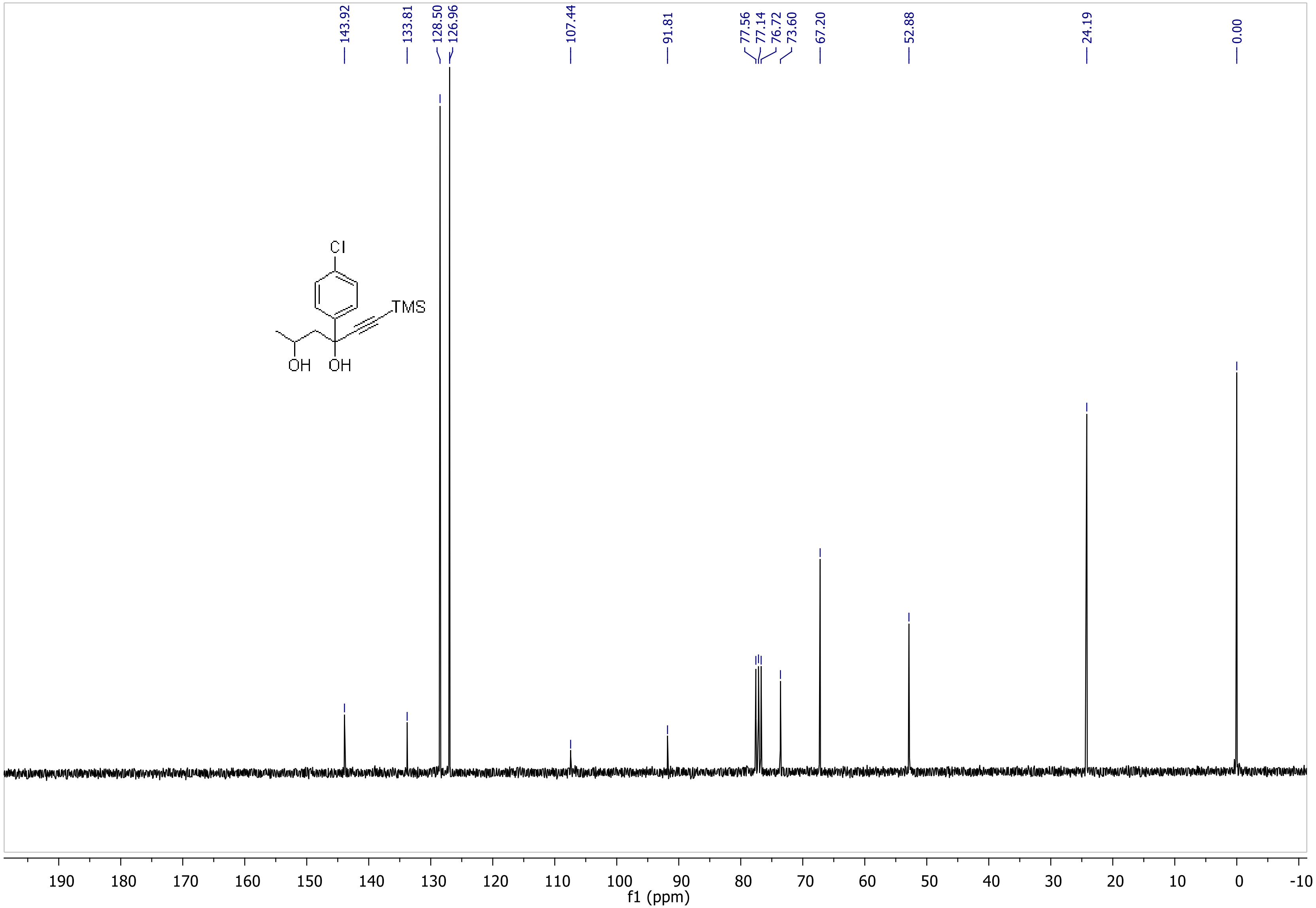

Figure S27. ^{1}H-NMR ($CDCl_3$) of (2*RS*,4*RS*)-**1j**, Related to **Figure 1** and **Table 1**

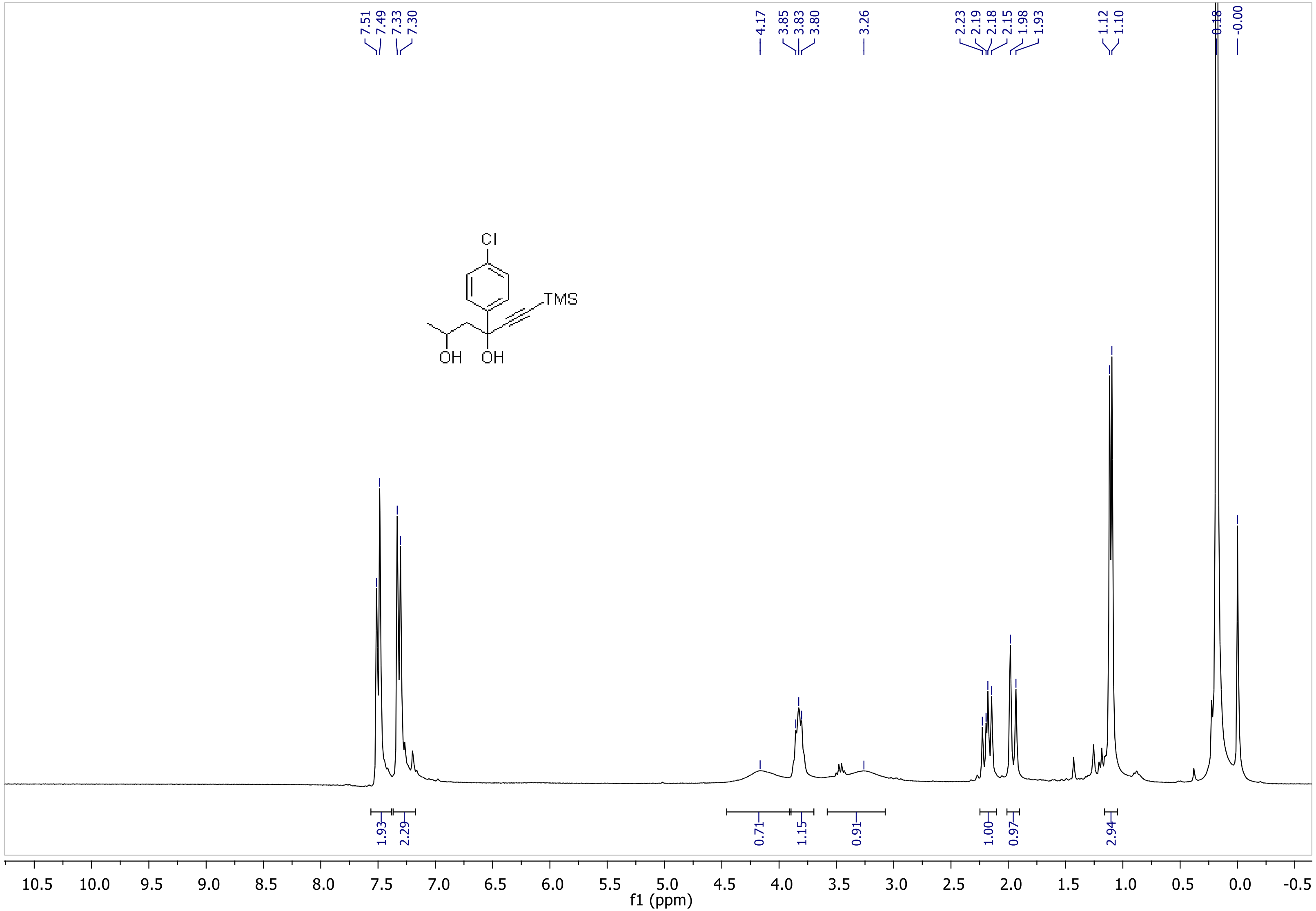

Figure S28. ^{13}C-NMR ($CDCl_3$) of (2*RS*,4*RS*)-**1j**, Related to **Figure 1** and **Table 1**

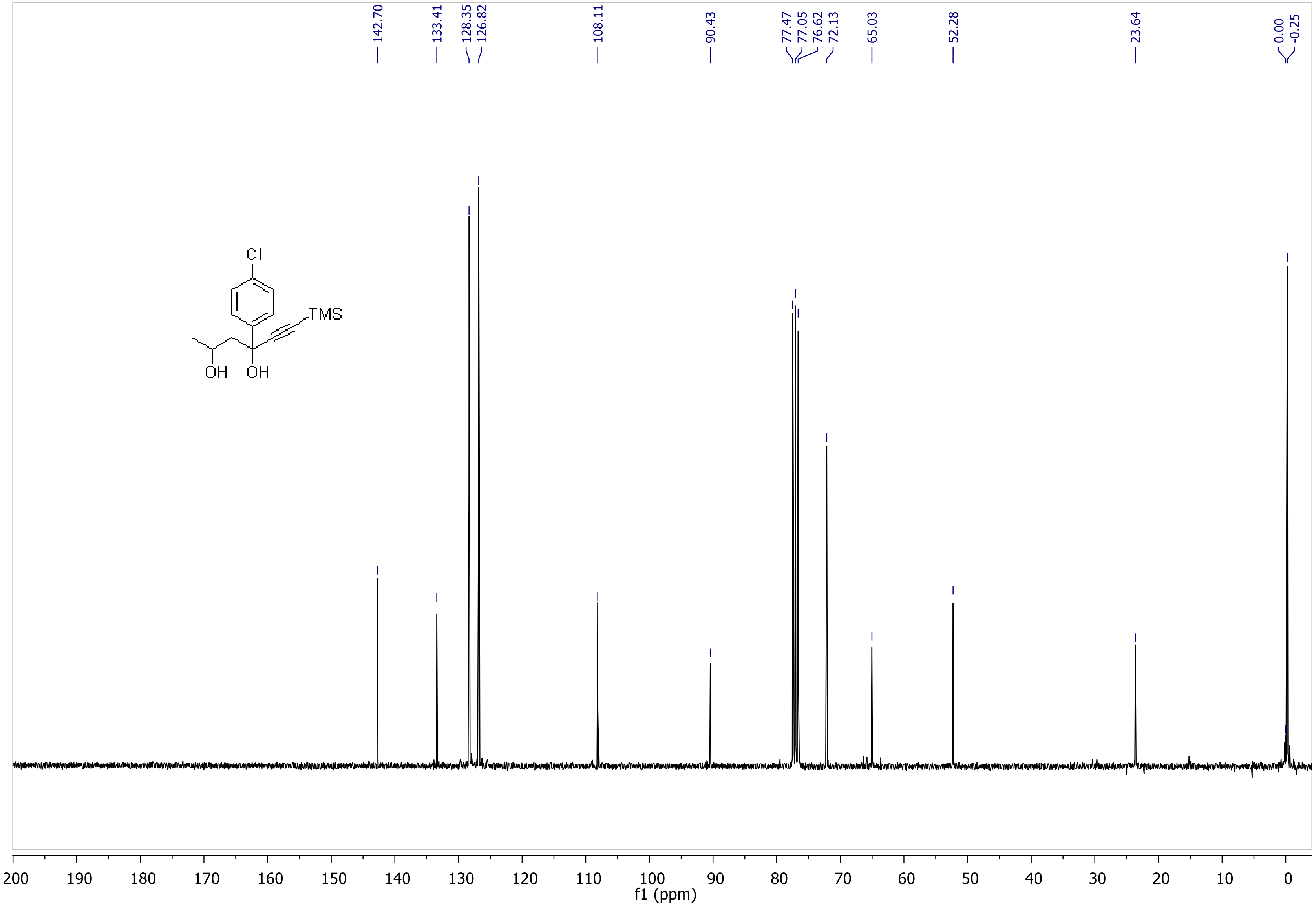

Figure S29. ^{1}H-NMR ($CDCl_3$) of (2*RS*,4*SR*)-**1k**, Related to **Figure 1** and **Table 1**

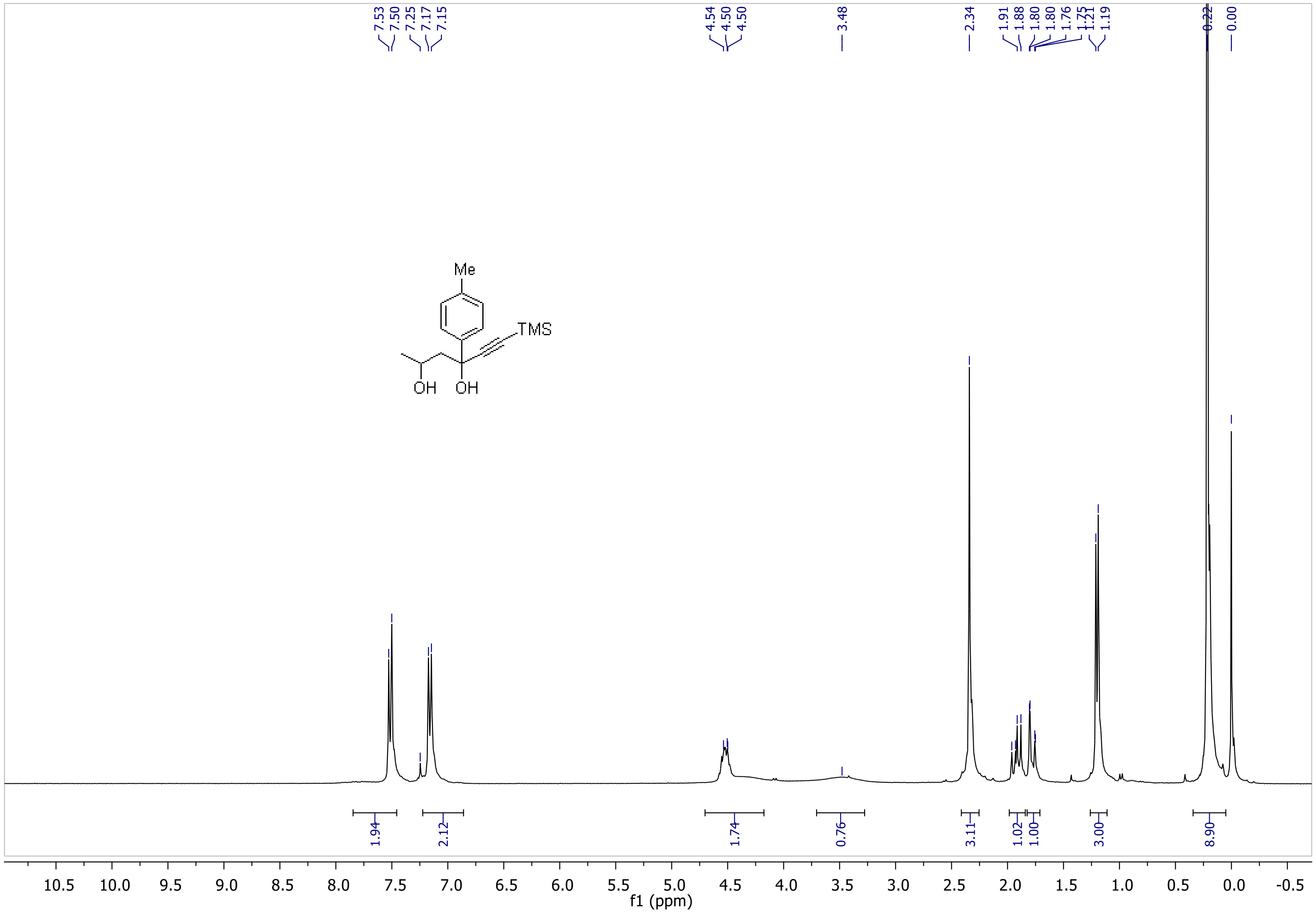

Figure S30. ^{13}C-NMR ($CDCl_3$) of (2*RS*,4*SR*)-**1k**, Related to **Figure 1** and **Table 1**

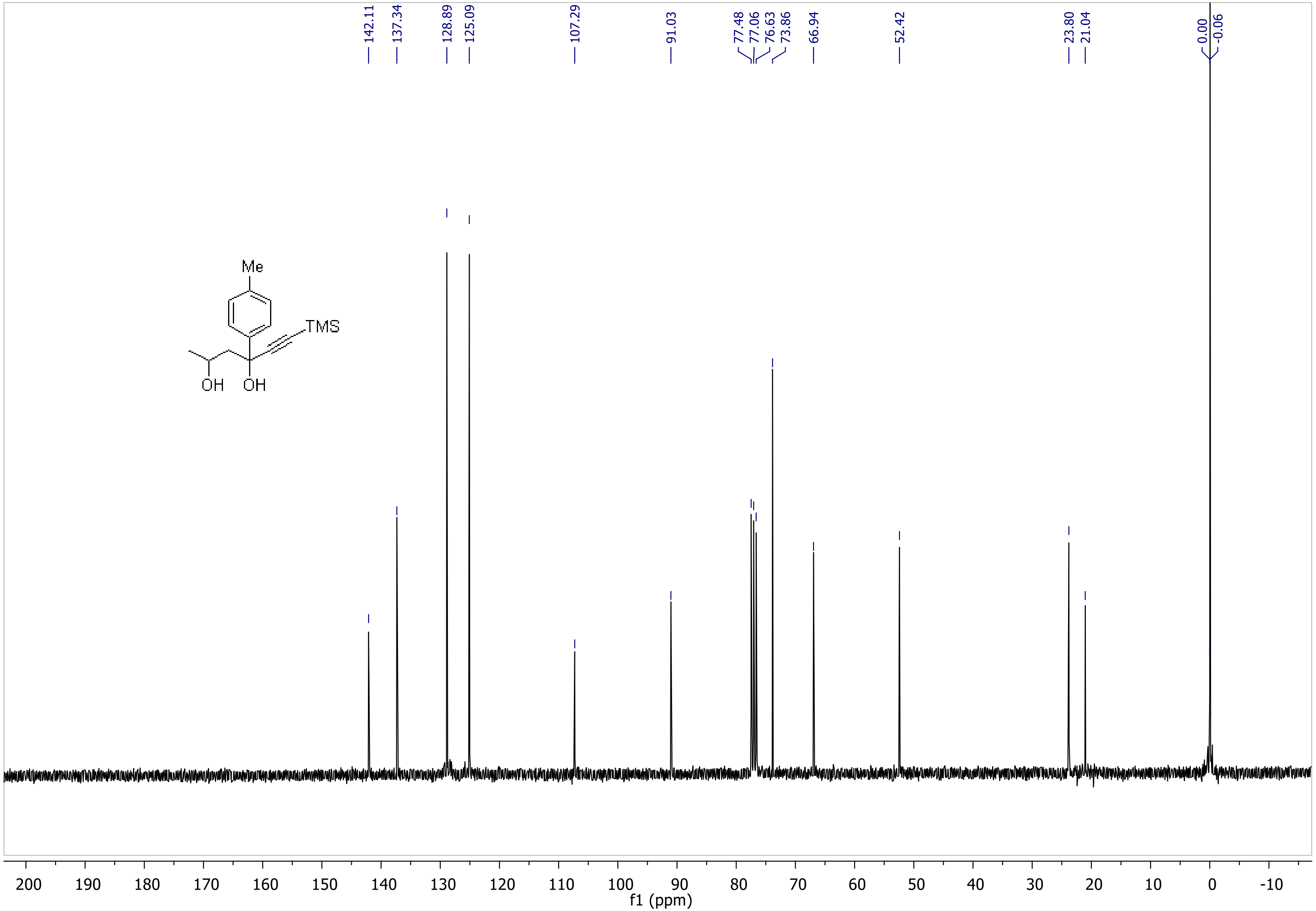

Figure S31. ^{1}H-NMR ($CDCl_3$) of (2*RS*,4*RS*)-**1k**, Related to **Figure 1** and **Table 1**

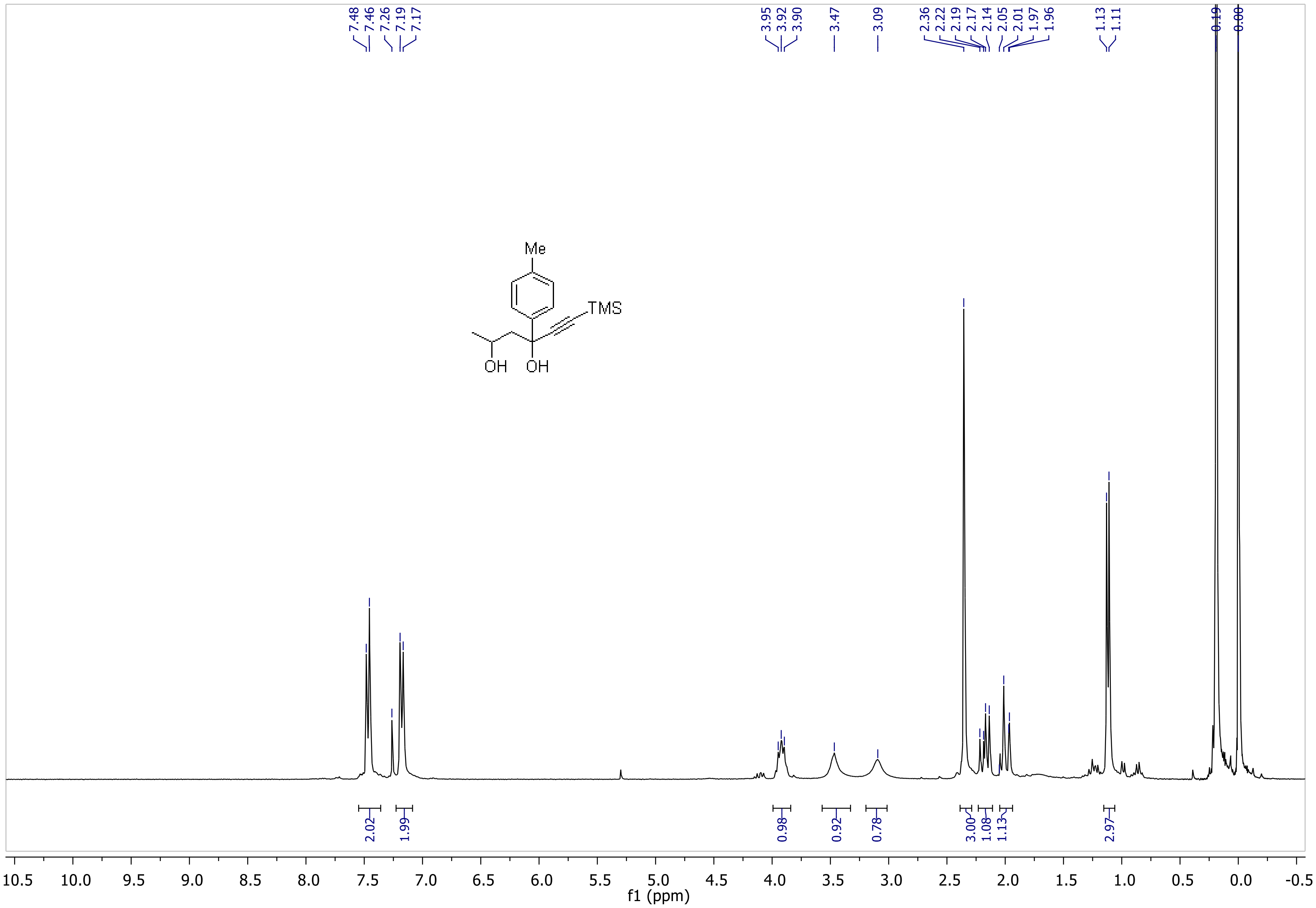

Figure S32. ^{13}C-NMR ($CDCl_3$) of (2*RS*,4*RS*)-**1k**, Related to **Figure 1** and **Table 1**

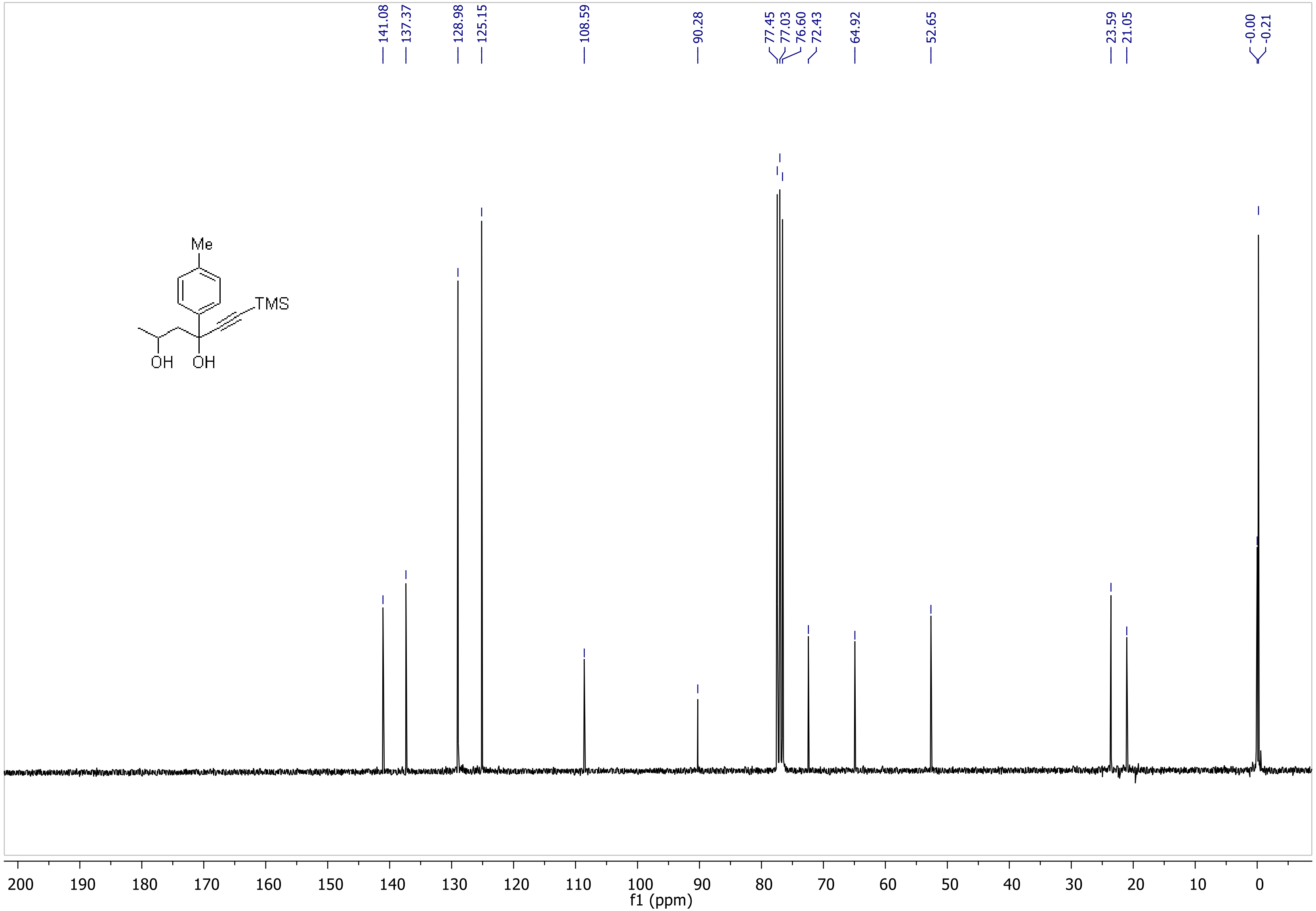

Figure S33. ^{1}H-NMR ($CDCl_3$) of **1l**, Related to **Figure 1** and **Scheme 3**

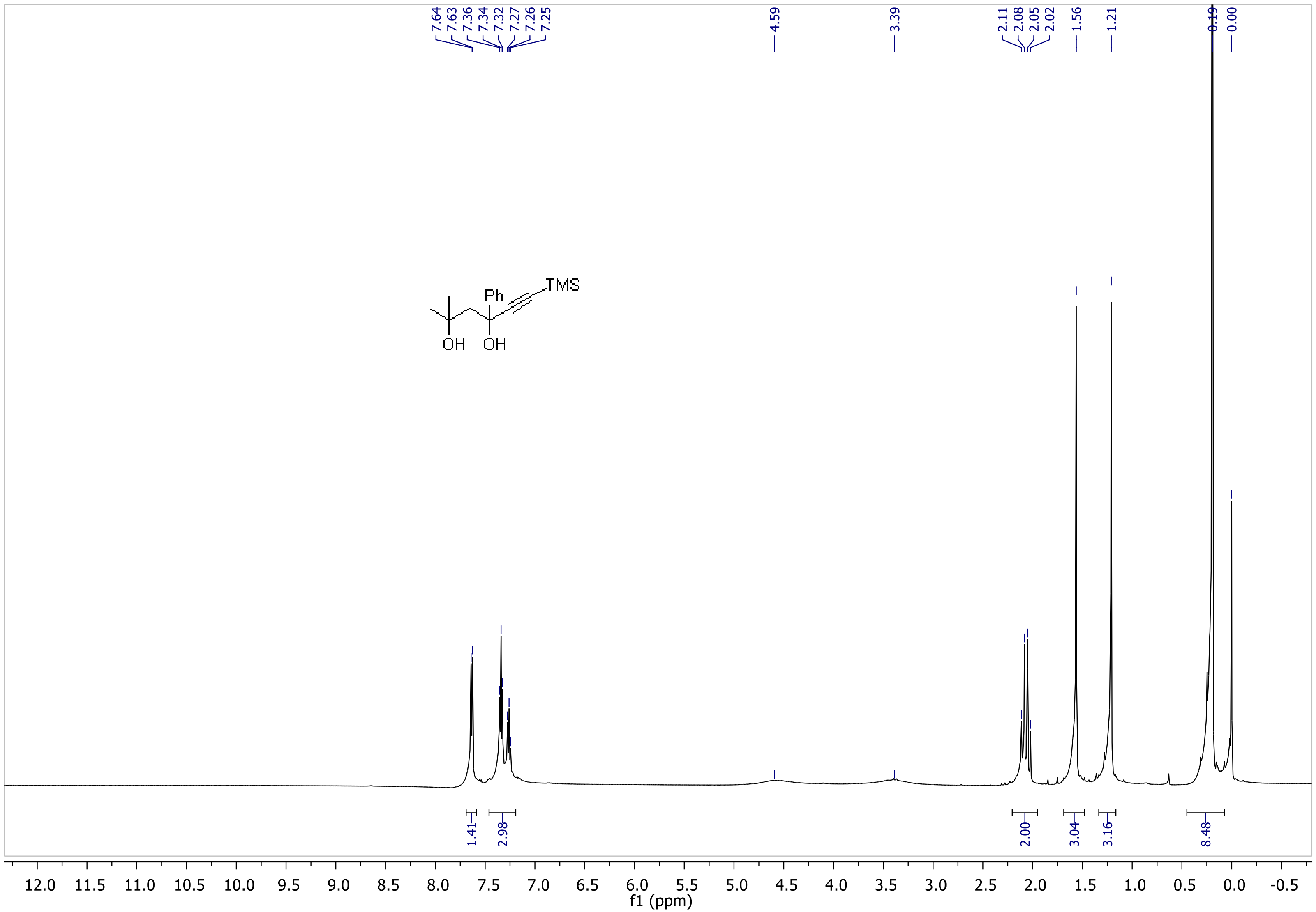

Figure S34. ^{13}C-NMR ($CDCl_3$) of **1l**, Related to **Figure 1** and **Scheme 3**

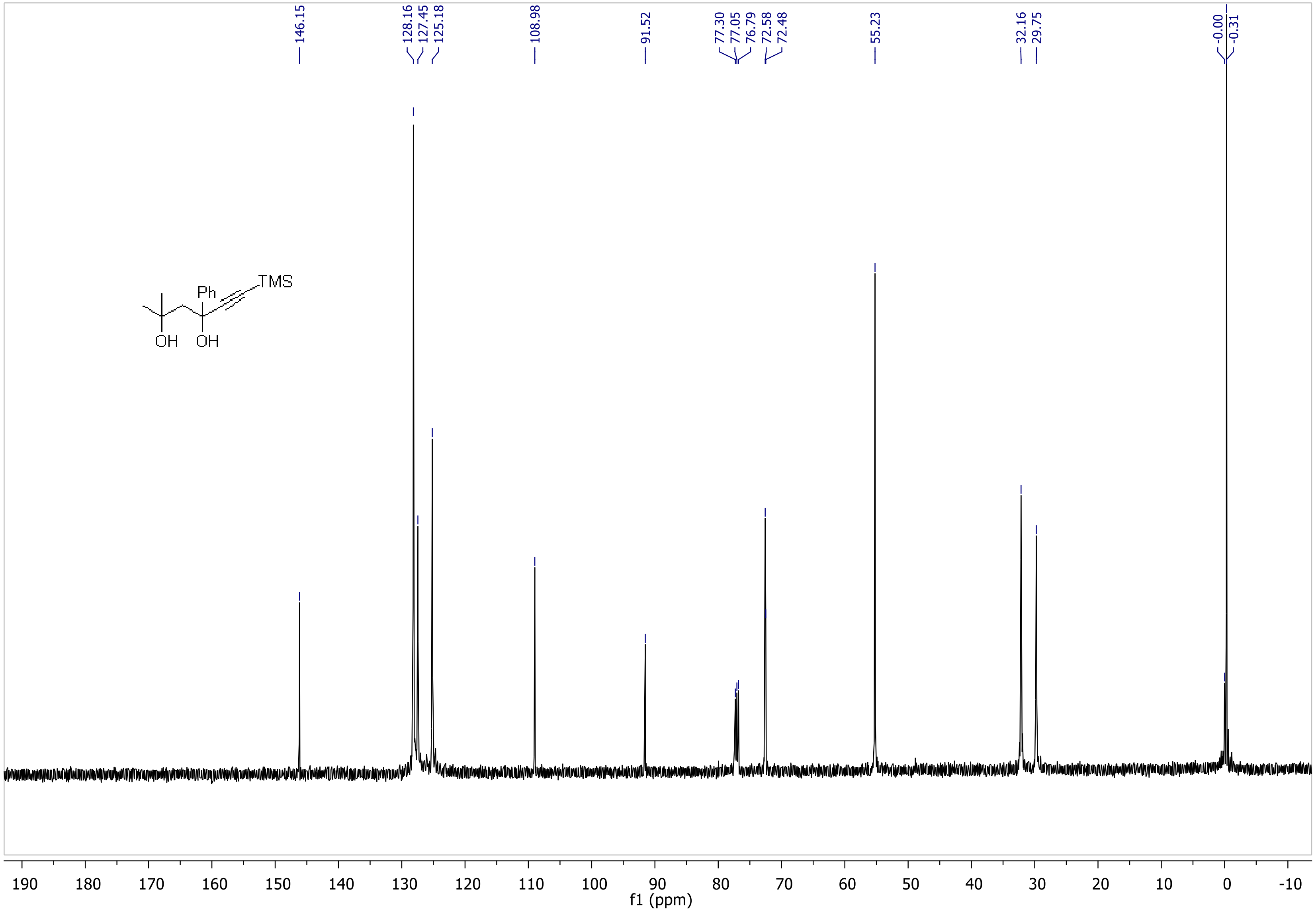

Figure S35. ^{1}H-NMR ($CDCl_3$) of **1m**, Related to **Figure 1** and **Scheme 3**

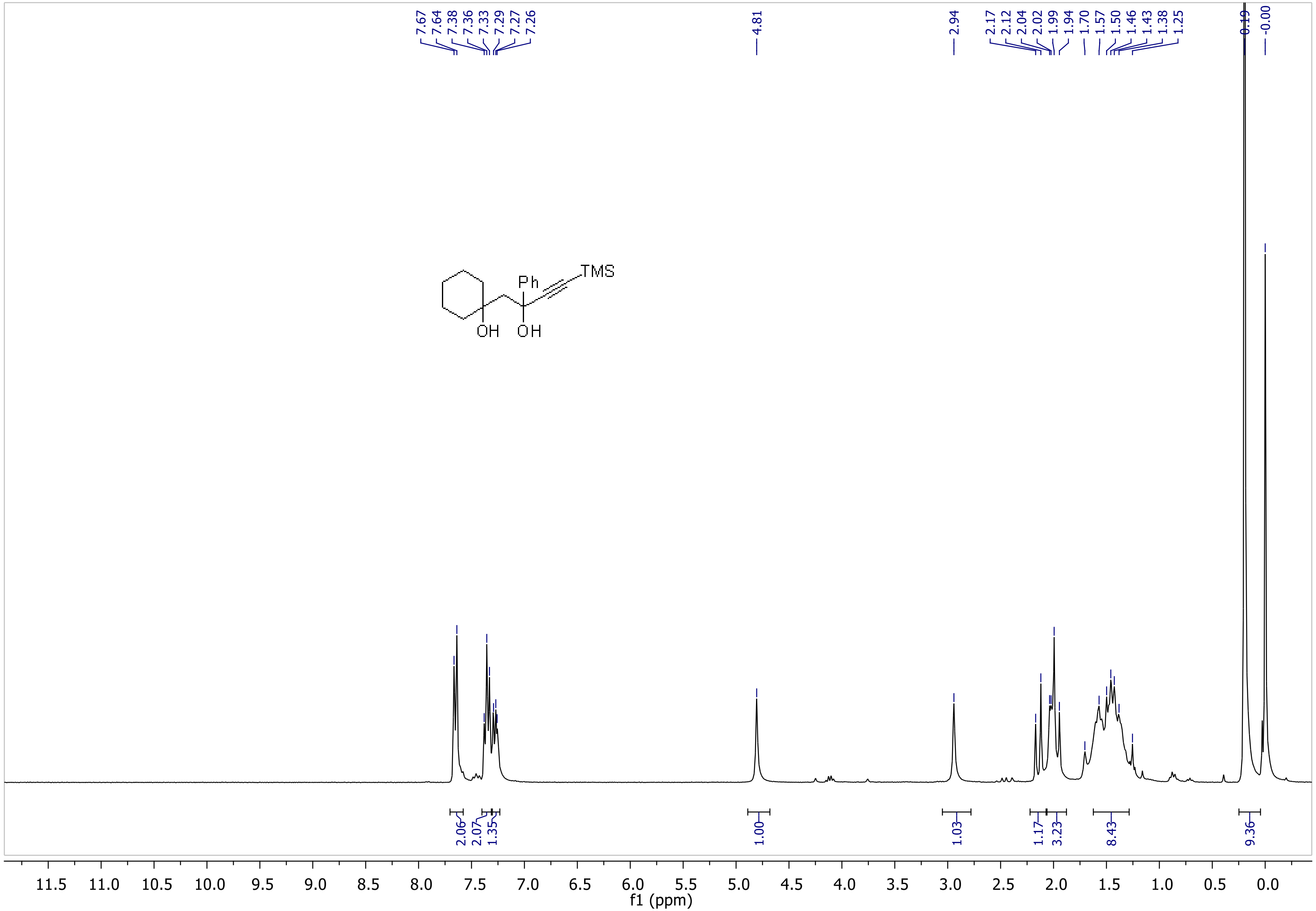

Figure S36. ^{13}C-NMR ($CDCl_3$) of **1m**, Related to **Figure 1** and **Scheme 3**

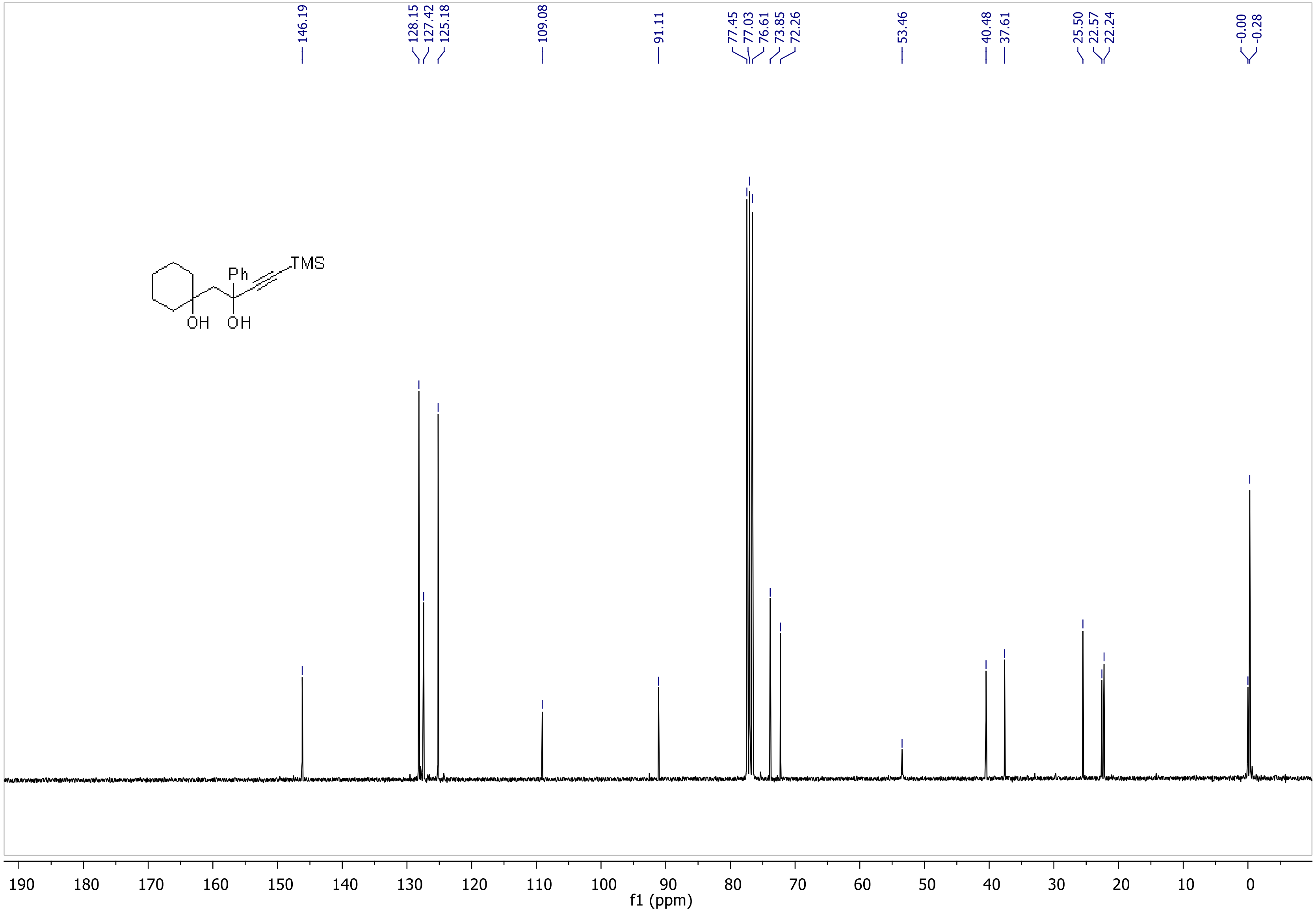

Figure S37. ^{1}H-NMR ($CDCl_3$) of **2a**, Related to **Scheme 2**

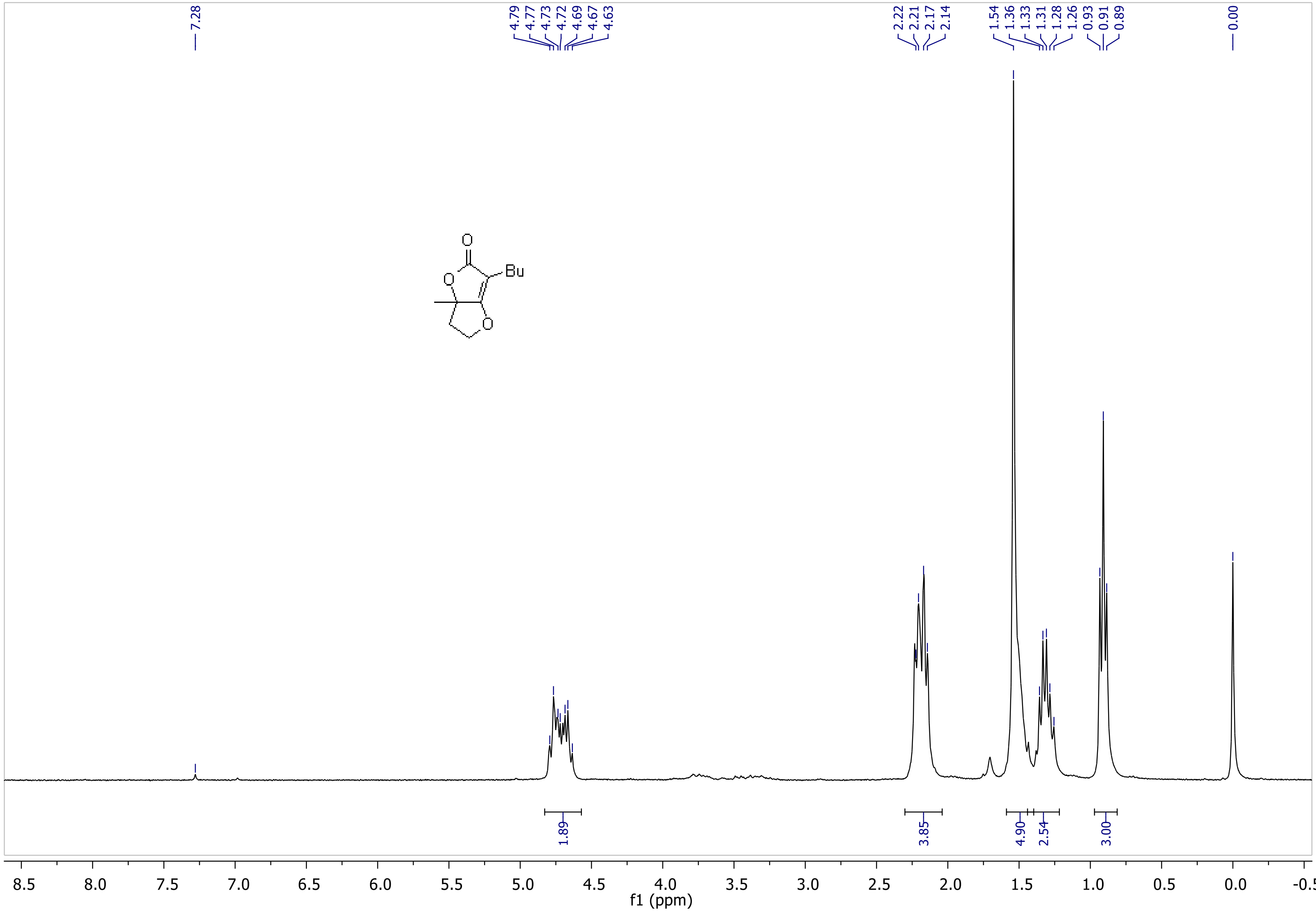

Figure S38. ^{13}C-NMR ($CDCl_3$) of **2a**, Related to **Scheme 2**

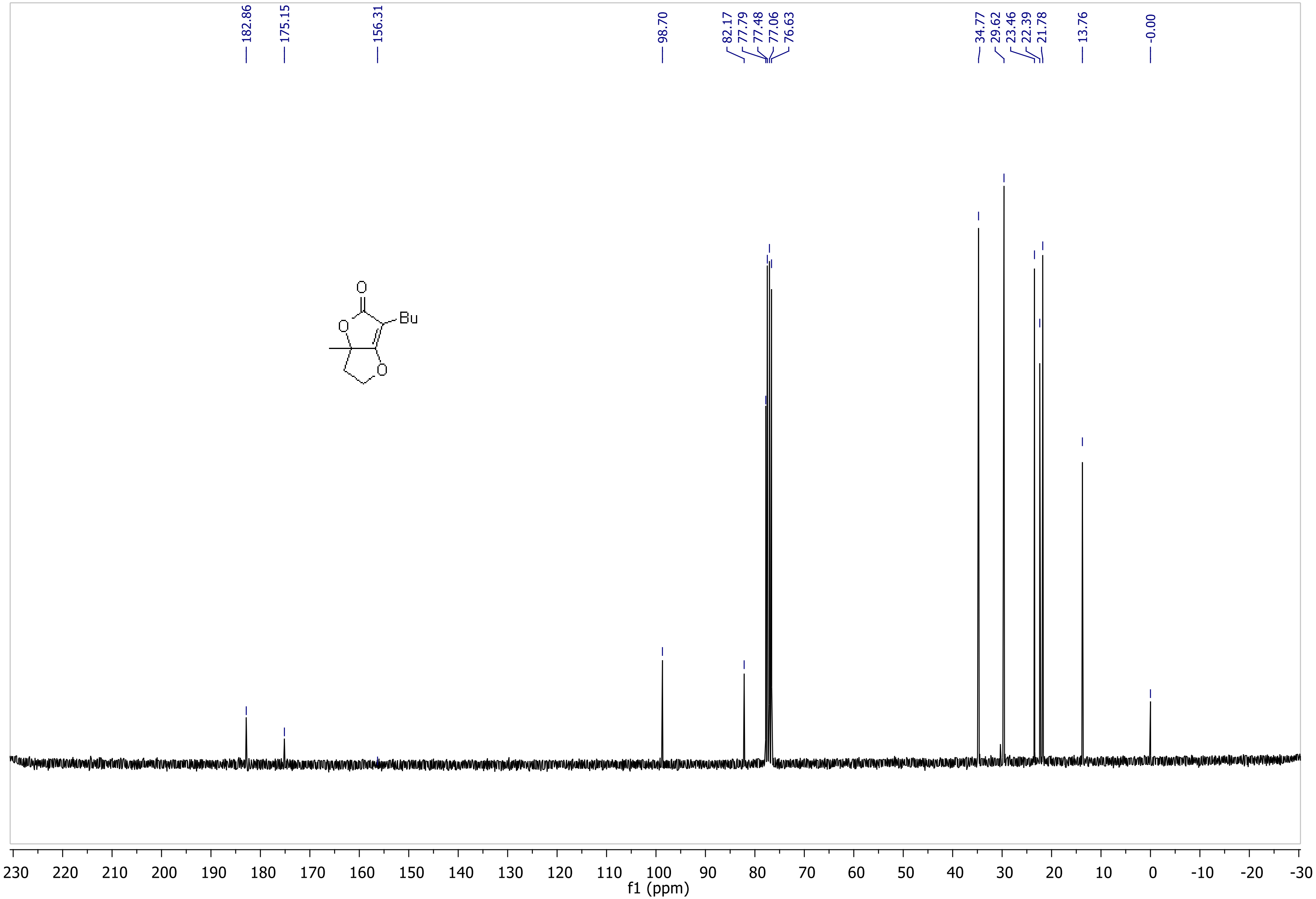

Figure S39. ^{1}H-NMR ($CDCl_3$) of **2b**, Related to **Scheme 2**

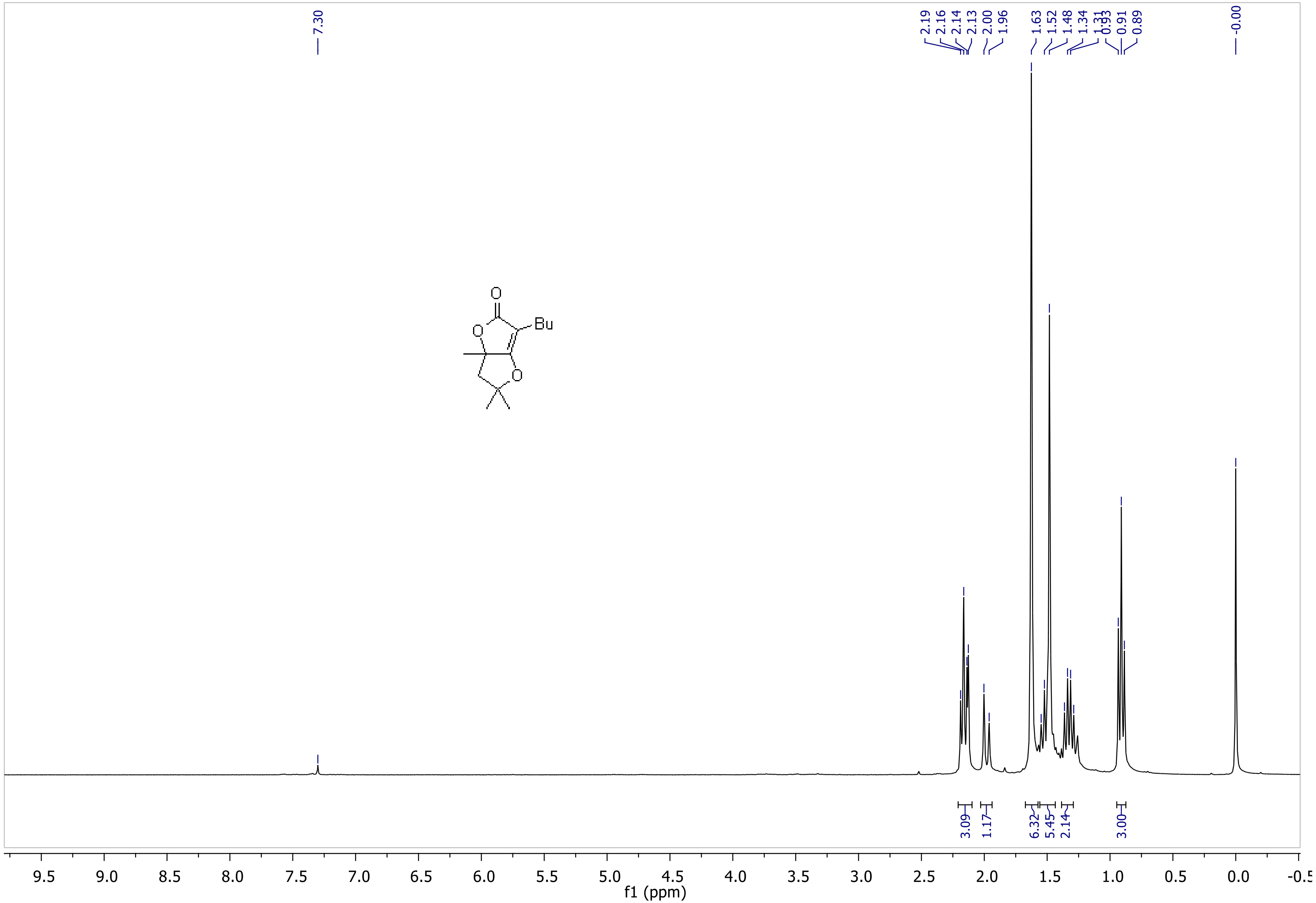

Figure S40. ^{13}C-NMR ($CDCl_3$) of **2b**, Related to **Scheme 2**

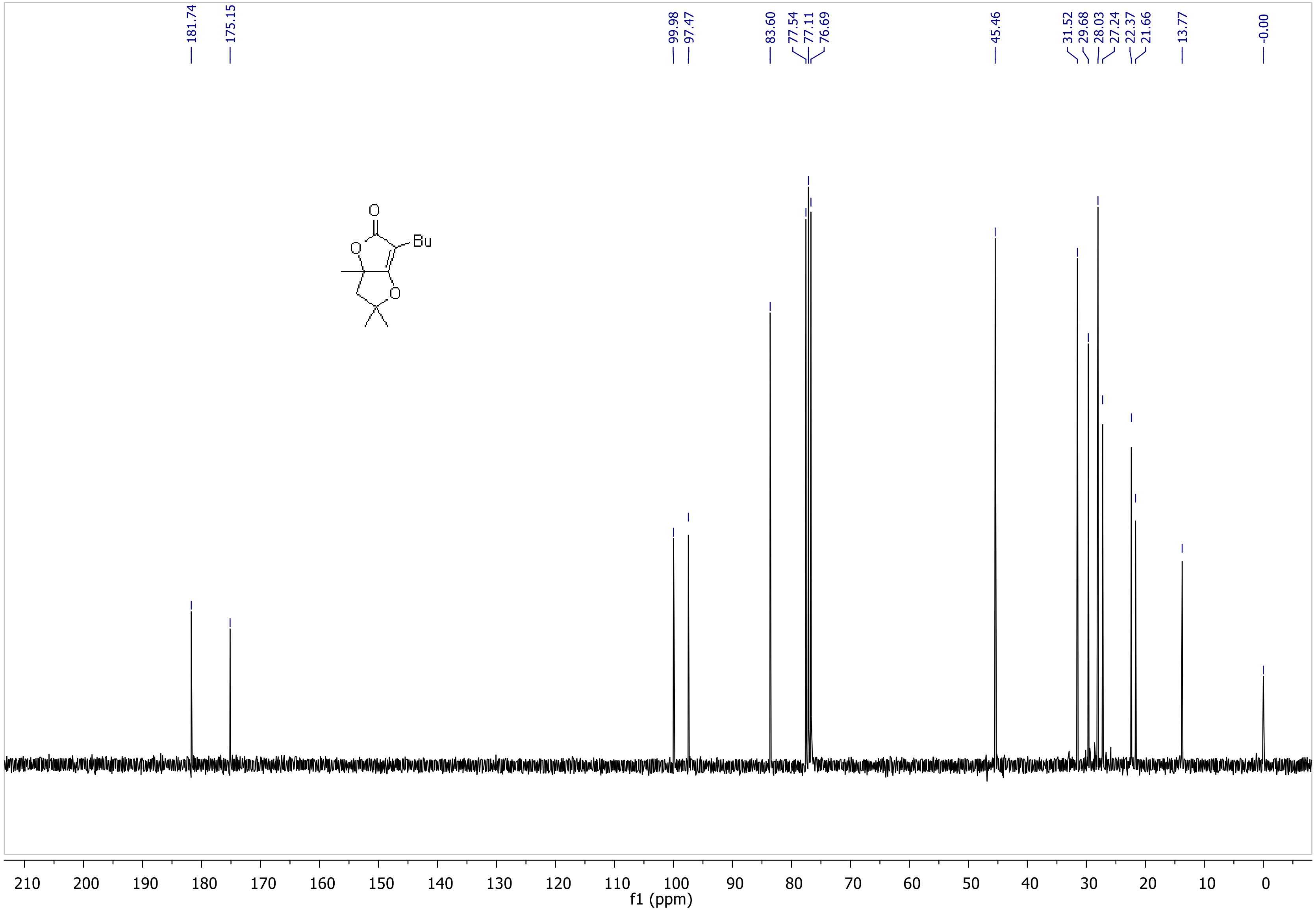

Figure S41. ^{1}H-NMR ($CDCl_3$) of **2c**, Related to **Scheme 2**

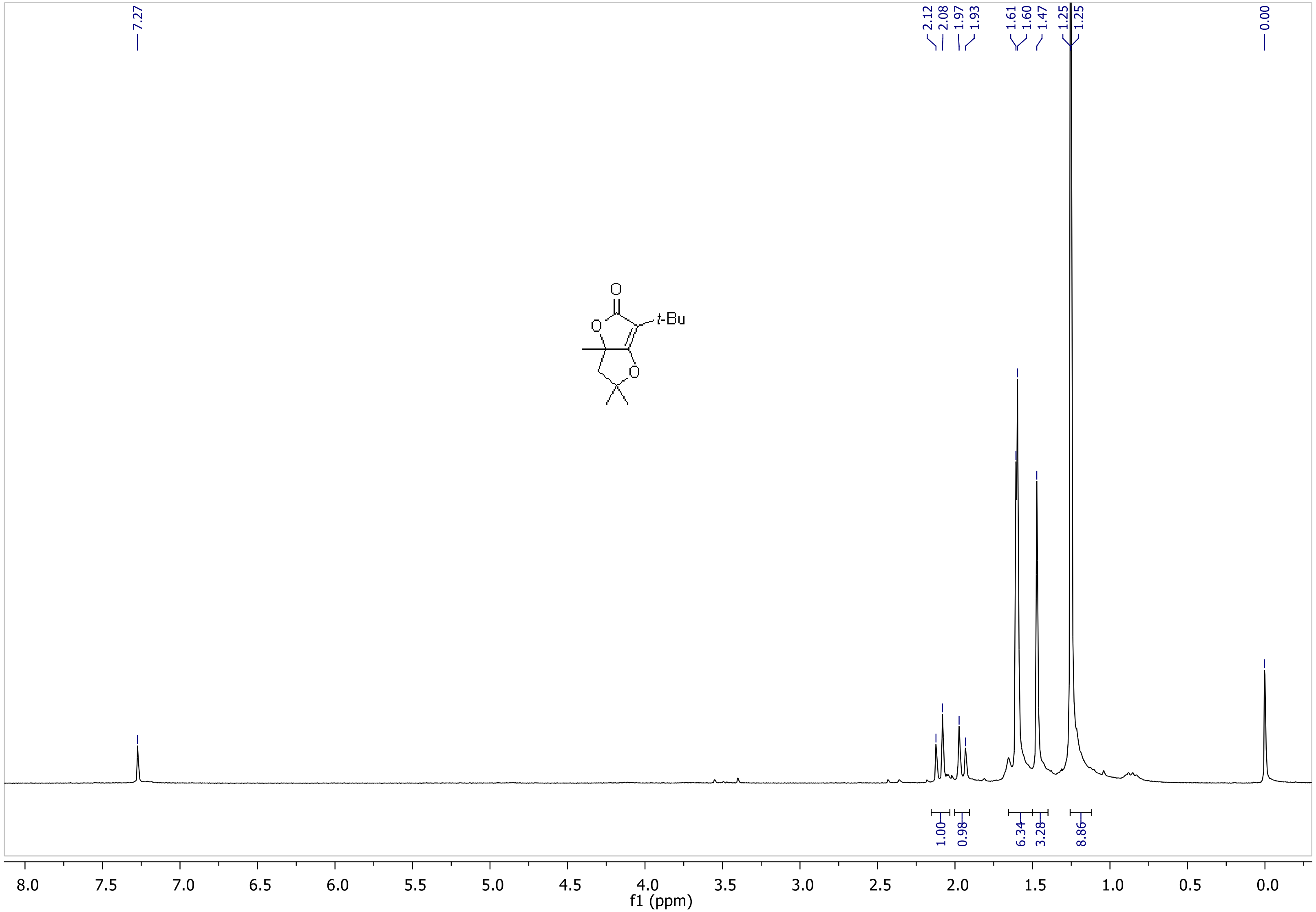

Figure S42. ^{13}C-NMR ($CDCl_3$) of **2c**, Related to **Scheme 2**

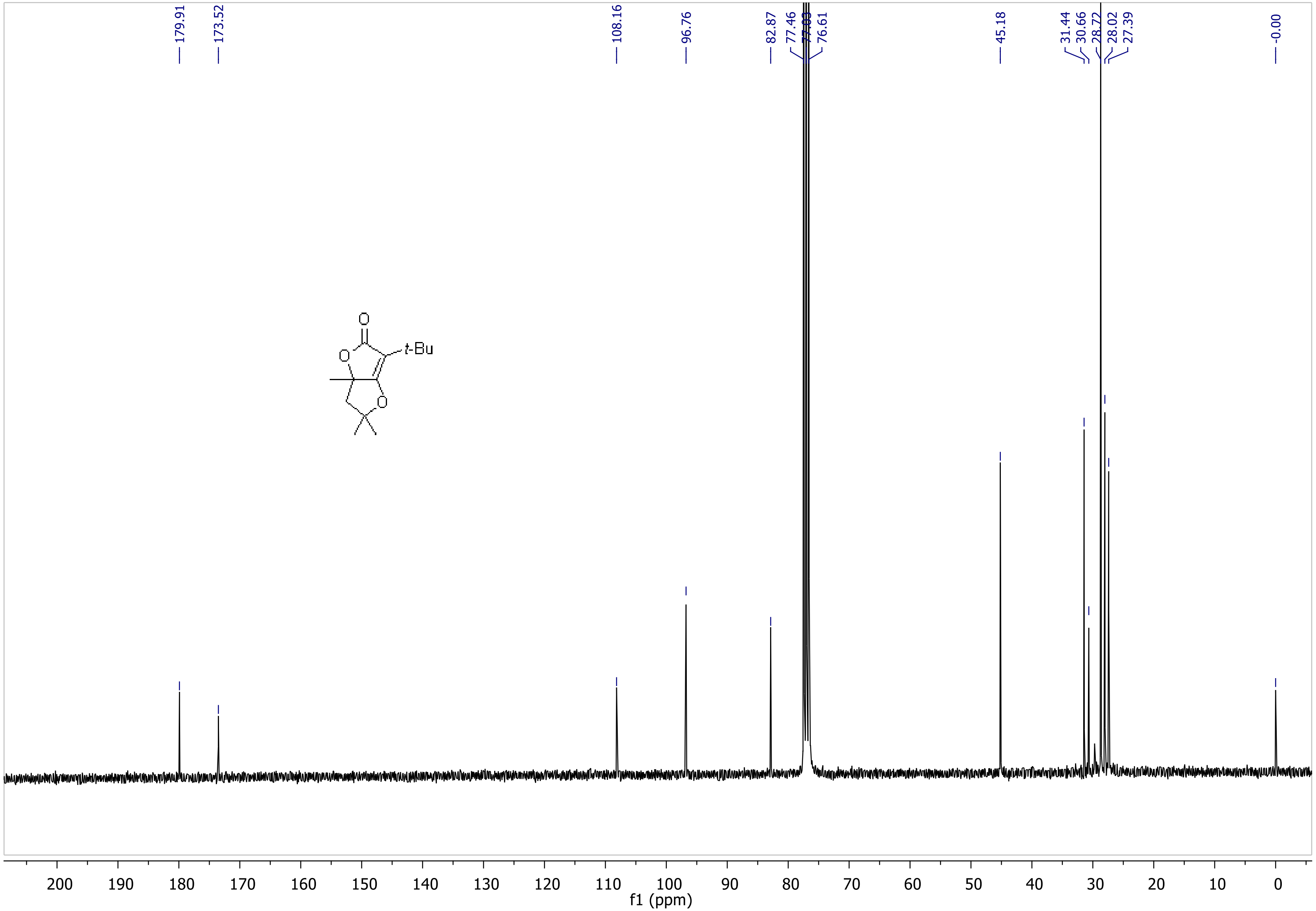

Figure S43. ^{1}H-NMR ($CDCl_3$) of **2d**, Related to **Scheme 2**

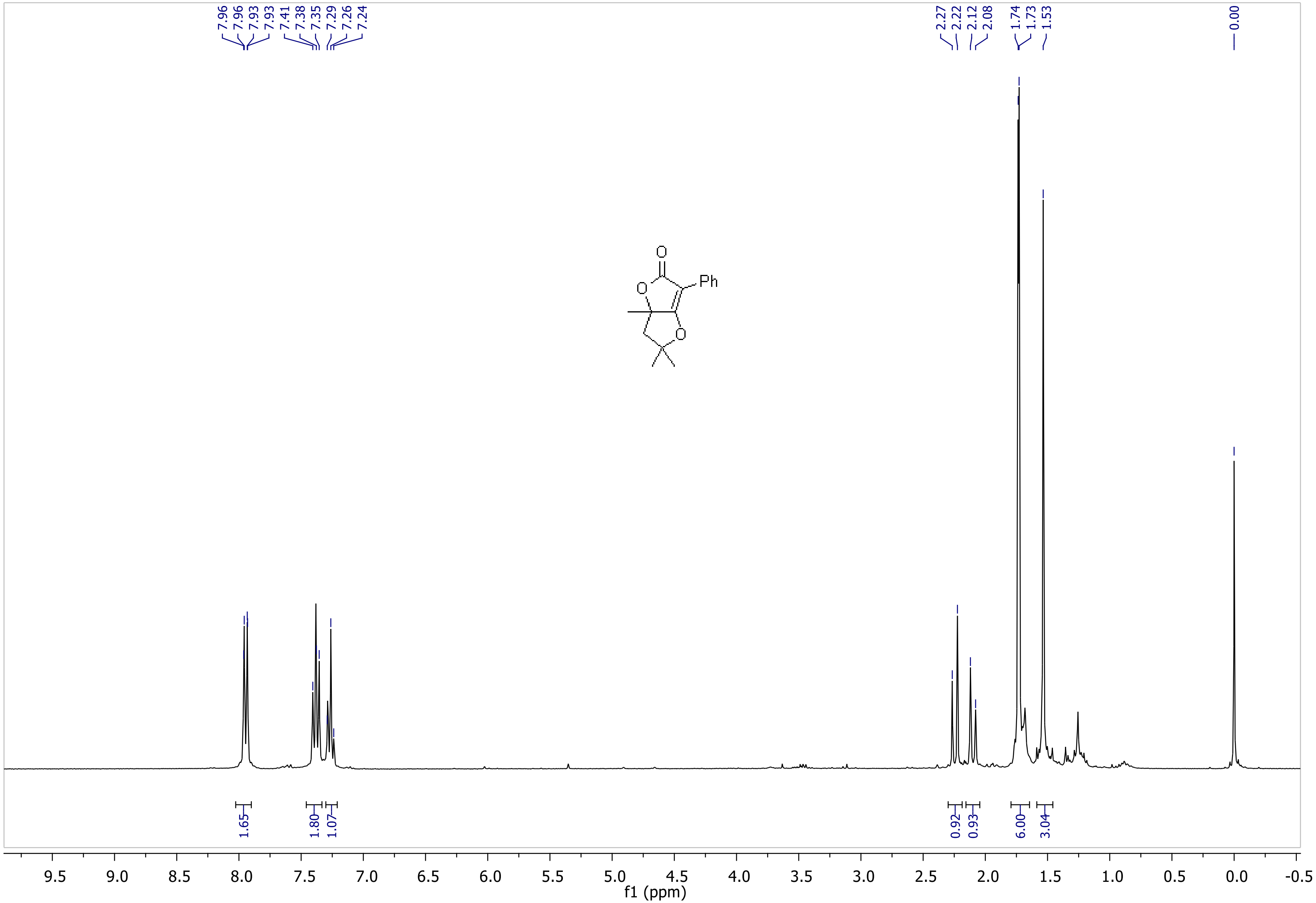

Figure S44. ^{13}C-NMR ($CDCl_3$) of **2d**, Related to **Scheme 2**

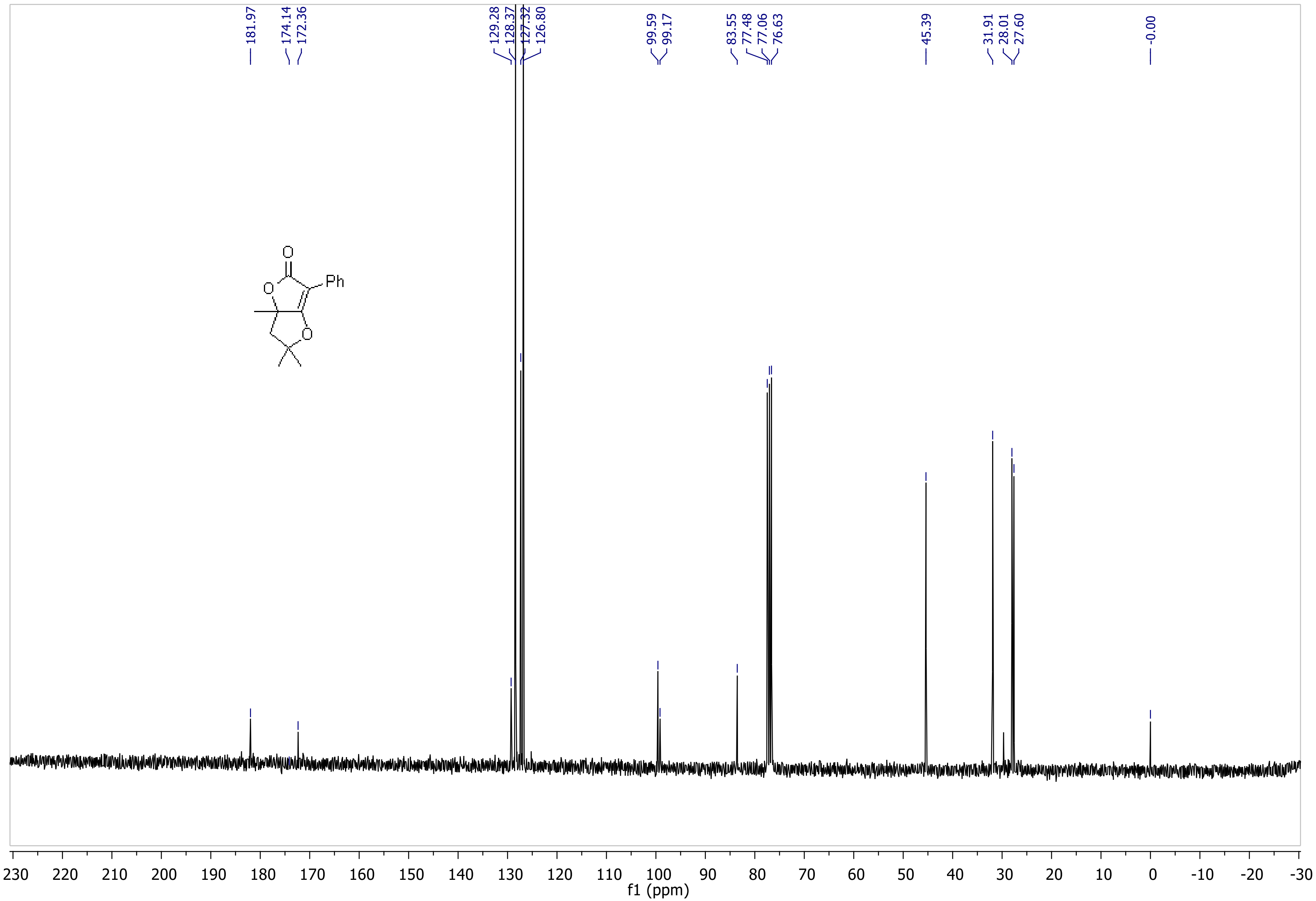

Figure S45. ^{1}H-NMR ($CDCl_3$) of **2e**, Related to **Figure 1**

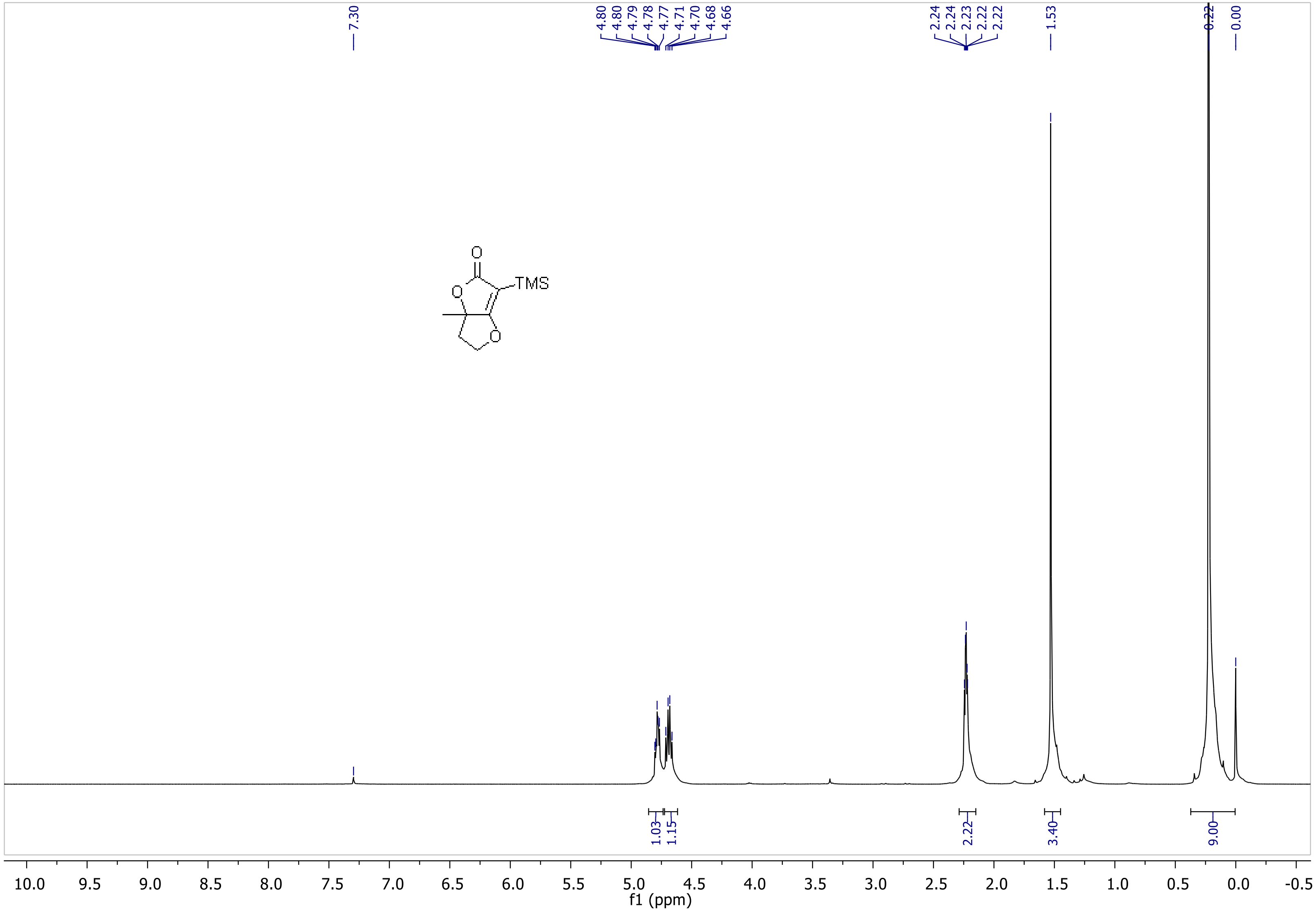

Figure S46. ^{13}C-NMR ($CDCl_3$) of **2e**, Related to **Figure 1**

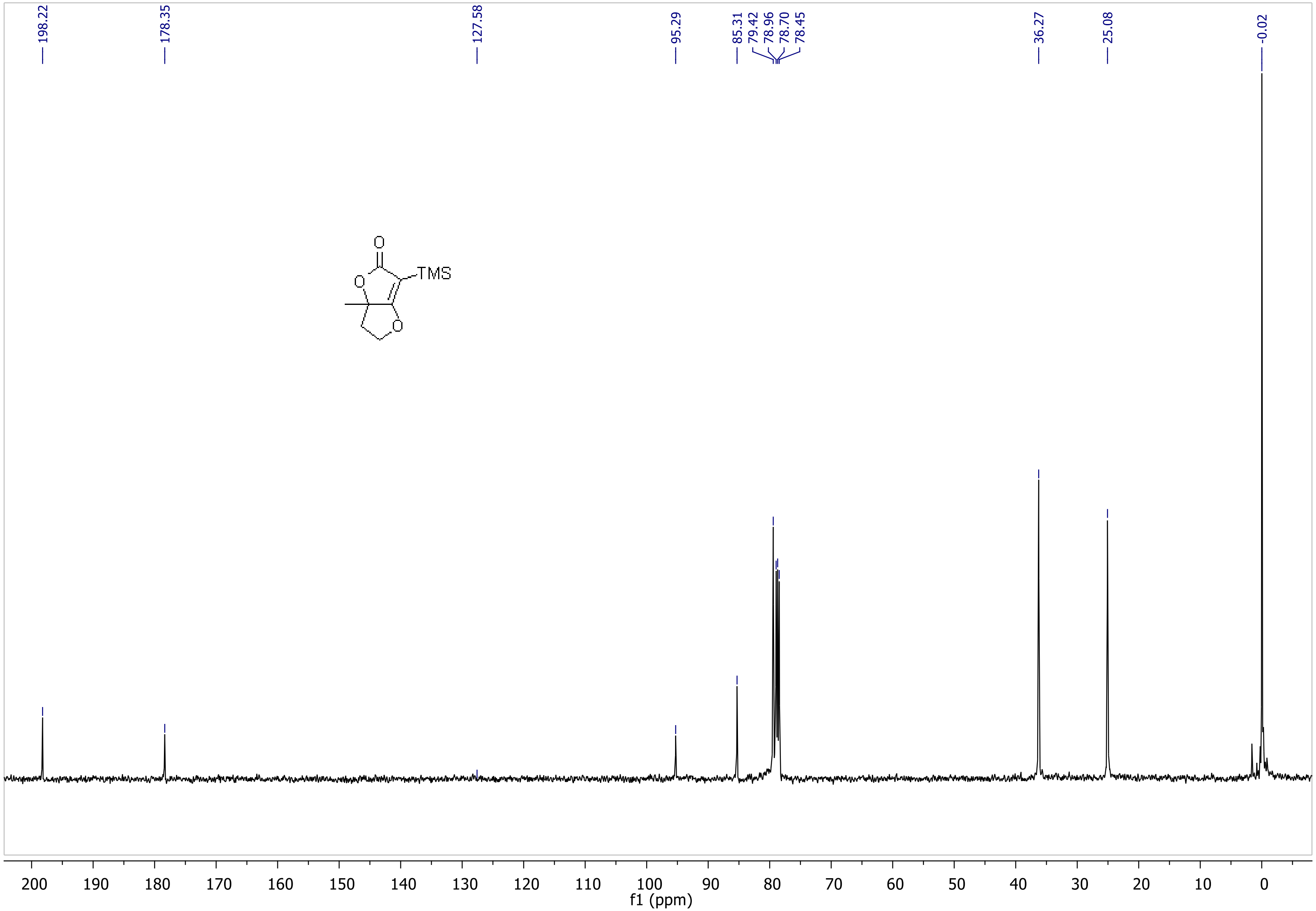

Figure S47. ^{1}H-NMR ($CDCl_3$) of **2f**, Related to **Figure 1**

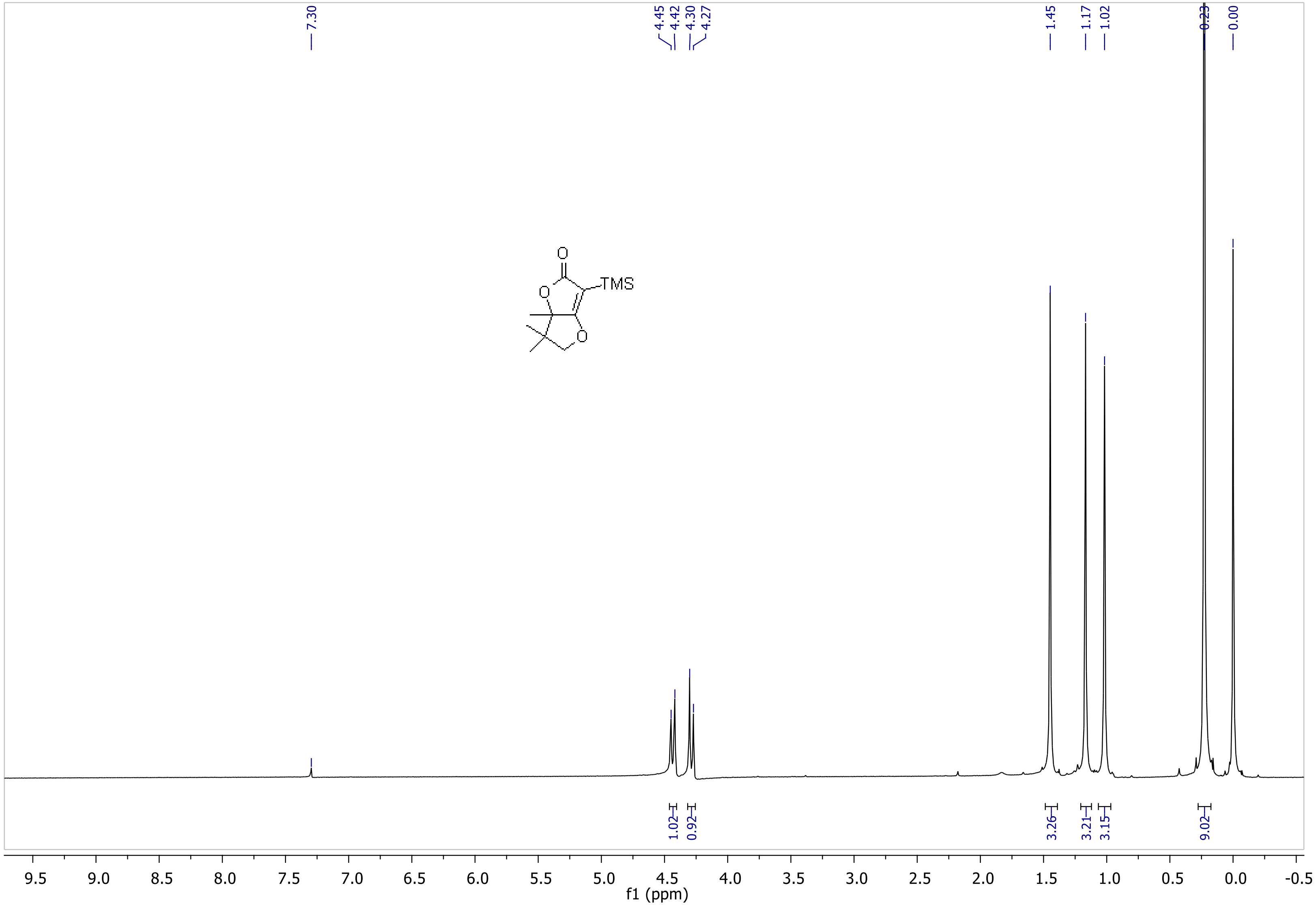

Figure S48. ^{13}C-NMR ($CDCl_3$) of **2f**, Related to **Figure 1**

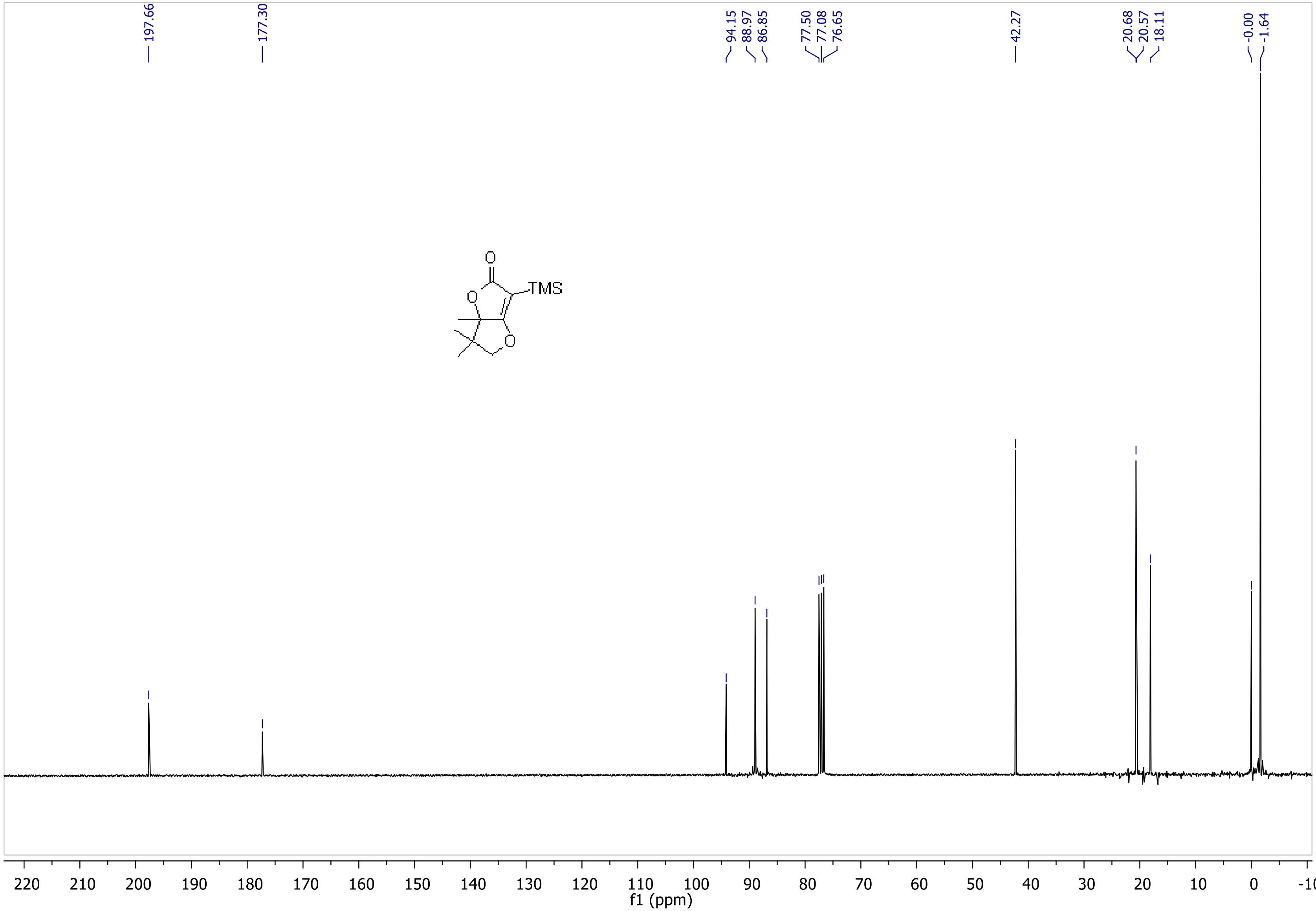

Figure S49. ^{1}H-NMR ($CDCl_3$) of **2g**, Related to **Figure 1**

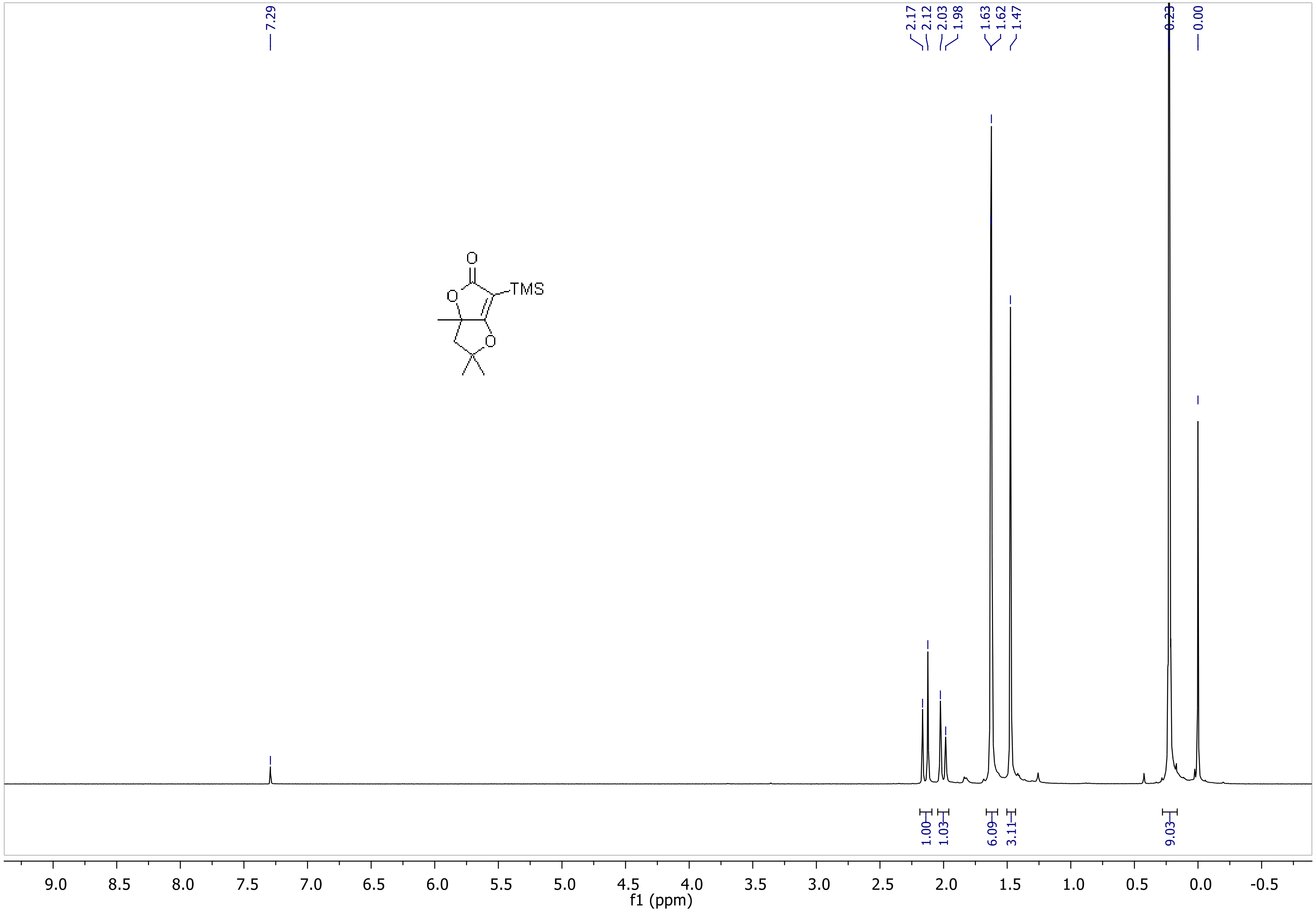

Figure S50. ^{13}C-NMR ($CDCl_3$) of **2g**, Related to **Figure 1**

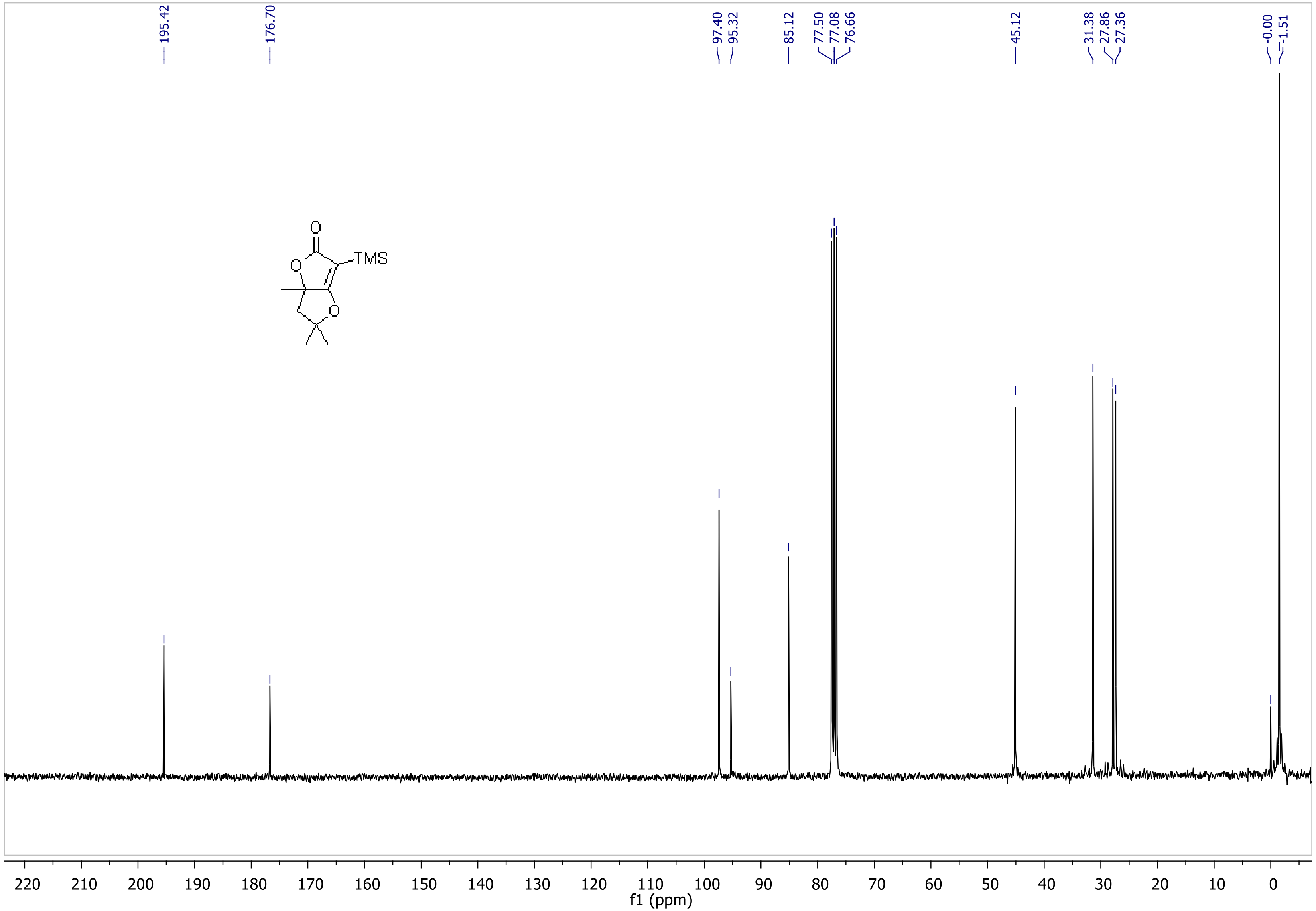

Figure S51. ^{1}H-NMR ($CDCl_3$) of **2h**, Related to **Figure 1**

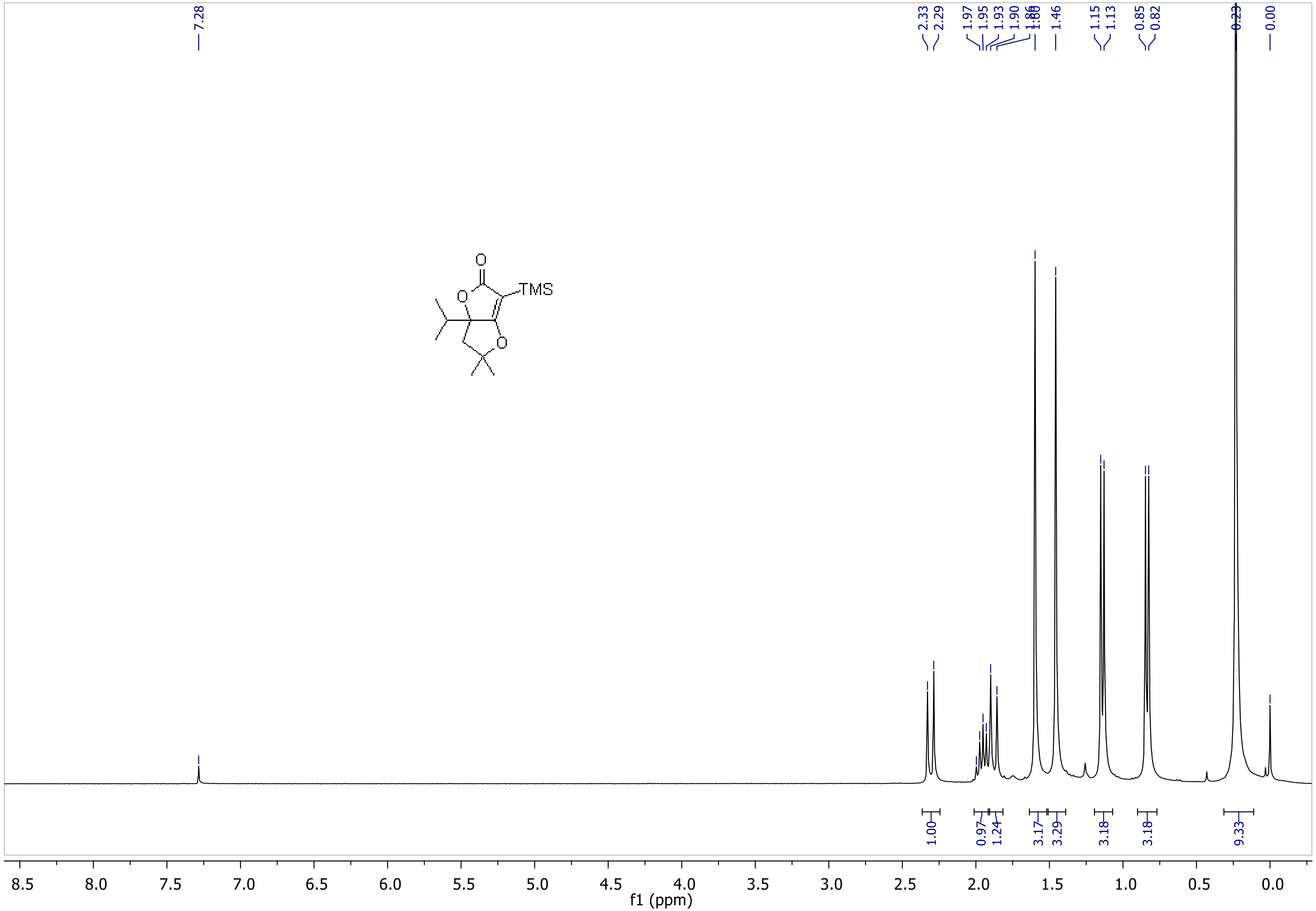

Figure S52. ^{13}C-NMR ($CDCl_3$) of **2h**, Related to **Figure 1**

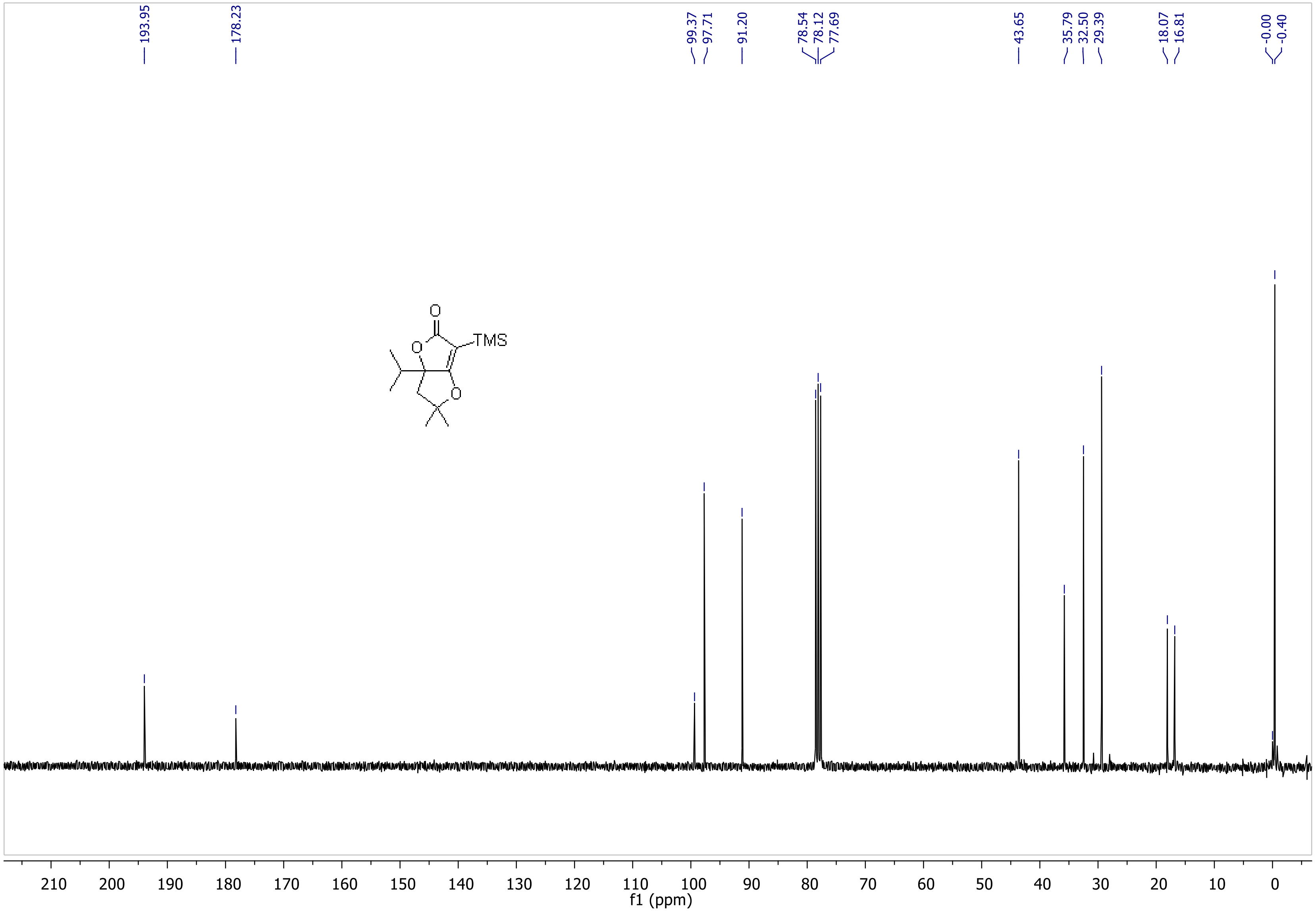

Figure S53. ^{1}H-NMR ($CDCl_3$) of (5*RS*,6*aSR*)-**2i**, Related to **Figure 1** and **Table 1**

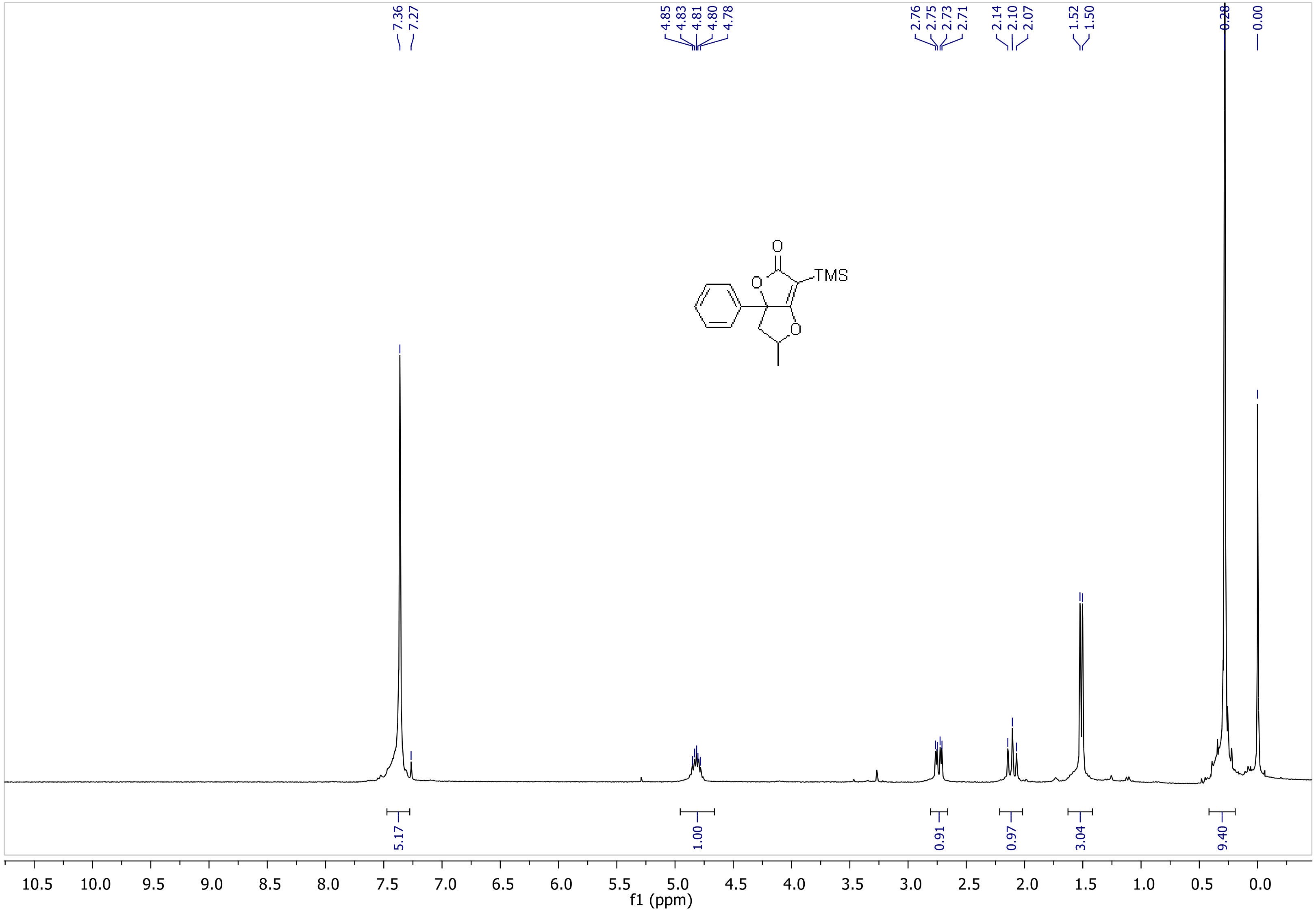

Figure S54. ^{13}C-NMR ($CDCl_3$) of (5*RS*,6a*SR*)-**2i**, Related to **Figure 1** and **Table 1**

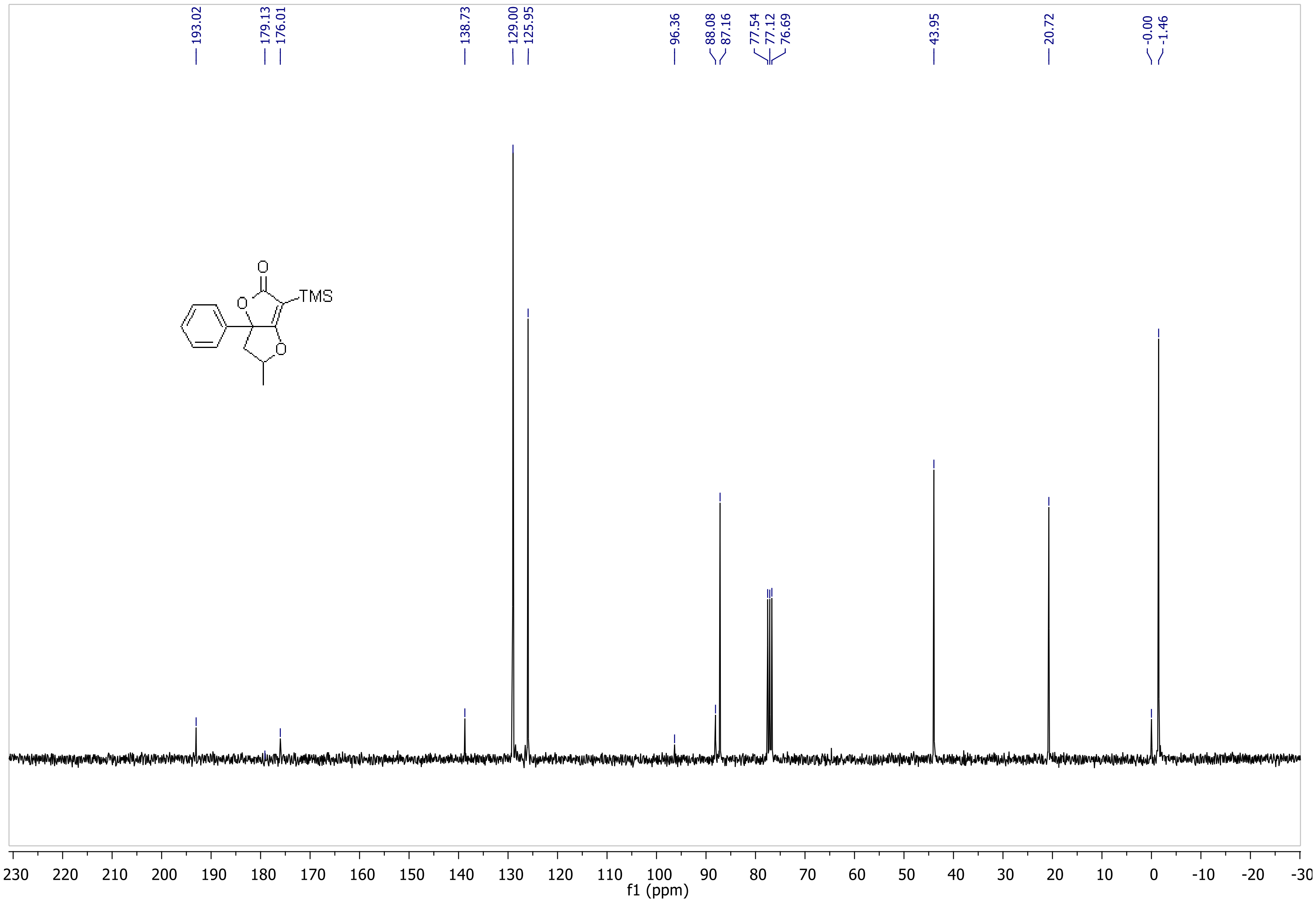

Figure S55. ^{1}H-NMR ($CDCl_3$) of (5*RS*,6a*RS*)-**2i**, Related to **Figure 1** and **Table 1**

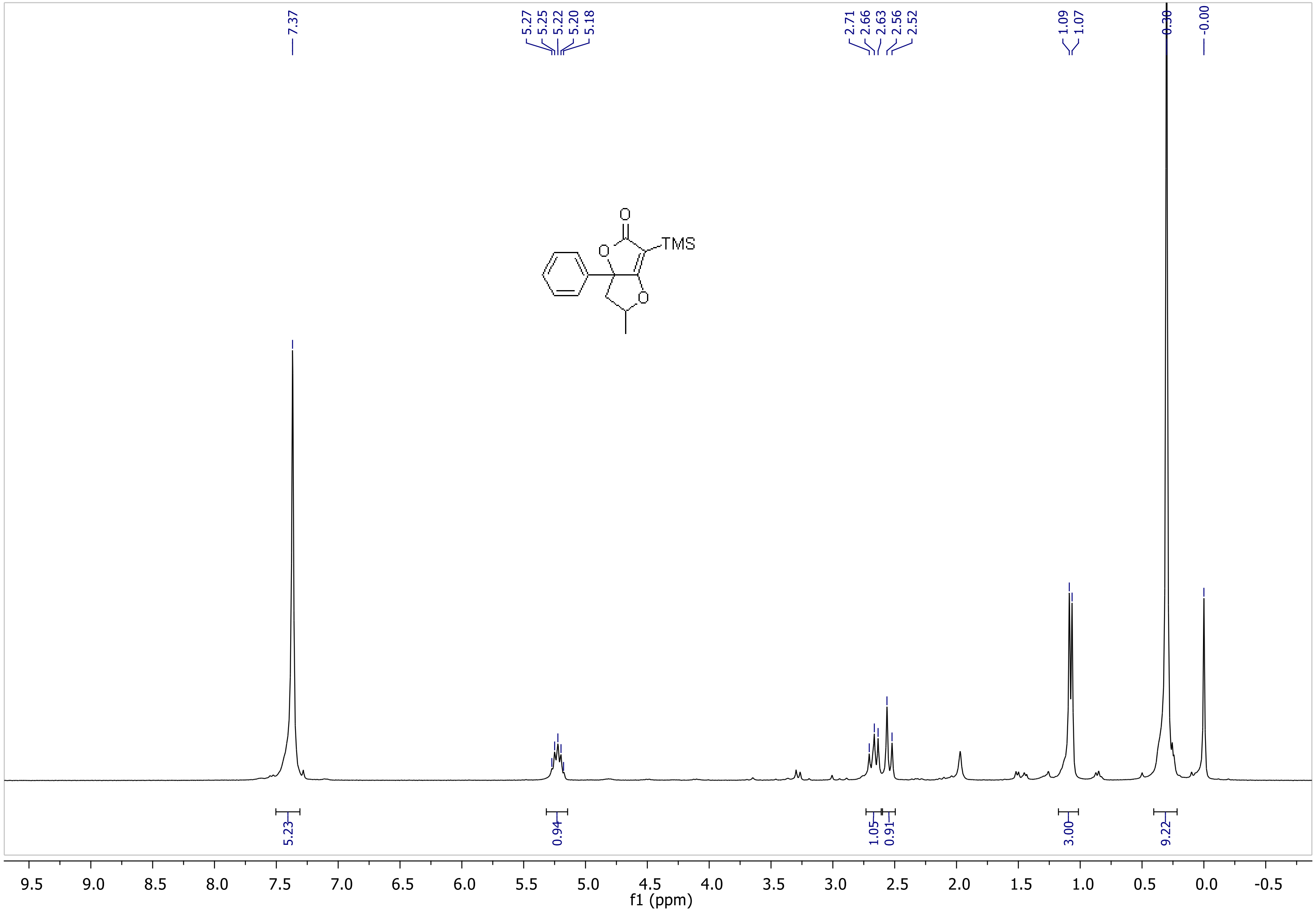

Figure S56. ^{13}C-NMR ($CDCl_3$) of (5*RS*,6a*RS*)-**2i**, Related to **Figure 1** and **Table 1**

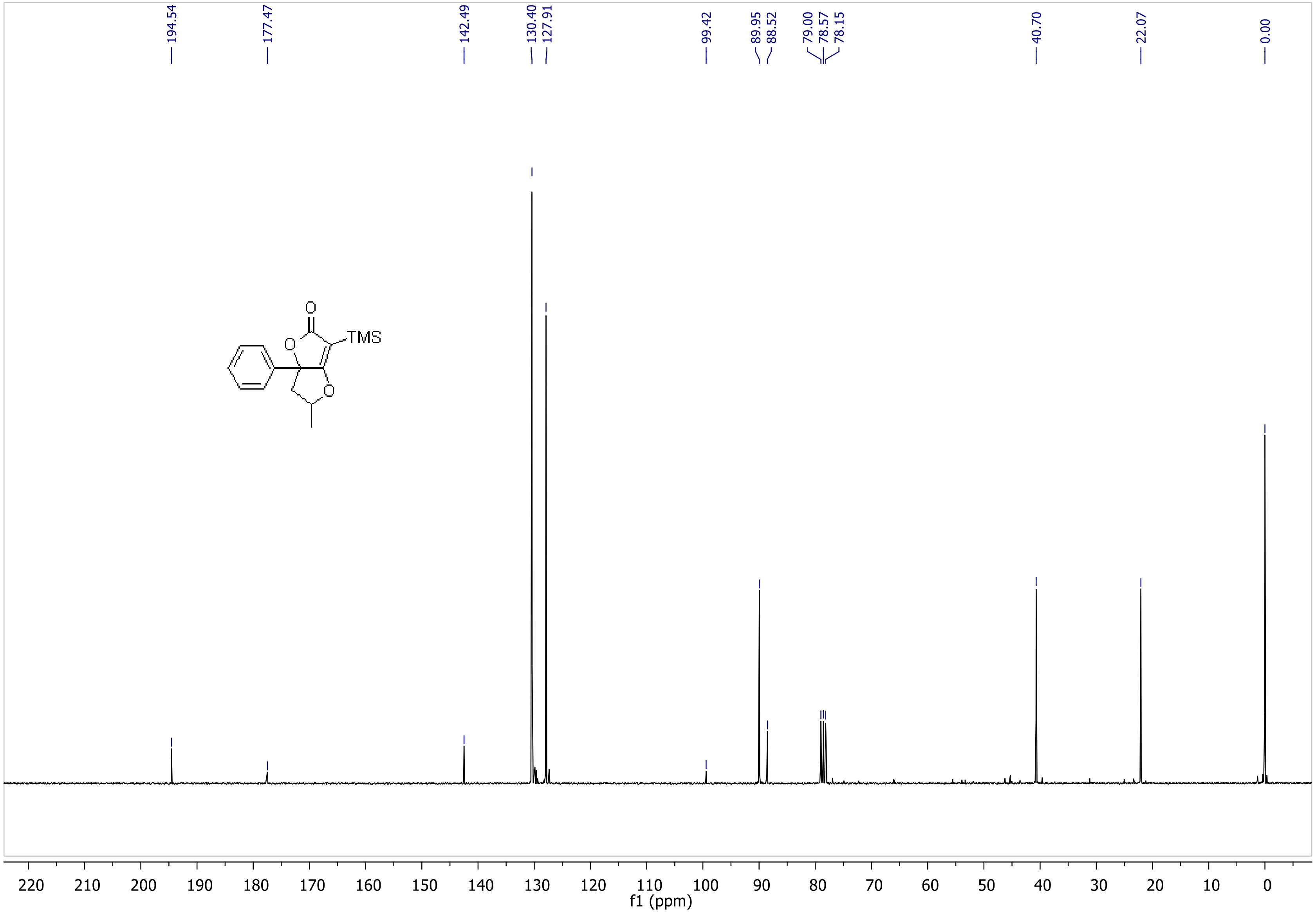

Figure S57. ^{1}H-NMR ($CDCl_3$) of (5*RS*,6a*SR*)-**2j**, Related to **Figure 1** and **Table 1**

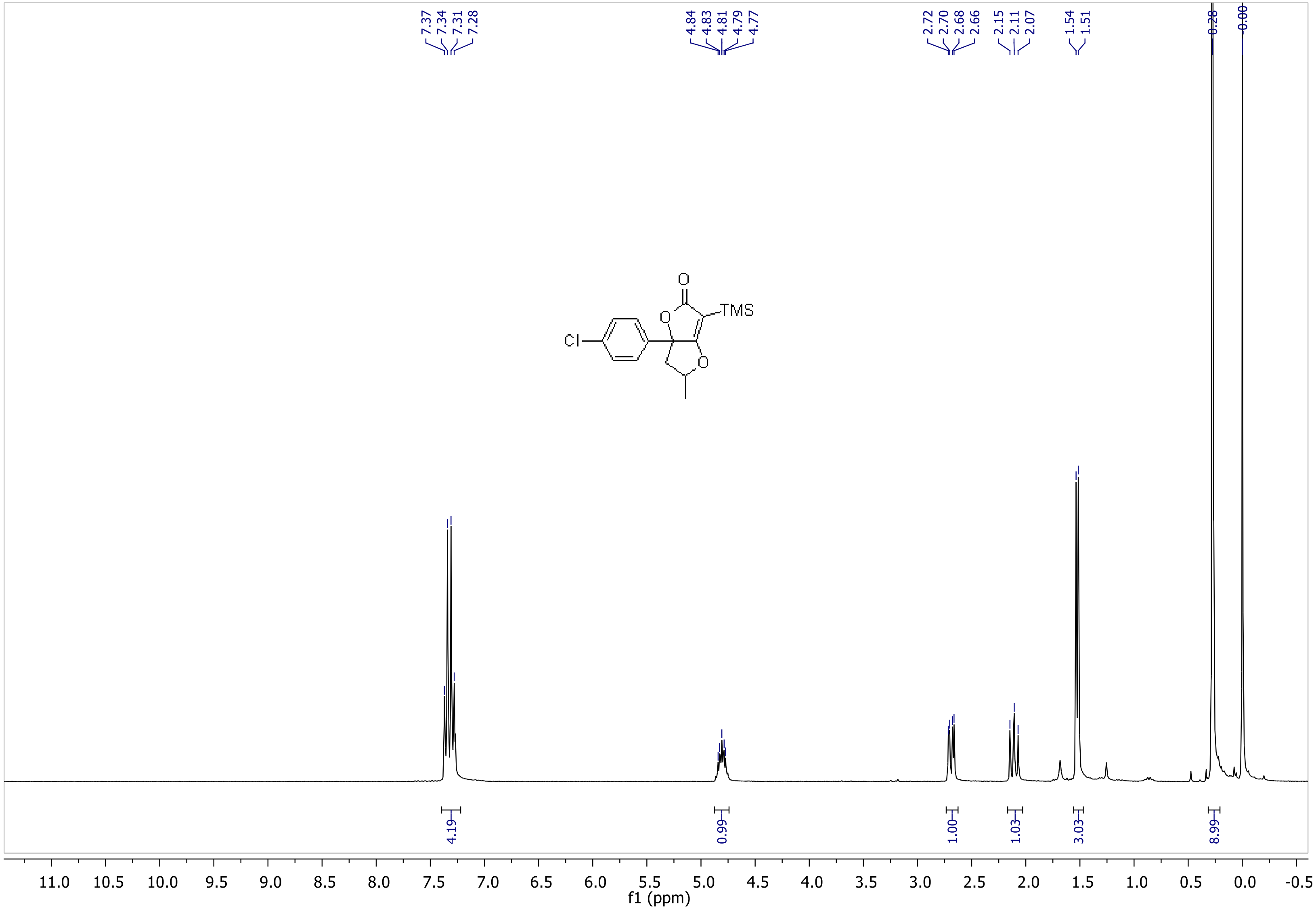

Figure S58. ^{13}C-NMR ($CDCl_3$) of (5*RS*,6a*SR*)-**2j**, Related to **Figure 1** and **Table 1**

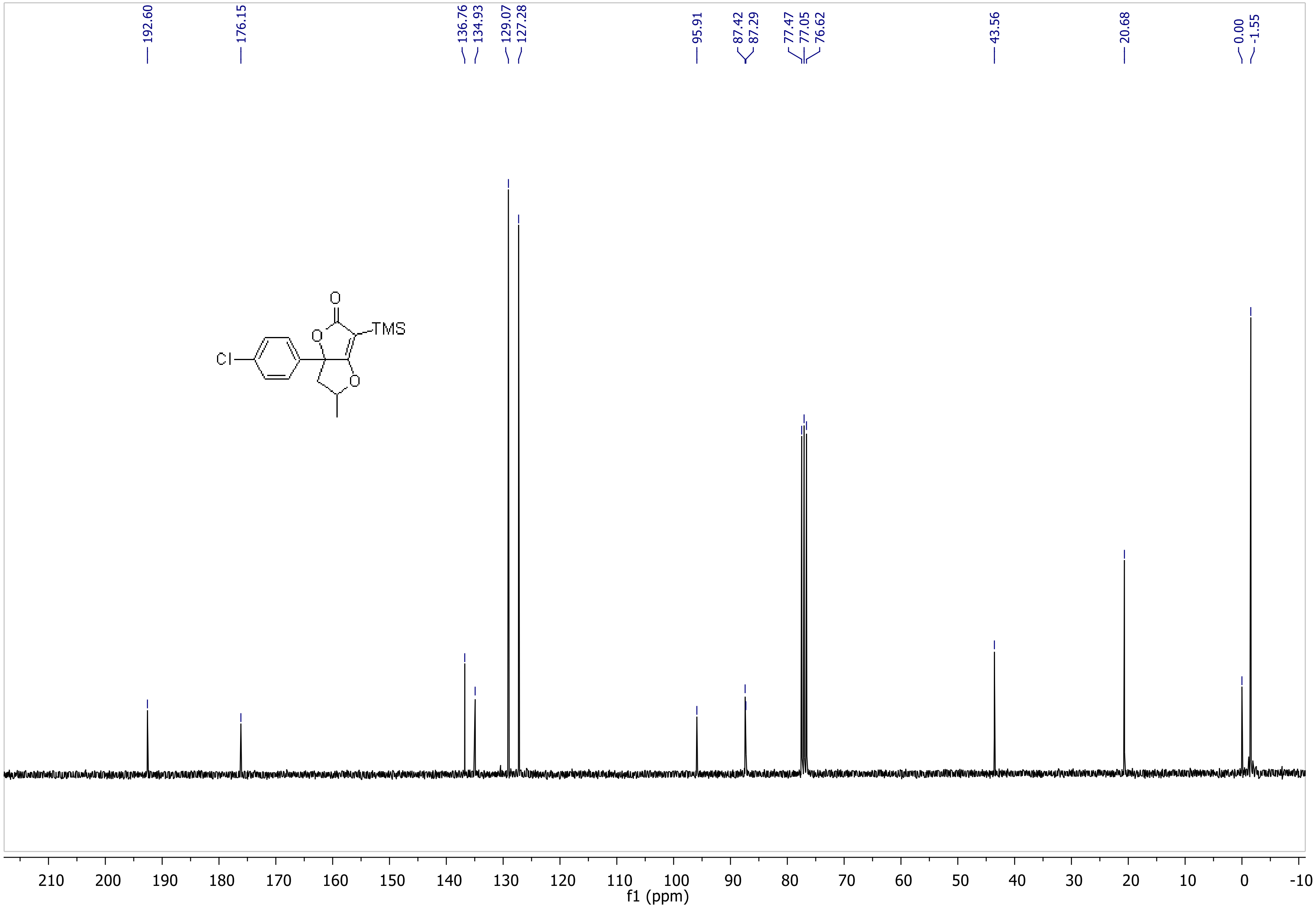

Figure S59. ^{1}H-NMR ($CDCl_3$) of (5*RS*,6a*RS*)-**2j**, Related to **Figure 1** and **Table 1**

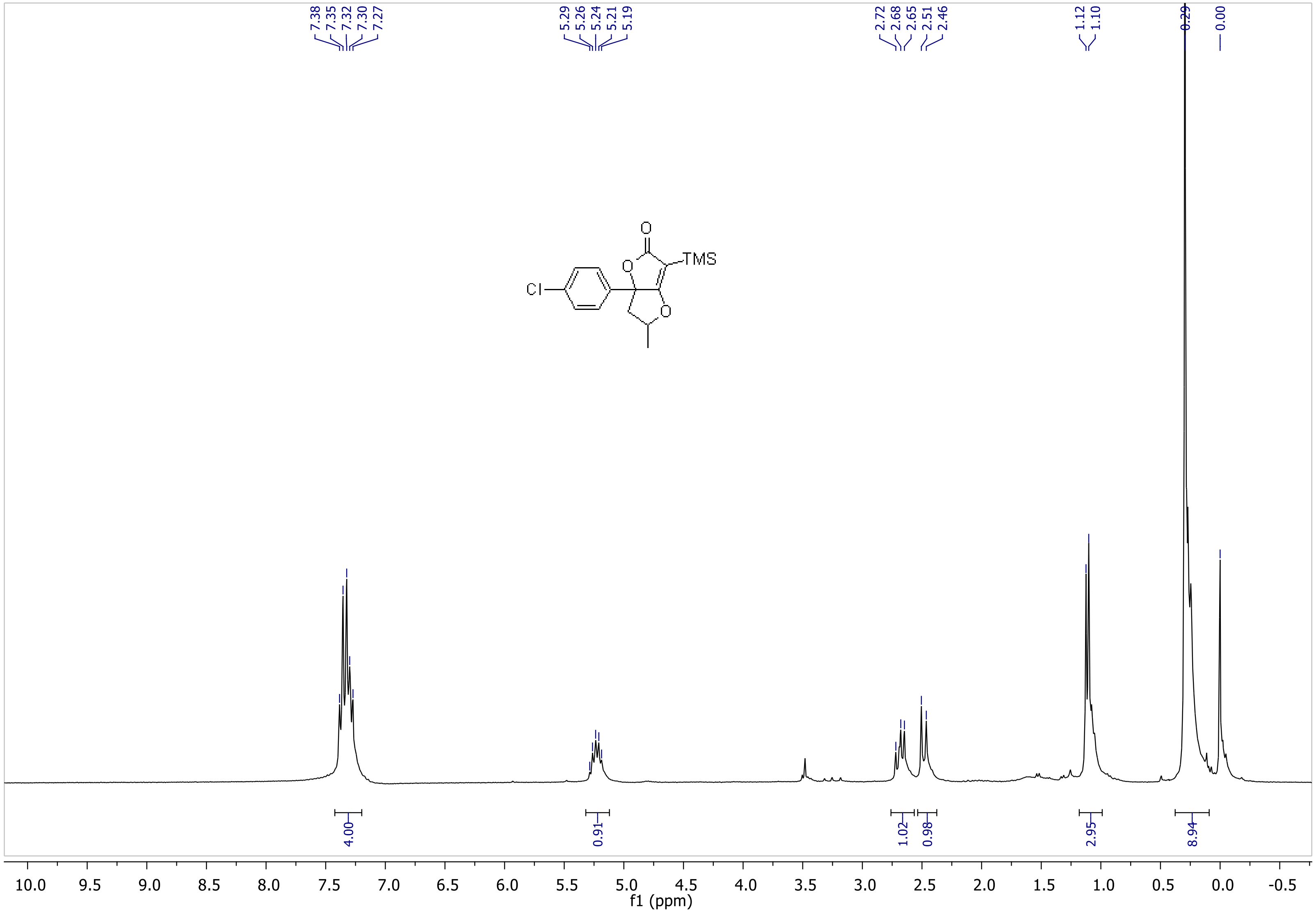

Figure S60. ^{13}C-NMR ($CDCl_3$) of (5*RS*,6a*RS*)-**2j**, Related to **Figure 1** and **Table 1**

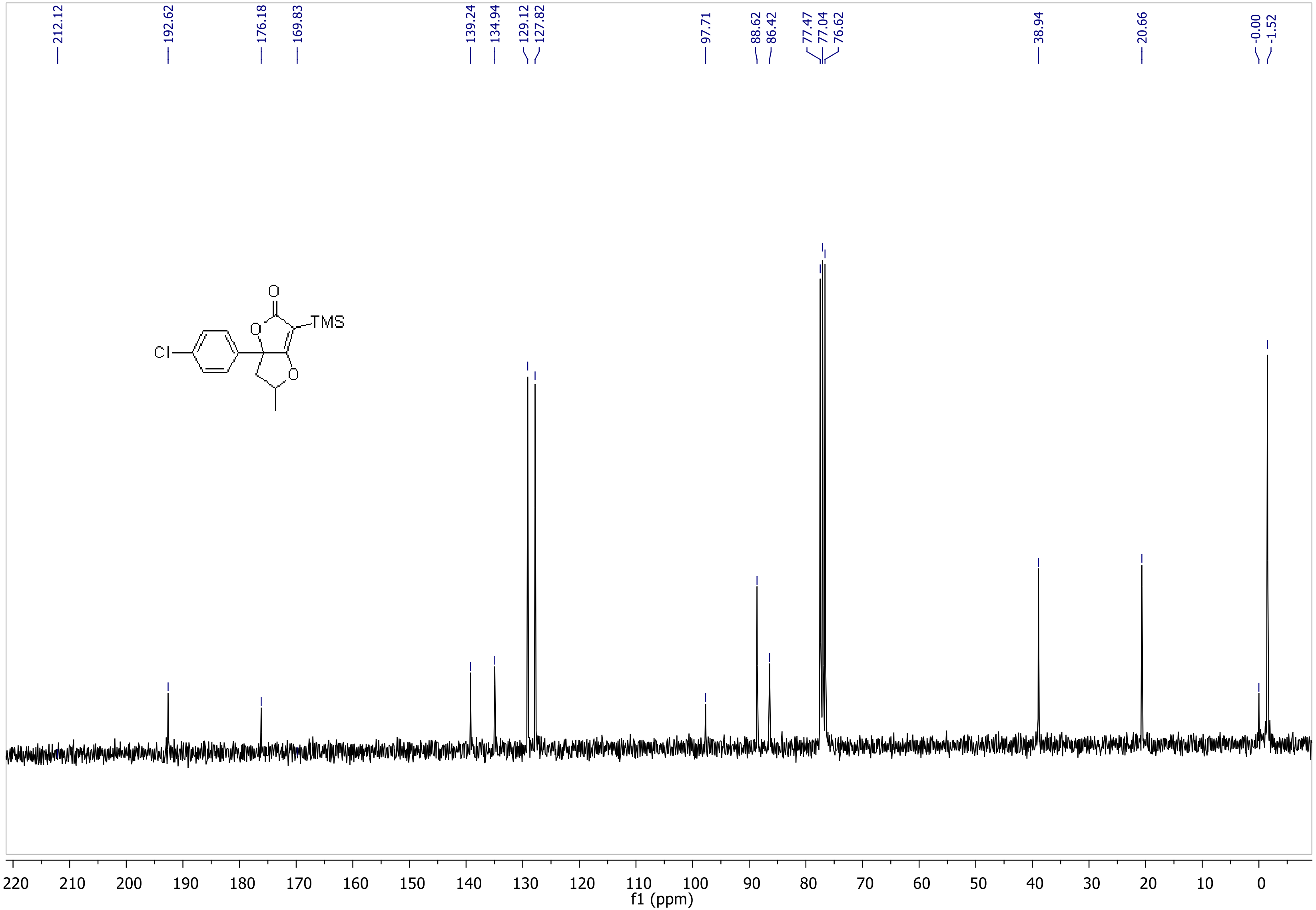

Figure S61. ^{1}H-NMR ($CDCl_3$) of (5*RS*,6a*SR*)-**2k**, Related to **Figure 1** and **Table 1**

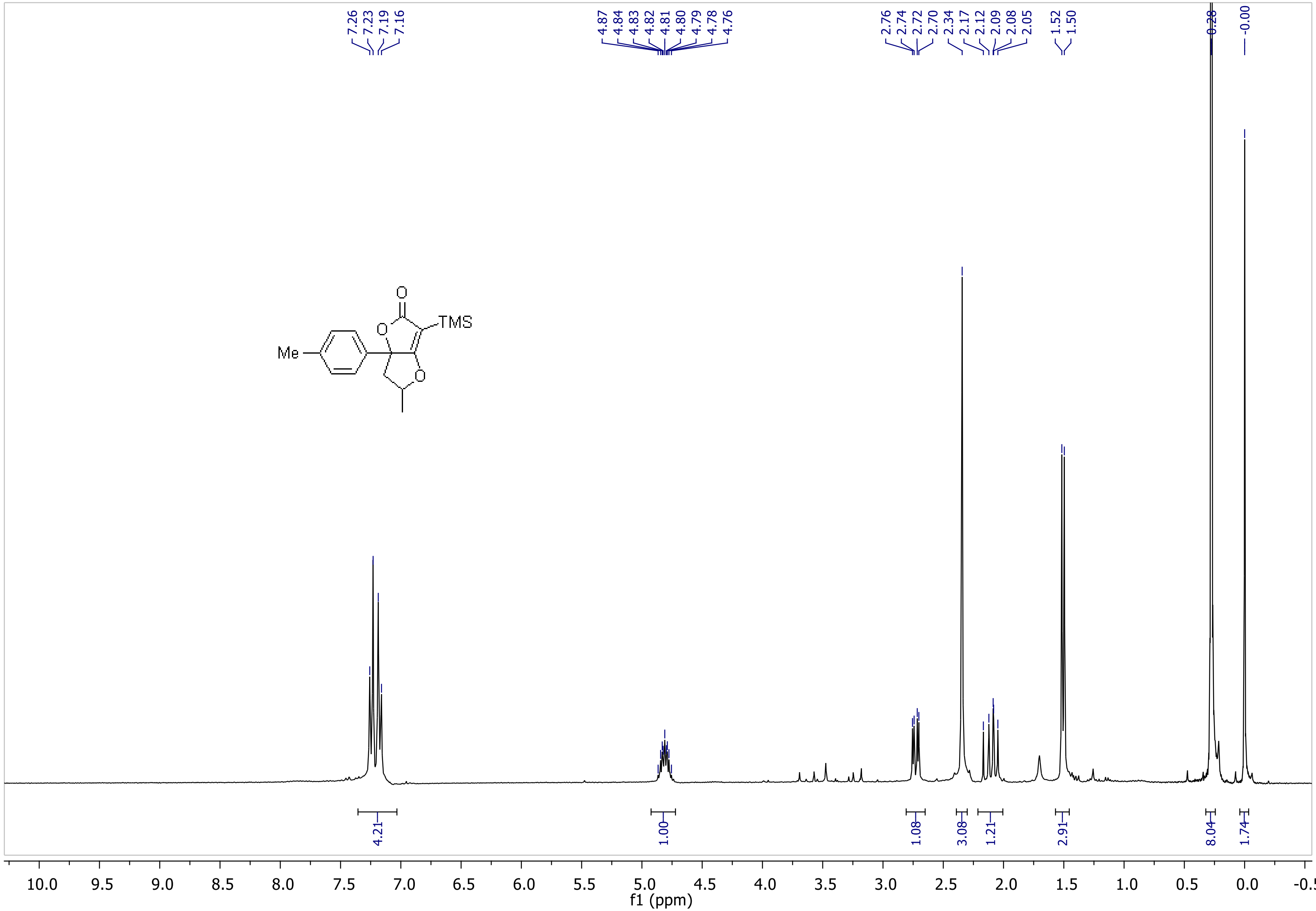

Figure S62. ^{13}C-NMR ($CDCl_3$) of (5*RS*,6*aSR*)-**2k**, Related to **Figure 1** and **Table 1**

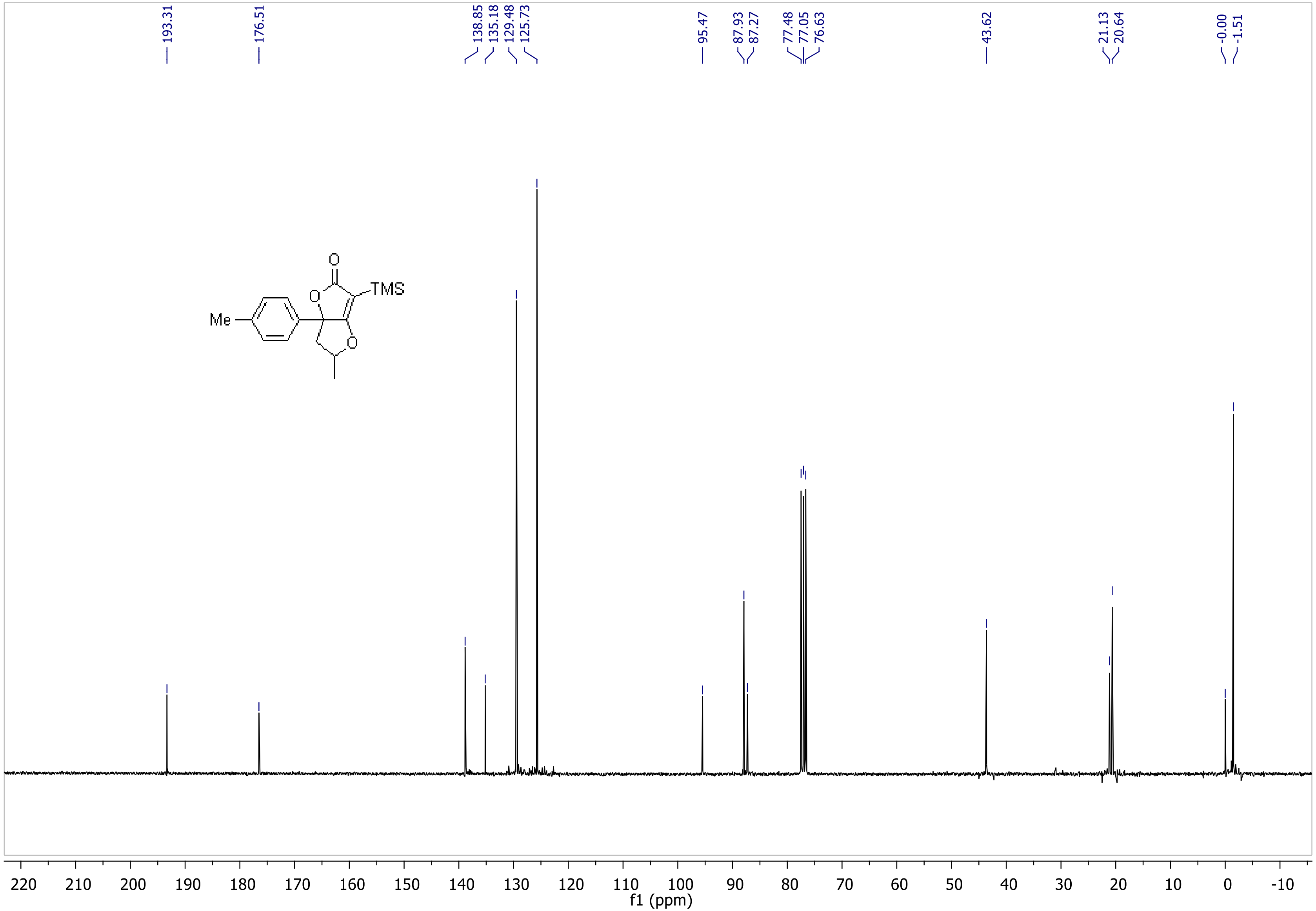

Figure S63. ^{1}H-NMR ($CDCl_3$) of (5*RS*,6a*RS*)-**2k**, Related to **Figure 1** and **Table 1**

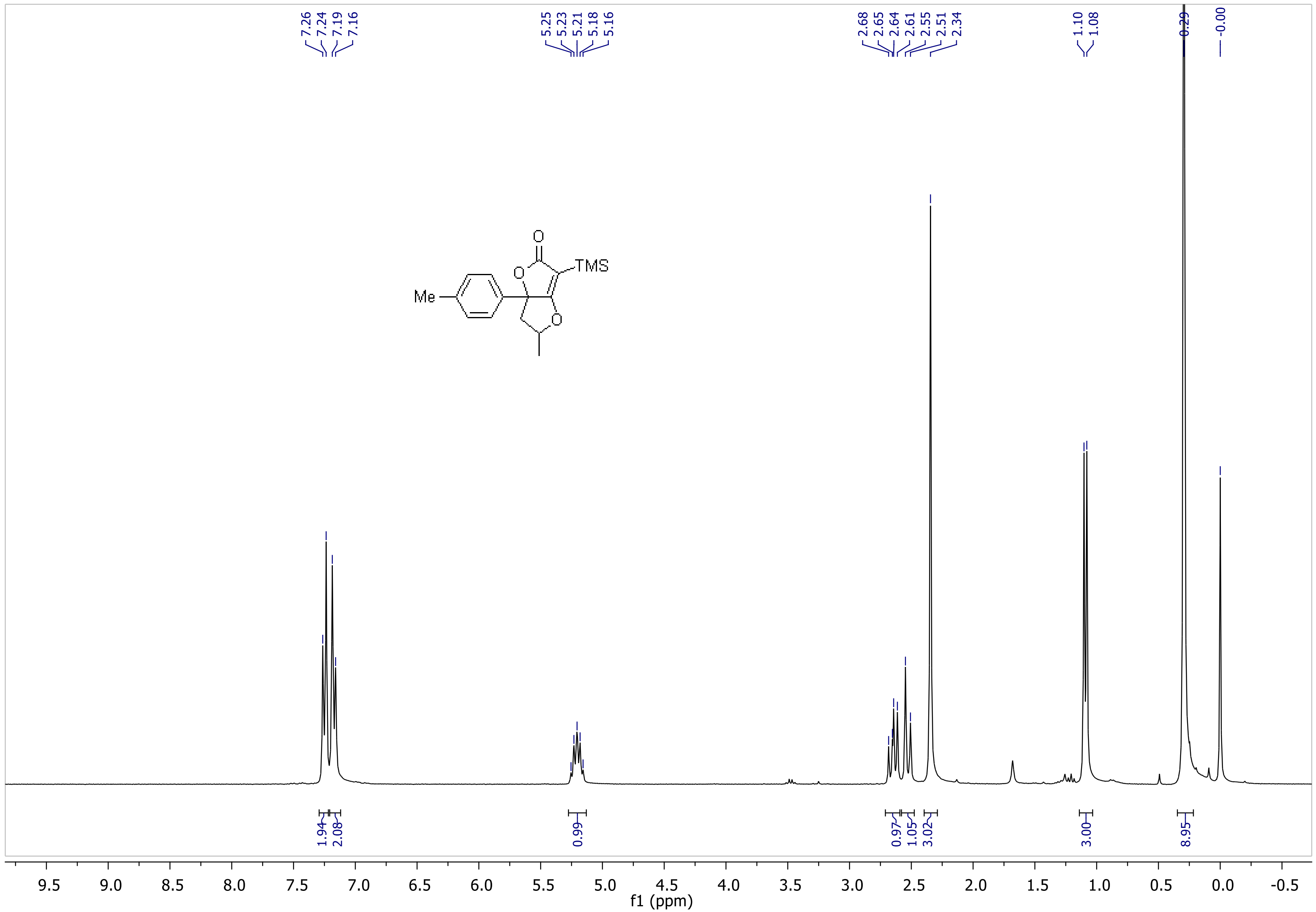

Figure S64. ^{13}C-NMR ($CDCl_3$) of (5*RS*,6a*RS*)-**2k**, Related to **Figure 1** and **Table 1**

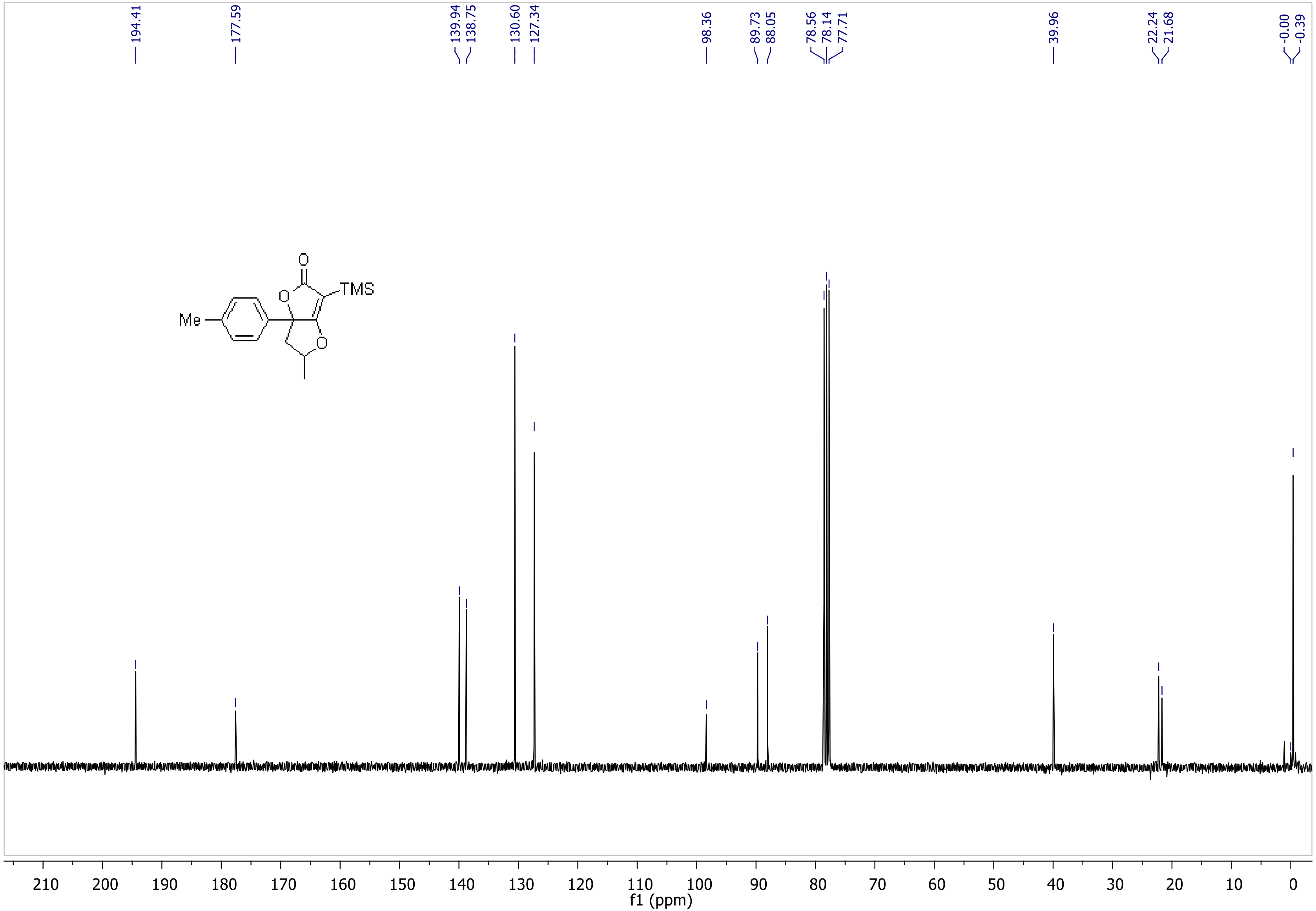

Figure S65. ^{1}H-NMR ($CDCl_3$) of **2l**, Related to **Figure 1**

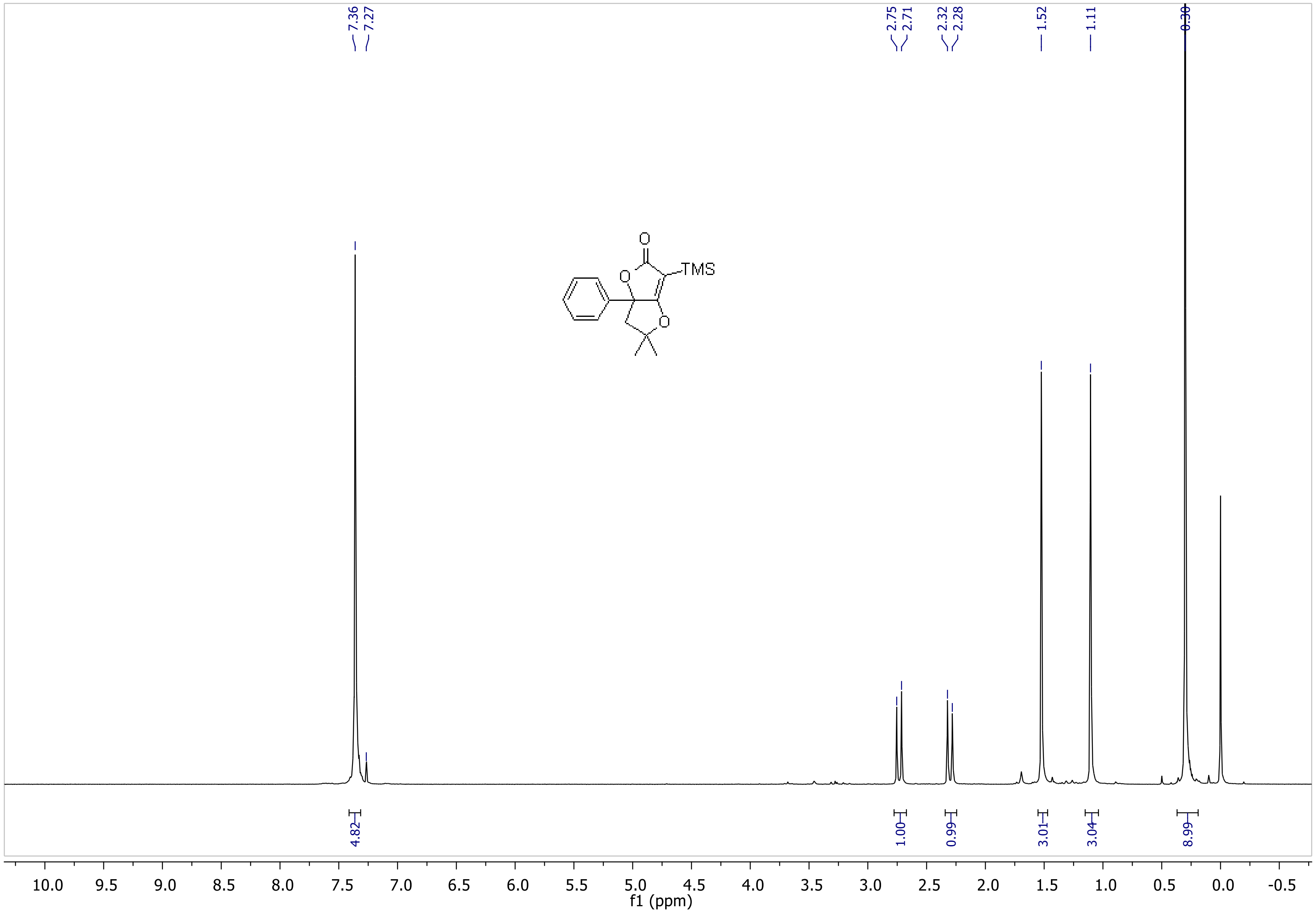

Figure S66. ^{13}C-NMR ($CDCl_3$) of **2l**, Related to **Figure 1**

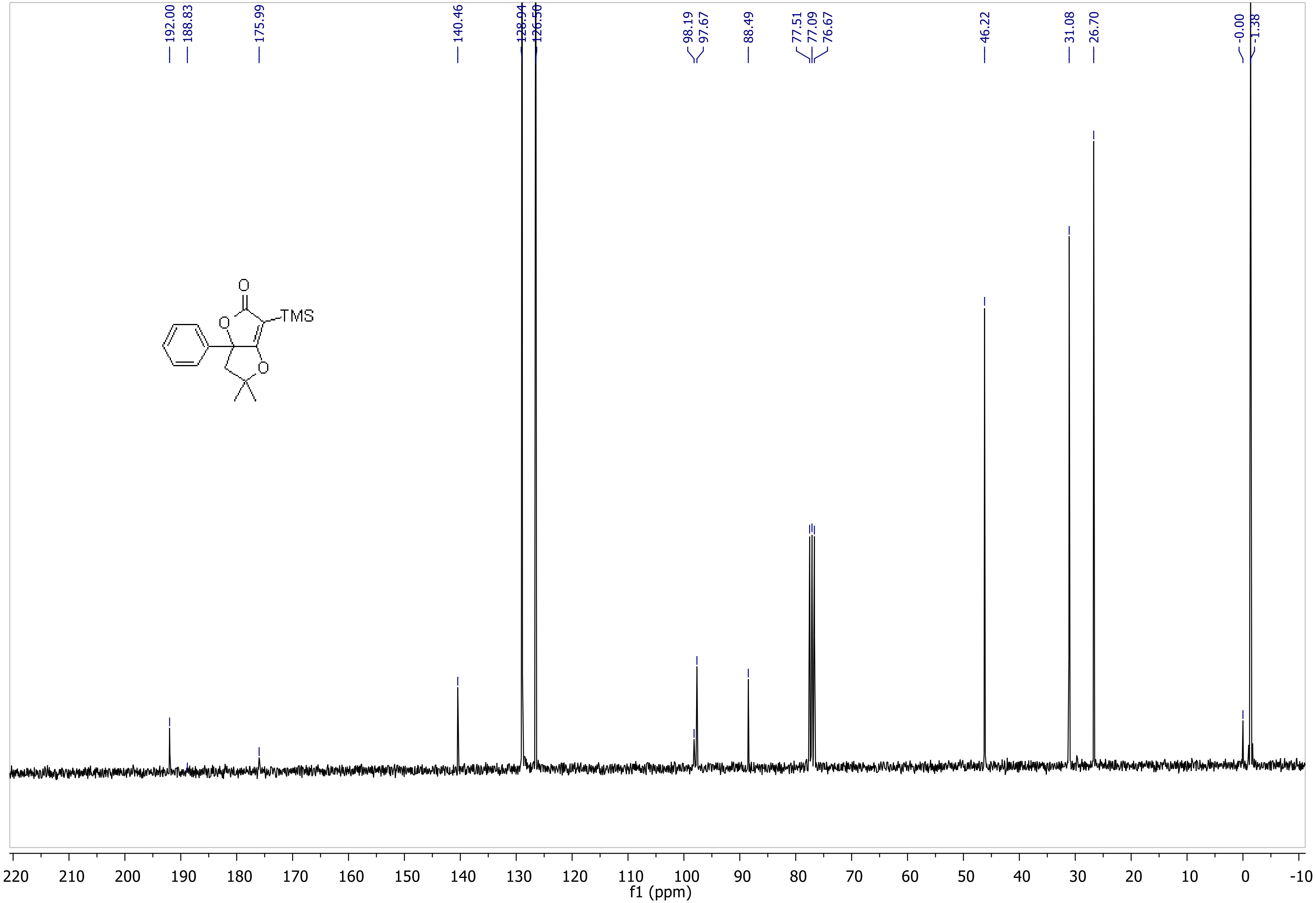

Figure S67. ^{1}H-NMR ($CDCl_3$) of **2m**, Related to **Figure 1**

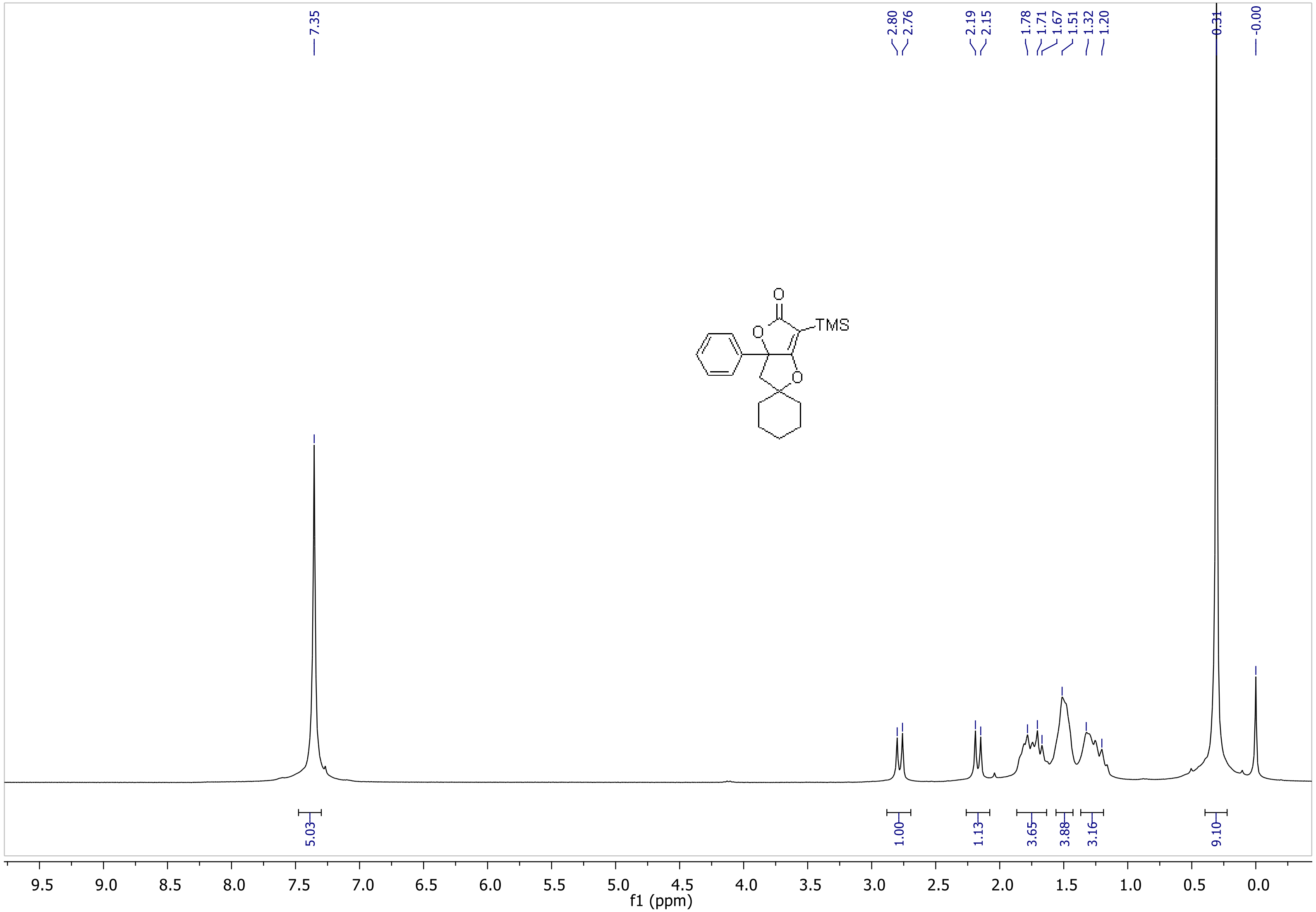

Figure S68. ^{13}C-NMR ($CDCl_3$) of **2m**, Related to **Figure 1**

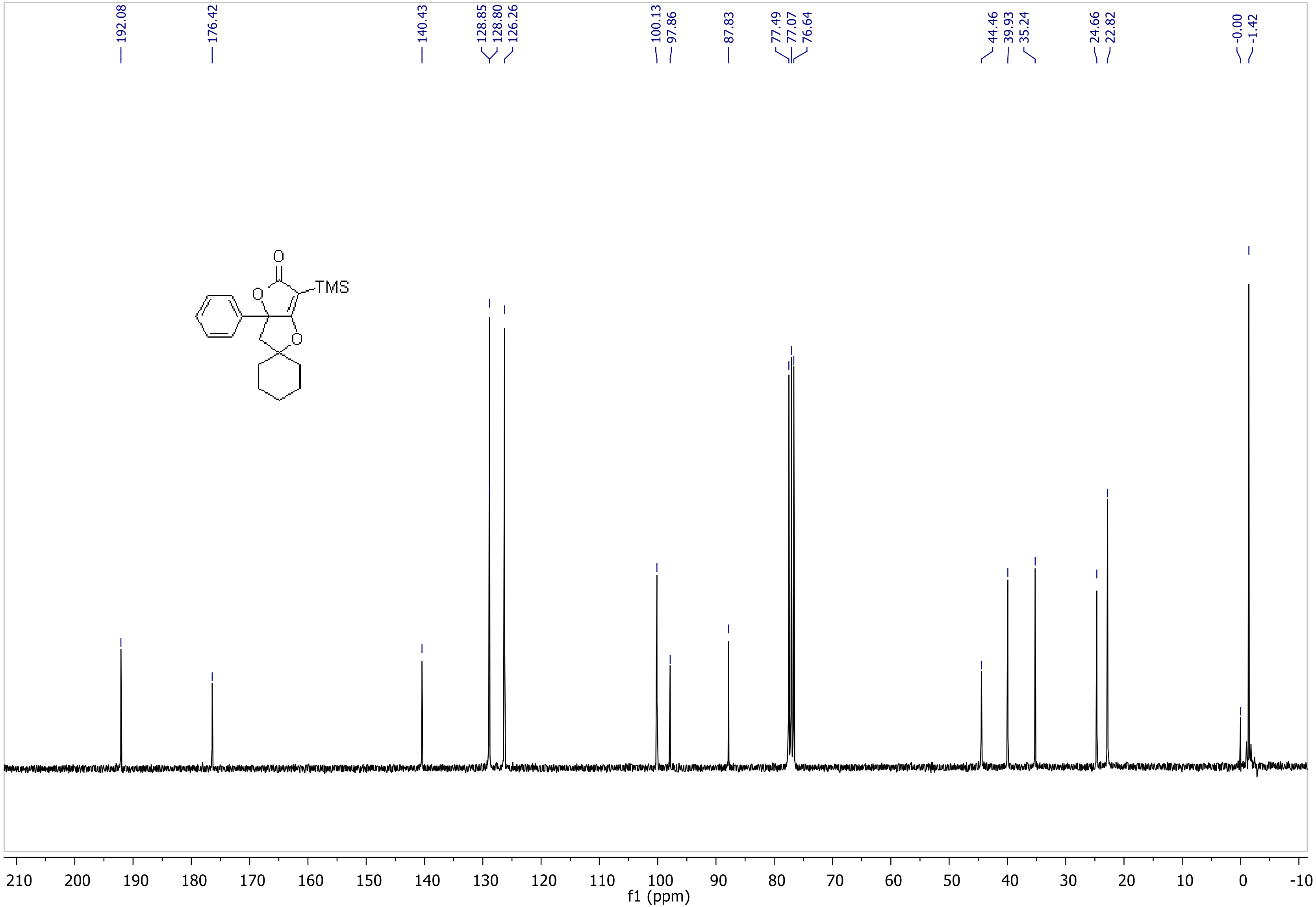

Figure S69. ^{1}H-NMR ($CDCl_3$) of **3h**, Related to **Scheme 3**

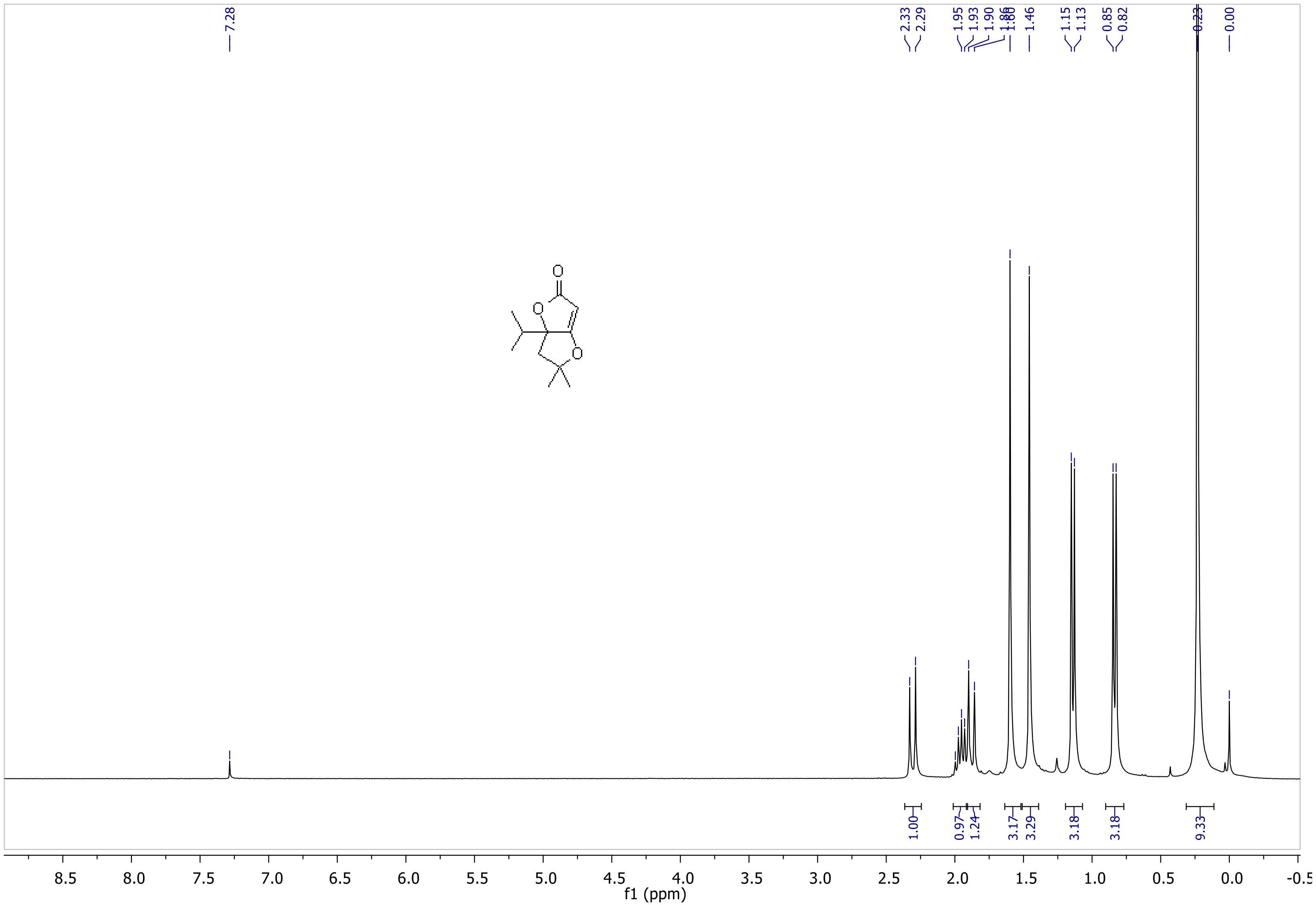

Figure S70. ^{13}C-NMR ($CDCl_3$) of **3h**, Related to **Scheme 3**

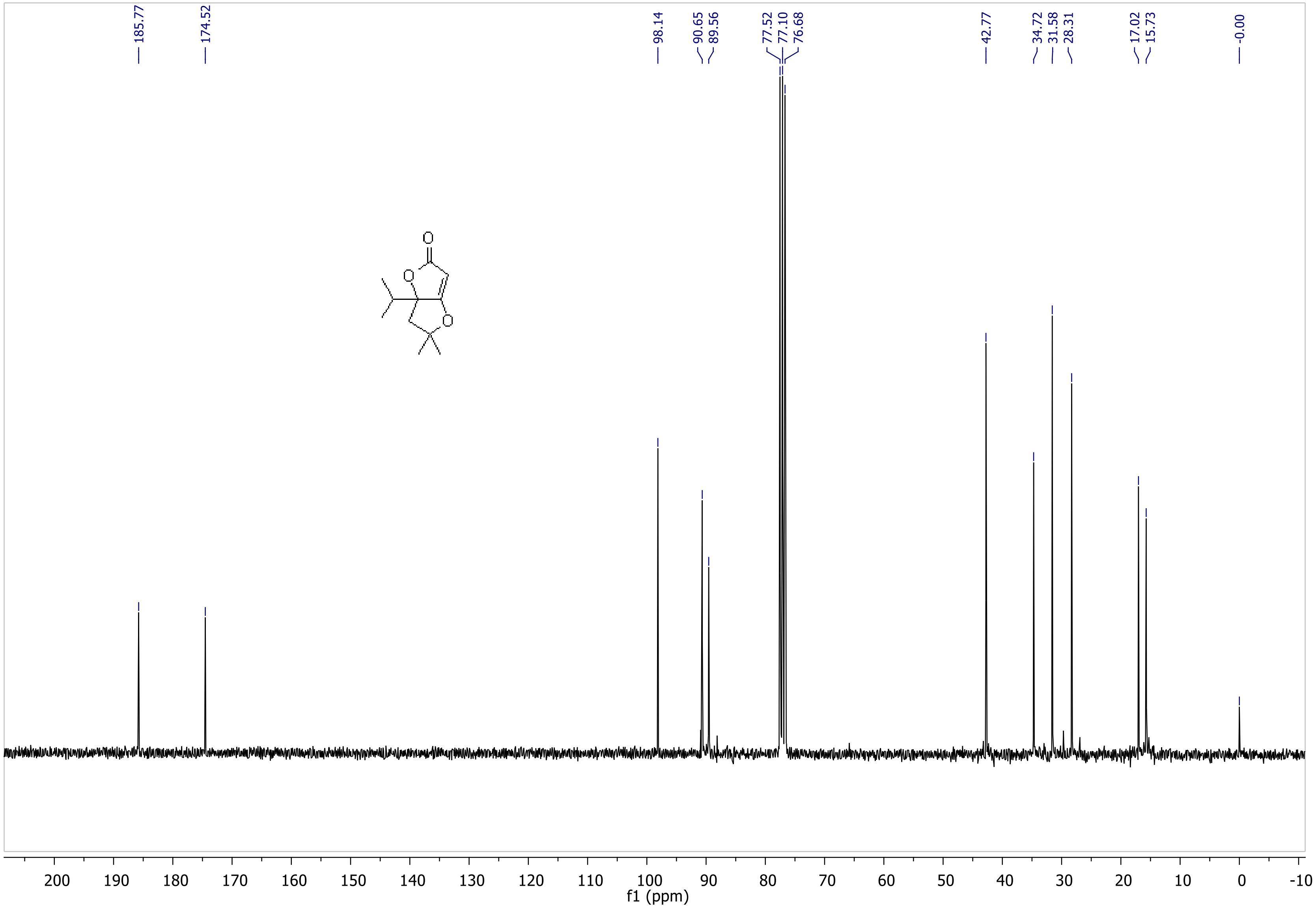

Figure S71. ^{1}H-NMR ($CDCl_3$) of **3l**, Related to **Scheme 3**

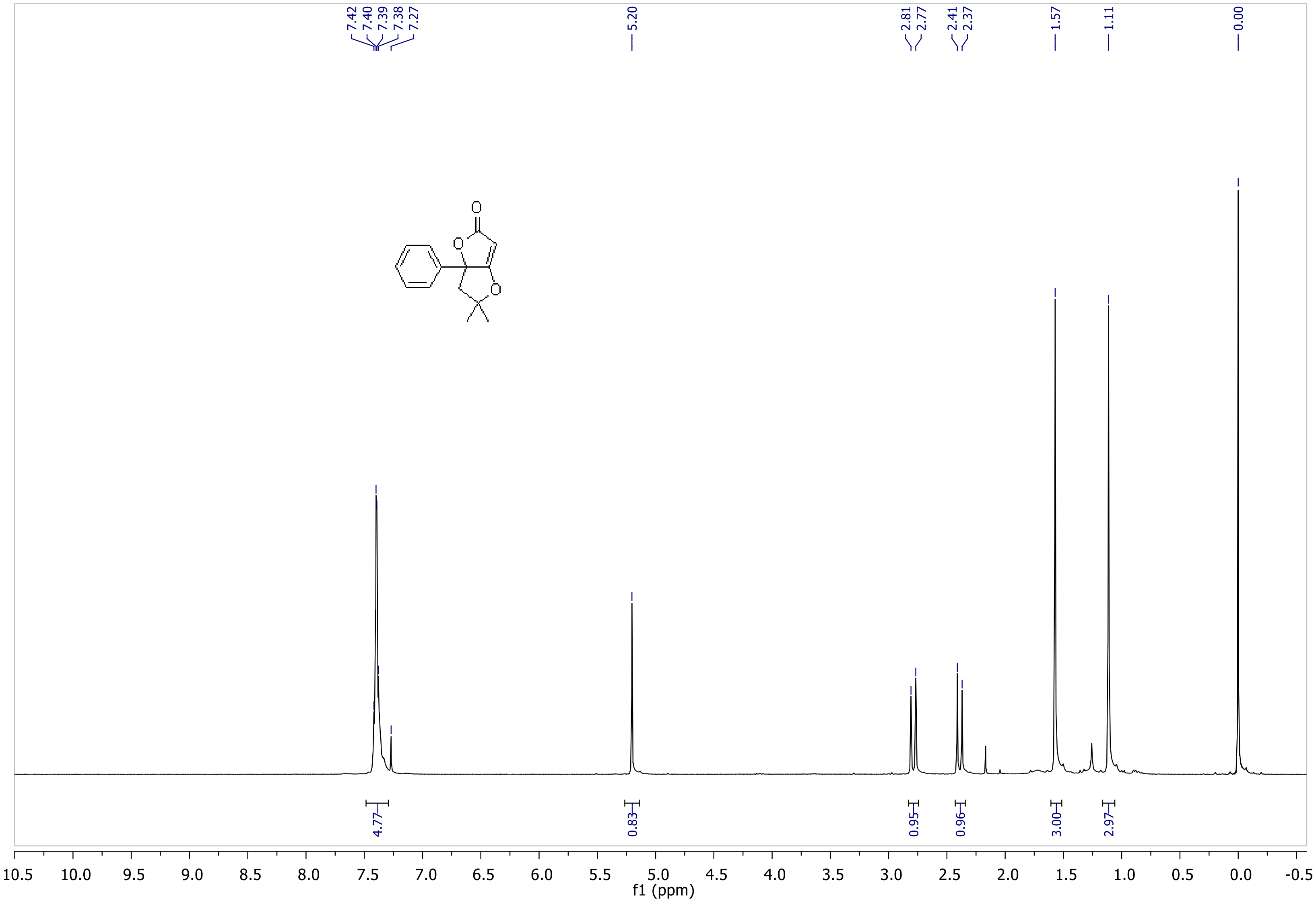

Figure S72. ^{13}C-NMR ($CDCl_3$) of **3l**, Related to **Scheme 3**

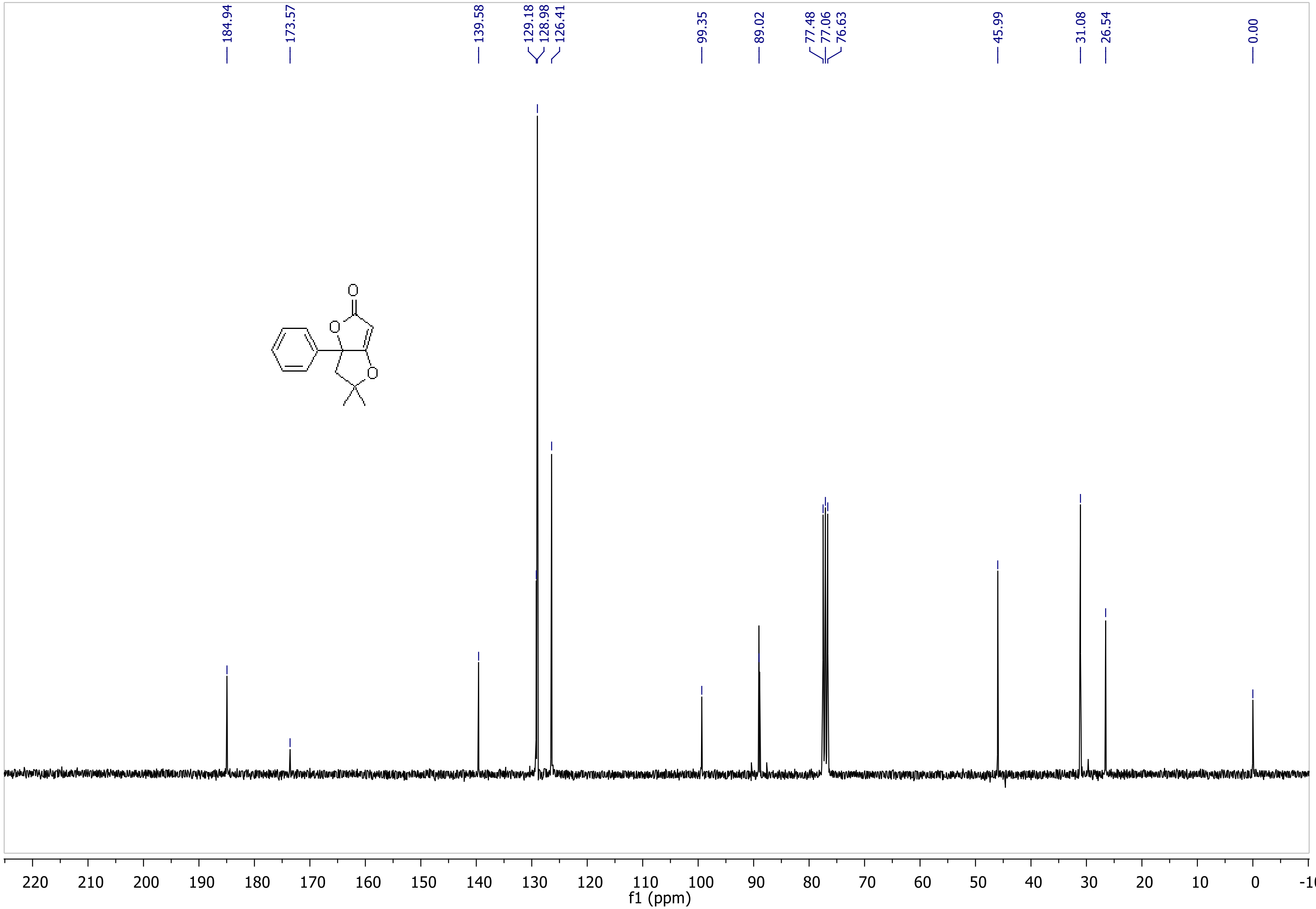

Figure S73. ^{1}H-NMR ($CDCl_3$) of **3m**, Related to **Scheme 3**

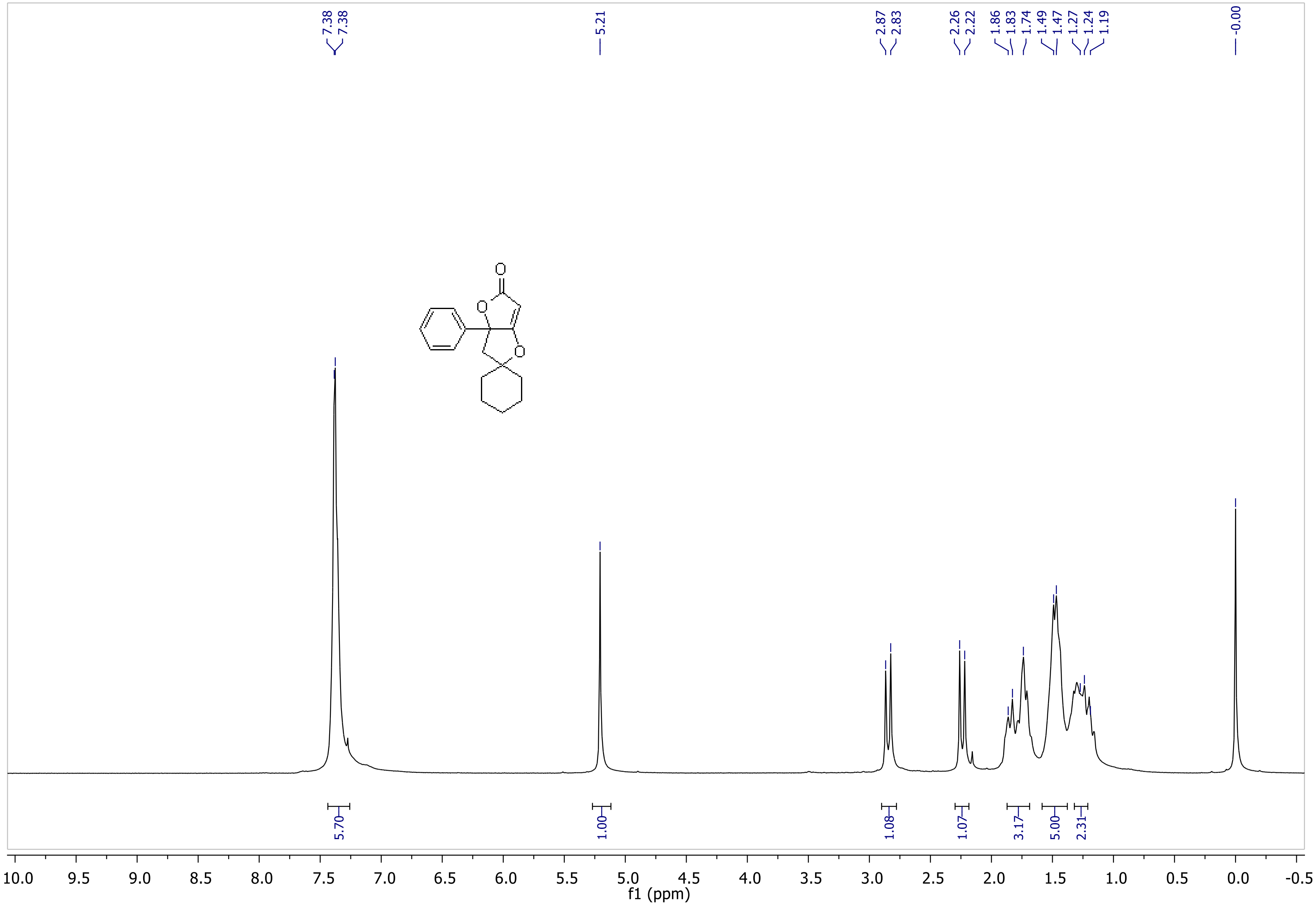

Figure S74. ^{13}C-NMR ($CDCl_3$) of **3m**, Related to **Scheme 3**

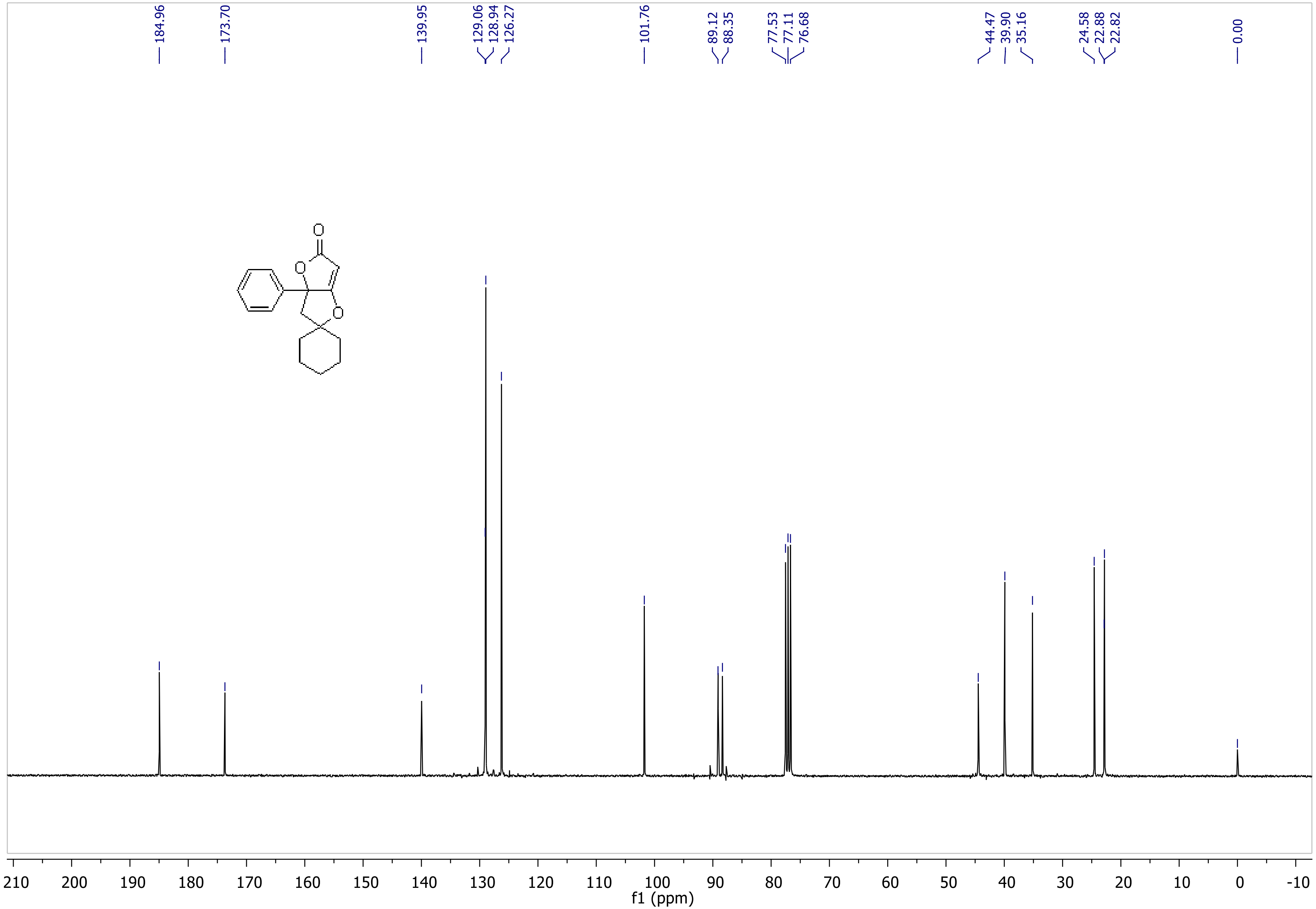

Table S1. Crystal data and structure refinement for compound **2g**, Related to **Figure 1**

Empirical formula	C12 H20 O3 Si	
Formula weight	240.37	
Temperature	296(2) K	
Wavelength	0.71073 Å	
Crystal system	Monoclinic	
Space group	$P2_1/c$	
Unit cell dimensions	a = 10.192(4) Å	α= 90°.
	b = 24.816(8) Å	β= 102.166(18)°.
	c = 11.873(4) Å	γ = 90°.
Volume	2935.5(18) Å^3	
Z^a	8	
Density (calculated)	1.088 Mg/m^3	
Absorption coefficient	0.152 mm^{-1}	
F(000)	1040	
Crystal size	0.200 x 0.140 x 0.060 mm^3	
Theta range for data collection	1.641 to 28.777°.	
Index ranges	-13<=h<=12, -33<=k<=33, -15<=l<=15	
Reflections collected	41809	
Independent reflections	6861 [R(int) = 0.0452]	
Completeness to theta = 25.242°	96.2 %	
Refinement method	Full-matrix least-squares on F^2	
Data / restraints / parameters	6861 / 0 / 289	
Goodness-of-fit on F^2	1.038	
Final R indices [I >2sigma(I)]	R_1 = 0.0720, wR_2 = 0.1695	
R indices (all data)	R_1 = 0.1303, wR_2 = 0.1916	
Largest diff. peak and hole	0.361 and -0.295 e.Å^{-3}	

[a] There are two independent molecules in the asymmetric unit.

Table S2. Crystal data and structure refinement for compound (5*RS*,6*aRS*)-**2j**, Related to **Figure 1** and **Table 1**

Empirical formula	C16 H19 Cl O3 Si	
Formula weight	322.85	
Temperature	296(2) K	
Wavelength	0.71073 Å	
Crystal system	Orthorhombic	
Space group	*Pbca*	
Unit cell dimensions	*a* = 14.7150(17) Å	α= 90°.
	b = 10.6681(12) Å	β= 90°.
	c = 21.569(3) Å	γ = 90°.
Volume	3385.9(7) $Å^3$	
Z	8	
Density (calculated)	1.267 Mg/m^3	
Absorption coefficient	0.303 mm^{-1}	
F(000)	1360	
Crystal size	0.230 x 0.170 x 0.100 mm^3	
Theta range for data collection	2.341 to 27.024°.	
Index ranges	-18<=h<=18, -13<=k<=13, -27<=l<=27	
Reflections collected	69219	
Independent reflections	3661 [*R*(int) = 0.0351]	
Completeness to theta = 25.242°	99.7 %	
Refinement method	Full-matrix least-squares on F^2	
Data / restraints / parameters	3661 / 0 / 190	
Goodness-of-fit on F^2	1.045	
Final *R* indices [*I* >2sigma(*I*)]	R_1 = 0.0338, wR_2 = 0.0910	
R indices (all data)	R_1 = 0.0421, wR_2 = 0.0972	
Largest diff. peak and hole	0.240 and -0.180 e.$Å^{-3}$	

TRANSPARENT METHODS

General experimental methods

Solvents and chemicals were reagent grade and used without further purification. All reactions were analyzed by TLC on silica gel 60 F254 (Merck) and by GLC (Shimadzu GC-2010) using capillary columns with polymethylsilicone +5% phenylsilicone as the stationary phase (HP-5). Column chromatography was performed on silica gel 60 (Merck, 70−230 mesh). Evaporation refers to the removal of solvent under reduced pressure. Melting points are uncorrected. ^{1}H NMR and ^{13}C NMR spectra were recorded at 25 °C on 300 or 500 MHz spectrometers (Bruker DPX Avance 300 or 500, respectively) in $CDCl_3$ solutions with Me_4Si as the internal standard. Chemical shifts (δ) and coupling constants (J) are given in ppm and Hz, respectively. IR spectra were taken with a JASCO FTIR 4200 spectrometer. Mass spectra were obtained using a GC-MS apparatus (Shimadzu QP-2010) at 70 eV ionization voltage. Microanalyses were carried out in our analytical laboratory (Thermo –Fischer Elemental Analyzer Flash 2000).

Preparation of substrates

Substrates **1a-m** were prepared by alkynylation of the appropriate β-hydroxy ketone using an excess of the corresponding alkynylmagnesium bromide (Gabriele et al., 2012), as described below. β-Hydroxy ketones 4-hydroxybutan-2-one and 4-hydroxy-4-methylpentan-2-one were commercially available and were used without further purification. All other necessary β-hydroxy ketones were prepared as described below.

Preparation of β-hydroxy ketones. 4-Hydroxy-3,3-dimethylbutan-2-one was prepared starting from 3-methyl-2-butanone by addition of paraformaldehyde, as reported in the literature (Markó and Schevenels, 2013). β-hydroxy ketones 3-hydroxy-1-phenylbutan-1-one, 1-(4-chlorophenyl)-3-hydroxybutan-1-one, 3-hydroxy-1-*p*-tolylbutan-1-one, 5-hydroxy-2,5-dimethylhexan-3-one, 3-hydroxy-3-methyl-1-phenylbutan-1-one, and 2-(1-hydroxycyclohexyl)-1-phenylethanone were prepared from the corresponding methyl ketones by aldol condensation with acetaldehyde, acetone, or cyclohexanone, according to literature procedures (Chopade et al., 2004; Ma et al., 2014; Martin et al., 1990; Schneider et al., 2006). 4-Hydroxy-3,3-dimethylbutan-2-one (Markó and Schevenels, 2013), 3-hydroxy-1-phenylbutan-1-one (Chopade et al., 2004), 1-(4-chlorophenyl)-3-hydroxybutan-1-one (Ma et al., 2014), 3-hydroxy-1-*p*-tolylbutan-1-one (Martin et al., 1990), 5-

hydroxy-2,5-dimethylhexan-3-one (Schneider et al., 2006), and 3-hydroxy-3-methyl-1-phenylbutan-1-one (Schneider et al., 2006) are known compounds. Characterization data for 2-(1-hydroxycyclohexyl)-1-phenylethanone are given below.

Preparation of 4-hydroxy-3,3-dimethylbutan-2-one (Markó and Schevenels, 2013). To a solution of 3-methyl-2-butanone (8.61 g, 100.0 mmol) in TFA (7.7 mL) was added paraformaldehyde (3.0 g, 100.0 mmol). The mixture was heated at 90 °C for 10 h. After cooling to room temperature, aqueous $NaHCO_3$ (180 mL) was carefully added to the mixture, until the solution turned yellow. The aqueous layer was extracted with CH_2Cl_2 (120 mL, followed by 2 × 60 mL). The collected organic phases were dried over Na_2SO_4, filtered and concentrated. Purification over silica gel using as eluent 8:2 hexane-EtOAc provided pure 4-hydroxy-3,3-dimethylbutan-2-one as a colorless oil (4.53 g, 39%).

Preparation of other β*-hydroxy ketones* (Chopade et al., 2004; Ma et al., 2014; Martin et al., 1990; Schneider et al., 2006). To a stirred solution of diisopropylamine (5.57 g, 55 mmol) in anhydrous diethyl ether (150 mL) cooled to 0°C was slowly added, under nitrogen and dropwise, a 1.6 M solution of *n*-BuLi in hexane (34.4 mL, 55 mmoL). The resulting solution was stirred for 30 min at 0 °C prior to cooling to -78°C. The appropriate methyl ketone (50 mmol; acetophenone, 6.01 g; *p*-chloroacetophenone, 7.73 g; *p*-methylacetophenone, 6.71 g; 3-methylbutan-2-one, 4.31 g) was then slowly added to this solution. The resulting solution was stirred for 1 h at 78°C prior to slow addition of the dry aldehyde or ketone (60 mmoL; acetaldehyde, 2.64 g; acetone, 3.49 g; cyclohexanone, 5.89 g). Stirring was continued for 3 h at -78 °C before the reaction was quenched with saturated aqueous ammonium chloride solution (50 mL). The reaction mixture was then allowed to reach room temperature. The layers were separated, and the aqueous layer was extracted twice with diethyl ether (50 mL). The combined organic layers were dried over Na_2SO_4 and filtered, and the solvent was removed under reduced pressure. Crude products were purified by flash chromatography on silica gel using as eluent 9:1 hexane-acetone for 3-hydroxy-1-phenylbutan-1-one; 8:2 hexane-acetone for 1-(4-chlorophenyl)-3-hydroxybutan-1-one; 9:1 hexane-diethyl ether for 3-hydroxy-1-*p*-tolylbutan-1-one; 7:3 hexane-EtOAc for 5-hydroxy-2,5-dimethylhexan-3-one; 8:2 pentane-diethyl ether for 3-hydroxy-3-methyl-1-phenylbutan-1-one; 9:1 hexane-EtOAc for 2-(1-hydroxycyclohexyl)-1-phenylethanone.

2-(1-Hydroxycyclohexyl)-1-phenylethan-1-one. Yield: 6.44 g, starting from 6.01 g of acetophenone (59%). Colorless solid, mp = 70-71 °C, lit. 78 °C (Yasuda et al., 1998). IR (KBr): ν = 3515 (s), 2937 (m), 2851 (m), 1674 (s), 1447 (m), 1394 (m), 1311 (w), 1219 (w), 1176 (w), 1051 (w), 983 (m), 751 (m), 737 (w), 680 (m) cm^{-1}; ^1H NMR (300 MHz, $CDCl_3$): δ = 7.99-7.93 (m, 2 H, aromatic), 7.63-7.53 (m, 1 H, aromatic), 7.52-7.42 (m, 2 H, aromatic), 3.89 (s, br, 1 H, OH), 3.11 [s, 2 H, $CH_2(CO)$], 1.83-1.64 (m, 4 H, cyclohexane ring), 1.64-1.37 (m, 5 H, cyclohexane ring), 1.37-1.21 (m, 1 H, cyclohexane ring); ^{13}C NMR (75 MHz, $CDCl_3$): δ = 201.9, 137.6, 133.5, 128.7, 128.1, 71.0, 47.8, 37.8, 25.8, 22.0; GC-MS: m/z = 218 (1) [M^+], 200 (7), 176 (4), 162 (18), 147 (5), 120 (27), 105 (100), 91 (3), 77 (30); anal. calcd for $C_{14}H_{18}O_2$ (218.29): C, 77.03; H, 8.31; found: C, 76.06; H, 8.32.

Preparation of 4-yne-1,3-diols 1 (Gabriele et al., 2012). To a suspension of Mg turnings (1.74 g, 71.4 mmol) in anhydrous THF (14.8 mL), maintained under nitrogen and under reflux, was added pure ethyl bromide (1.3 mL, 17,5 mmoL) to start the formation of the Grignard reagent. The remaining bromide was added dropwise in THF solution (3.9 mL, 52.5 mmoL of EtBr in 42.9 mL of THF; total amount of EtBr added 7.63 g, 70.0 mmol). The mixture was then refluxed for an additional 20 min. After cooling, the resulting solution of EtMgBr was transferred under nitrogen into a dropping funnel and added dropwise under nitrogen to a solution of the 1-alkyne (70 mmol: trimethylsilylacetylene, 6.88 g; 1-hexyne, 5.75 g; *tert*-butylacetylene, 5.75 g; phenylacetylene, 7.15 g) in anhydrous THF (21 mL) at 0 °C with stirring. After additional stirring at 0 °C for 15 min, the mixture was warmed to room temperature and then maintained at 40 °C for 2 h. While warm, to the solution of [trimethylsilyl)ethynyl]magnesium bromide or alkynylmagnesium bromide thus obtained was then added dropwise under nitrogen a solution of β-hydroxy ketone (28 mmol; 4-hydroxybutan-2-one, 2.47 g; 4-hydroxy-3,3-dimethylbutan-2-one, 3.25 g; 3-hydroxy-1-phenylbutan-1-one, 4.6 g; 1-(4-chlorophenyl)-3-hydroxybutan-1-one, 5.56 g; 3-hydroxy-1-*p*-tolylbutan-1-one, 4.99 g; 4-hydroxy-4-methylpentan-2-one, 3.25 g; 5-hydroxy-2,5-dimethylhexan-3-one, 4.04 g; 3-hydroxy-3-methyl-1-phenylbutan-1-one, 4.99 g; 2-(1-hydroxycyclohexyl)-1-phenylethanone, 6.11 g) in anhydrous THF (34 mL). The resulting mixture was stirred at 40 °C for an additional 2 h. After the mixture was cooled to room temperature, saturated NH_4Cl (80 mL) and EtOAc (30 mL) were sequentially added. Phases were separated, and the aqueous phase was extracted with EtOAc (3 × 80 mL). The collected organic layers were washed with brine and dried over Na_2SO_4. After filtration and evaporation of the solvent, the product was purified by column chromatography on silica gel using as eluent 8:2 hexane-EtOAc for **1a**, **1f**, **1i**, **1j**; 9:1 hexane-EtOAc for **1b**, **1c**, **1d**; 7:3 hexane-EtOAc for **1e**, **1h**, **1l**; 95:5 hexane-EtOAc for **1g**, **1k**, **1m.**

*3-Methylnon-4-yne-1,3-diol (**1a**).* Yield: 3.77 g, starting from 2.47 g of 4-hydroxybutan-2-one (79%). Colorless oil. IR (film): ν = 3361 (s, br), 2967 (s), 2931 (s), 2864 (m), 2235 (w), 1453 (m), 1427 (m), 1376 (m), 11330 (w), 1269 (w), 1141 (m), 1090 (m), 1053 (m), 890 (w) cm^{-1}; ^1H NMR (300 MHz,

$CDCl_3$): δ =4.19-4.07 (m, 1 H, HOC*H*H), 3.88 (dt, *J* = 11.0, 4.5, 1H, HOCH*H*), 3.52 (s br, 2H, 2 OH), 2.21 (t, *J* = 6.9, 2 H, ≡CCH_2), 2.02-1.89 (m, 1 H, HOCH$_2$C*H*H), 1.84-1.75 (m, 1 H, HOCH$_2$CH*H*), 1.55-1.33 (m, 4 H, CH_2CH_2CH$_3$), 1.49 (s, 3 H, MeCOH), 0.91 (t, *J* =7.1, 3 H, CH$_2$CH_3); ^{13}C NMR (75 MHz, $CDCl_3$): δ = 84.5, 83.3, 68.8, 60.6, 44.1, 31.1, 30.8, 22.0, 18.3, 13.6; GC-MS: *m/z* = 170 (absent) [M$^+$], 155 (3), 137 (2), 125 (100), 109 (11), 91 (7), 81 (8), 73 (13), 65 (4), 55 (8); anal. calcd for $C_{10}H_{18}O_2$ (170.25): C, 70.55; H, 10.66; found: C, 70.68; H, 10.65.

*2,4-Dimethyldec-5-yne-2,4-diol (**1b**).* Yield: 3.22 g, starting from 3.25 g of 4-hydroxy-4-methylpentan-2-one (58%). Yellow oil. IR (film): *ν* = 3350 (s, br), 2982 (s), 2936 (s), 2875 (m), 2240 (w), 1473 (m), 1417 (m), 1386 (s), 1366 (s), 1330 (m), 1289 (m), 1187 (s), 1074 (m), 896 (m) cm^{-1}; ^{1}H NMR (300 MHz, $CDCl_3$): δ = 4.16 (s, br, 1 H, OH), 3.41 (s br, 1 H, OH), 2.20 (t, *J* = 7.0, 2 H, ≡CCH_2), 1.97-1.82 (m, 2 H, CH_2COH), 1.53-1.32 (m, 4 H, CH_2CH_2CH$_3$), 1.52 (s, 3 H, Me), 1.50 (s, 3 H, Me), 1.29 (s, 3 H, Me), 0.90 (t, *J* = 6.8, 3 H, CH$_2$CH_3); ^{13}C NMR (75 MHz, $CDCl_3$): δ =85.0, 84.8, 72.2, 67.3, 52.8, 33.7, 32.4, 30.6, 29.7, 22.0, 18.4, 13.6; GC-MS: *m/z* = 198 (absent) [M$^+$], 183 (2), 165 (19), 151 (6), 142 (5), 138 (6), 125 (100), 109 (33), 107 (19), 93 (15), 91 (10), 81 (13), 79 (22), 69 (11), 59 (25); anal. calc for $C_{12}H_{22}O_2$ (198.30): C, 72.68; H, 11.18; found: C, 72.79; H, 11.15.

*2,4,7,7-Tetramethyloct-5-yne-2,4-diol (**1c**).* Yield: 2.67 g, starting from 3,25 g of 4-hydroxy-4-methylpentan-2-one (48%). White solid, mp 53.2-54.2 °C. IR (KBr): *ν* = 3335 (m, br), 2971 (s), 2936 (m), 2868 (m), 2228 (w), 1457 (m), 1361 (m), 1266 (m), 1191 (s), 1066 (m), 983 (m), 945 (w), 893 (m), 851 (m) cm^{-1}; ^{1}H NMR (300 MHz, $CDCl_3$): δ = 3.71 (s, br, 1 H, OH), 1.97-1.82 (m, 2 H, CH_2COH), 1.51 (s, 3 H, Me), 1.49 (s, 3 H, Me), 1.29 (s, 3 H, Me), 1.21 (s, 9 H, *t*-Bu); ^{13}C NMR (75 MHz, $CDCl_3$): δ = 93.1, 83.1, 72.1, 67.2, 52.9, 33.7, 32.3, 30.8, 29.8, 27.3; GC-MS: *m/z* = 198 (absent) [M$^+$], 183 (5), 165 (55), 137 (12), 125 (100), 109 (48), 107 (71), 91 (22), 81 (21), 59 (26); anal. calc for $C_{12}H_{22}O_2$ (198.30): C, 72.68; H, 11.18; found: C, 72.76; H, 11.15.

*2,4-Dimethyl-6-phenylhex-5-yne-2,4-diol (**1d**).* Yield: 3.30 g, starting from 3,25 g of 4-hydroxy-4-methylpentan-2-one (54%). White solid, mp 57-58 °C. IR (film): *ν* = 3337 (s, br), 2975 (s), 2932 (m), 2235 (w), 1598 (w), 1490 (m), 1368 (m), 1297 (w), 1260 (m), 1184 (s), 1068 (m), 897 (m), 873 (m), 757 (s), 691 (s) cm^{-1}; ^{1}H NMR (300 MHz, $CDCl_3$): δ = 7.44-7.36 (m, 2 H, aromatic), 7.32-7.22 (m, 2 H, aromatic), 4.87 (s, br, 1 H, OH), 3.48 (s, br, 1 H, OH), 2.07-1.92 (m, 2 H, CH_2COH), 1.63 (s, 3 H, Me), 1.62 (s, 3 H, Me), 1.31 (s, 3 H, Me); ^{13}C NMR (75 MHz, $CDCl_3$): δ = 131.6, 128.4, 128.3, 123.3, 94.2, 84.5, 72.4, 67.8, 53.3, 33.3, 32.8, 29.9; GC-MS: *m/z*= 218 (absent) [M$^+$], 200 (16), 185 (38), 162 (18), 157 (7), 145 (100), 129 (96), 119 (22), 115 (21), 102 (11), 91 (34), 77 (11), 59 (19); anal. calc for $C_{14}H_{18}O_2$ (218.29): C, 77.03; H, 8.31; found: C, 77.16; H, 8.34.

*3-Methyl-5-(trimethylsilyl)pent-4-yne-1,3-diol (**1e**).* Yield: 3.44 g, starting from 2.47 g of 4-hydroxybutan-2-one (66%). White solid, mp 34-35 °C. IR (KBr): ν = 3399 (s, br), 3193 (m), 2963 (w), 2168 (w), 1637 (m), 1402 (m), 1286 (w), 1247 (m), 1125 (m), 930 (m), 842 (s), 759 (m) cm^{-1}; ^1H NMR (300 MHz, $CDCl_3$): δ = 4.20-4.09 (m, 1 H, HOC*H*H), 3.94-3.86 (m, 1 H, HOCH*H*), 3.69 (s, br, 2 H, 2 O*H*), 2.00-1.92 (m, 1 H, $HOCH_2C$*H*H), 1.85-1.78 (m, 1 H, $HOCH_2CH$*H*), 1.52 (s, 3 H, Me), 0.17 (s, 9 H, $SiMe_3$); ^{13}C NMR (75 MHz, $CDCl_3$): δ = 109.1, 88.1, 68.9, 60.5, 43.9, 30.7, 0.0; GC-MS: *m/z* = 186 (absent) [M^+], 171 (4), 153 (6), 141 (100), 125 (14), 123 (34), 101 (13), 75 (18); anal. calcd for $C_9H_{18}O_2Si$ (186.32): C, 58.02; H, 9.74; Si,15.07; found: C, 58.05; H, 9.75; Si,15.09.

*2,2,3-Trimethyl-5-(trimethylsilyl)pent-4-yne-1,3-diol (**1f**)*. Yield: 4.5 g, starting from 3.25 g of 4-hydroxy-3,3-dimethylbutan-2-one (75%). White solid, mp 45-46 °C. IR (KBr): ν = 3335 (s, br), 2963 (s), 2898 (m), 2875 (m), 2167 (m), 1474 (m), 1393 (m), 1251 (s), 1192 (w), 1145 (m), 1111 (m), 1042 (m), 935 (m), 860 (s), 842 (s), 816 (m) cm^{-1}; ^1H NMR (300 MHz, $CDCl_3$): δ = 3.94 (d, *J* = 10.8, 1 H, HOC*H*H), 3.72 (s, br, 2 H, 2O*H*), 3.49 (d, *J* = 10.8, 1 H, HOCH*H*), 1.44 (s, 3 H, Me), 1.05 (s, 3 H, Me), 0.98 (s, 3H, Me), 0.17 (s, 9 H, $SiMe_3$); ^{13}C NMR (75 MHz, $CDCl_3$): δ = 108.9, 88.3, 75.0, 71.4, 40.8, 25.2, 21.8, 19.2, –0.05; GC-MS: *m/z* = 214 (absent) [M^+], 181 (35), 165 (4), 151 (10), 141 (100), 127 (8), 101 (24), 99 (23), 83 (12), 75 (36), 73 (44); anal. calcd for $C_{11}H_{22}O_2Si$ (214.38): C, 61.63; H, 10.34; Si, 13.10; found: C, 61.76; H, 10.31; Si, 13.12.

*2,4-Dimethyl-6-(trimethylsilyl)hex-5-yne-2,4-diol (**1g**).* Yield: 2.46 g, starting from 3.25 g of 4-hydroxy-4-methylpentan-2-one (41%). White solid, mp 69-70 °C. IR (KBr): ν = 3335 (m, br), 2971 (s), 2936 (m), 2167 (m), 1408 (m), 1368 (m), 1251 (s), 1191 (s), 1066 (w), 965 (w), 932 (w), 878 (s), 843 (s) cm^{-1}; ^1H NMR (300 MHz, $CDCl_3$): δ = 3.91 (s, br, 2 H, 2 O*H*), 1.97-1.84 (m, 2 H, CH_2COH), 1.54 (s, 3 H, Me), 1.51 (s, 3 H, Me), 1.29 (s, 3 H, Me), 0.15 (s, 9 H, $SiMe_3$); ^{13}C NMR (75 MHz, $CDCl_3$): δ = 110.5, 88.5, 72.4, 67.3, 52.5, 33.1, 32.5, 29.5, –0.25; GC-MS: *m/z* = 214 (0.2) [M^+], 199 (2), 181 (61), 143 (34), 141 (96), 138 (24), 125 (73), 123 (100), 101 (30), 99 (41), 97 (22), 83 (41), 75 (59), 73 (76); 59 (40); anal. calc for $C_{11}H_{22}O_2Si$ (214.38): C, 61.63; H, 10.34; Si, 13.10; found: C, 61.60; H, 10.36; Si, 13.13.

*4-Isopropyl-2-methyl-6-(trimethylsilyl)hex-5-yne-2,4-diol (**1h**).* Yield: 3.26 g, starting from 4.04 g of 5-hydroxy-2,5-dimethylhexan-3-one (48%). White solid, mp 82-83 °C. IR (KBr): ν = 3230 (s, br), 2973 (s), 2916 (m), 2875 (m), 2164 (m), 1471 (m), 1409 (m), 1249 (m), 1195 (w), 1158 (w), 1062 (m), 1018 (m), 880 (m), 840 (s), 760 (m) cm^{-1}; ^1H NMR (300 MHz, $CDCl_3$): δ = 1.95-1.70 (m, 3 H, CH_2 + C*H*Me_2), 1.54 (s, 3 H, Me), 1.30 (s, 3 H, Me), 1.03 (d, *J* = 6.7, 3 H, C$H_3$$CHCH_3$), 0.97 (d, *J* = 6.7, 3 H, CH_3CHC*H_3*), 0.16 (s, 9 H, $SiMe_3$); ^{13}C NMR (75 MHz, $CDCl_3$): δ = 108.2, 90.8, 73.9, 72.3, 48.7, 40.4, 32.6, 29.8, 17.6, 16.8, –0.2; GC-MS: *m/z* = 242 (absent) [M^+], 224 (1), 209 (7), 199 (4), 181 (18), 169 (15), 151 (52), 141 (54), 125 (100), 97 (20), 83 (21), 75 (28), 73 (81), 59 (34); anal. calc for $C_{13}H_{26}O_2Si$ (242.43): C, 64.41; H, 10.81; Si, 11.59; found: C, 64.44; H, 10.80; Si, 11.56.

*4-Phenyl-6-(trimethylsilyl)hex-5-yne-2,4-diol (**1i**)*. Mixture of diastereomers, total yield: 4.12 g, starting from 4.6 g of 3-hydroxy-1-phenylbutan-1-one (56%). Column chromatography (8:2 hexane-Et_2O) gave three fractions containing pure (2*RS*,4*SR*) diastereomer (yield: 810 mg, 11%), a mixture (2*RS*,4*SR*)/(2*RS*,4*RS*) diastereomers (DR ca. 2.2, determined by ^{1}H NMR; total yield: 2.06 g, 28%), and pure (2*RS*,4*RS*) diastereomer (yield: 1.25 g, 17%).

(*2RS,4SR*) Diastereomer. White solid, mp 64-65 °C. IR (KBr): *v* = 3226 (s, br), 2964 (m), 2908 (w), 2168 (m), 1447 (m), 1426 (m), 1313 (w), 1252 (m), 1134 (m), 1086 (m), 914 (w), 893 (m), 776 (s), 759 (s), 699 (m), 669 (m) cm^{-1}; ^{1}H NMR (300 MHz, $CDCl_3$): δ = 7.68-7.59 (m, 2 H, aromatic), 7.40-7.22 (m, 3 H, aromatic), 4.66 (s, br, 1 H, OH), 4.61-4.47 (m, 1 H, C*H*CH_3), 3.63 (s, br, 1 H, OH), 1.91 (dist dd, *J* = 14.5, 10.0, 1 H, C*H*H), 1.77 (dist d, br, *J* = 14.5, 1 H, CH*H*), 1.19 (d, *J* = 6.2, 3 H, Me), 0.22 (s, 9 H, $SiMe_3$); ^{13}C NMR (75 MHz, $CDCl_3$): δ = 144.9, 128.2, 127.6, 125.2, 107.2, 91.1, 74.0, 67.0, 52.4, 23.8, –0.06; GC-MS: *m/z* = 262 (absent) [M^+], 243 (2), 229 (4), 217 (2), 203 (100), 187 (11), 185 (8), 161 (6), 159 (4), 135 (7), 125 (5), 105 (8), 77 (4), 73 (9); anal. calcd for $C_{15}H_{22}O_2Si$ (262.42): C, 68.65; H, 8.45; Si, 10.70; found: C, 68.89; H, 8.43; Si, 10.69.

(*2RS,4RS*) Diastereomer. Colorless oil. IR (film): *v* = 3323 (s, br), 2966 (m), 2168 (m), 1448 (w), 1423 (w), 1251 (m), 1139 (m), 1071 (m), 840 (s), 701 (m) cm^{-1}; ^{1}H NMR (300 MHz, $CDCl_3$): δ = 7.64-7.49 (m, 2 H, aromatic), 7.45-7.24 (m, 3 H, aromatic), 3.93-3.83 (m, 1 H, C*H*CH_3), 3.72 (s, br, 1 H, OH), 3.18 (s, br, 1 H, OH), 2.19 (dist dd, *J* = 14.6, 9.7, 1 H, C*H*H), 1.99 (dist dd, *J* = 14.6, 1.6, 1 H, CH*H*), 1.11 (d, *J* = 6.3, 3 H, Me), 0.19 (s, 9 H, $SiMe_3$); ^{13}C NMR (75 MHz, $CDCl_3$): δ = 144.0, 128.3, 127.6, 125.3, 108.5, 90.4, 72.5, 65.0, 52.6, 23.6, –0.25; GC-MS: *m/z* = 262 (absent) [M^+], 243 (1), 229 (5), 217 (1), 203 (100), 187 (10), 185 (7), 161 (7), 159 (4), 135 (8), 125 (5), 105 (10), 77 (5), 73 (10); anal. calcd for $C_{15}H_{22}O_2Si$ (262.42): C, 68.65; H, 8.45; Si, 10.70; found: C, 68.68; H, 8.46; Si, 10.64.

*4-(4-chlorophenyl)-6-(trimethylsilyl)hex-5-yne-2,4-diol (**1j**)*. Mixture of diastereomers, total yield: 5.90 g, starting from 5.56 g of 1-(4-chlorophenyl)-3-hydroxybutan-1-one (71%). Column chromatography (8:2 hexane-Et_2O) gave three fractions containing pure (2*RS*,4*SR*) diastereomer (yield: 2.50 g, 30%), a mixture (2*RS*,4*SR*)/(2*RS*,4*RS*) diastereomers (DR ca. 1.4, determined by ^{1}H NMR; total yield: 2.01 g, 24%), and pure (2*RS*,4*RS*) diastereomer (yield: 1.43 g, 17%).

(*2RS,4SR*) Diastereomer. White solid, mp 80-81 °C. IR (KBr): *v* = 3203 (s, br), 2965 (m), 2912 (m), 2897 (w), 2167 (m), 1489 (m), 1425 (m), 1400 (m), 1273 (m), 1252 (m), 1160 (m), 1132 (m), 1085 (m), 963 (m), 861 (s), 845 (s), 816 (m) cm^{-1}; ^{1}H NMR (300 MHz, $CDCl_3$): δ = 7.60-7.51 (m, 2 H, aromatic), 7.35-7.27 (m, 2 H, aromatic), 4.72 (s, br, 1 H, OH), 4.62-4.85 (m, 1 H, HOC*H*CH_3), 3.16 (s br, 1 H, OH), 1.88 (dist dd, *J* = 14.5, 10.0, 1 H, C*H*H), 1.76 (dist dd, *J* = 14.5, 1.9, 1 H, CH*H*), 1.21 (d, *J* = 6.3, 3 H, HOC*H*CH_3), 0.22 (s, 9 H, $SiMe_3$); ^{13}C NMR (75 MHz, $CDCl_3$): δ = 143.9, 133.8, 128.5, 127.0, 107.4, 91.8, 73.6, 67.2, 52.9, 24.2, 0.0; GC-MS: *m/z* = 296 (absent) [M$^+$], 278 (1), 263 (2), 251 (1), 240 (7), 237 (100), 221 (22), 219 (29), 195 (8), 169 (9), 152 (2), 139 (12), 125 (3), 111 (4), 99 (5), 75 (10), 73 (15); anal. calcd for $C_{15}H_{21}ClO_2Si$ (296.86): C, 60.69; H, 7.13; Cl, 11.94; Si, 9.46; found: C, 60.81; H, 7.11; Cl, 11.88; Si, 9.41.

(*2RS,4RS*) Diastereomer. White solid, mp 75-76 °C. IR (KBr): *ν* = 3392 (s), 3211 (s, br), 2962 (m), 2166 (m), 1490 (m), 1404 (m), 1249 (m), 1186 (m), 1136 (s), 1008 (s), 958 (m), 895 (m), 848 (s), 816 (m), 763 (m), 726 (m) cm^{-1}; ^{1}H NMR (300 MHz, $CDCl_3$): δ = 7.54-7.44 (m, 2 H, aromatic), 7.37-7.27 (m, 2 H, aromatic), 4.17 (s, br, 1 H, OH), 3.91-3.72 (m, 1 H, C*H*CH_3), 3.26 (s, br, 1 H, OH), 2.18 (dist dd, *J* = 14.6, 9.8, 1H, C*H*H), 1.96 (dist d, *J* = 14.6, 1 H, CH*H*), 1.11 (d, *J* = 6.3, 3 H, Me), 0.19 (s, 9 H, $SiMe_3$); ^{13}C NMR (75 MHz, $CDCl_3$): δ = 142.7, 133.4, 128.4, 126.8, 108.1, 90.4, 72.1, 65.0, 52.3, 23.6, –0.25; GC-MS: *m/z* = 296 (absent) [M$^+$], 239 (39), 237 (100), 221 (17), 219 (15), 195 (10), 169 (13), 141 (8), 139 (19), 125 (5), 111 (7), 99 (10), 83 (6), 75 (20), 73 (26); anal. calcd for $C_{15}H_{21}ClO_2Si$ (296.86): C, 60.69; H, 7.13; Cl, 11.94; Si, 9.46; found: C, 60.73; H, 7.12; Cl, 11.91; Si, 9.47.

*4-(p-Tolyl)-6-(trimethylsilyl)hex-5-yne-2,4-diol (**1k**).* Mixture of diastereomers, total yield: 3.87 g, starting from 4.99 g of 3-hydroxy-1-(*p*-tolyl)butan-1-one (50%). Column chromatography (8:2 hexane-Et_2O) gave three fractions containing pure (2*RS*,4*SR*) diastereomer (yield: 1.70 g, 22%), a mixture (2*RS*,4*SR*)/(2*RS*,4*RS*) diastereomers (DR ca. 1.0, determined by ^{1}H NMR; total yield: 1.01 g, 13%), and pure (2*RS*,4*RS*) diastereomer (yield: 1.16 g, 15%).

(*2RS,4SR*) Diastereomer. White solid, mp 63-64 °C. IR (KBr): *ν* = 3336 (m, br), 2965 (s), 2920 (m), 2167 (m), 1510 (w), 1422 (m), 1376 (m), 1311 (w), 1250 (m), 1132 (m), 1086 (m), 962 (m), 844 (s), 760 (m) cm^{-1}; ^{1}H NMR (300 MHz, $CDCl_3$): δ = 7.56-7.44 (m, 2 H, aromatic), 7.20-7.10 (m, 2 H, aromatic), 4.61-4.44 (m, 1 H, HOC*H*CH_3), 4.30 (s, br, 1 H, OH), 3.50 (s, br, 1 H, OH), 2.34 (s, 3 H, $C_6H_4CH_3$), 1.92 (dist dd, *J* = 14.5, 10.1, 1 H, C*H*H), 1.78 (dist dd, *J* = 14.5, 1.8, 1 H, CH*H*), 1.20 (d, *J* = 6.3, 3 H, HOCHC*H*$_3$), 0.22 (s, 9 H, $SiMe_3$); ^{13}C NMR (75 MHz, $CDCl_3$): δ = 142.1, 137.3, 128.9, 125.1, 107.3, 91.0, 73.9, 66.9, 52.4, 23.8, 21.0, –0.05; GC-MS: *m/z* = 276 (absent) [M$^+$], 243 (2), 231 (2), 217 (100), 201 (7), 175 (4), 149 (4), 119 (9), 97 (3), 75 (6), 73 (9); anal. calcd for $C_{16}H_{24}O_2Si$ (276.45): C, 69.51; H, 8.75; Si, 10.16; found: C, 69.54; H, 8.76; Si, 10.19.

<u>(*2RS,4RS*) Diastereomer.</u> White solid, mp 85-86 °C. IR (KBr): *ν* = 3335 (m, br), 2965 (m), 2921 (m), 2169 (m), 1421 (m), 1250 (m), 1140 (m), 1089 (m), 844 (s), 770 (m) cm^{-1}; ^{1}H NMR (300 MHz, $CDCl_3$): δ = 7.50-7.42 (m, 2 H, aromatic), 7.21-7.13 (m, 2 H, aromatic), 3.99-3.85 (m, 1 H, $HOCHCH_3$), 3.47 (s, br, 1 H, OH), 3.10 (s, br, 1 H, OH), 2.36 (s, 3 H, $C_6H_4CH_3$), 2.18 (dist dd, *J* = 14.5, 9.6, 1 H, C*H*H), 1.98 (dist dd, *J*= 14.5, 1.7, 1 H, CH*H*), 1.12 (d, *J* = 6.3, 3 H, $HOCHCH_3$), 0.19 (s, 9 H, $SiMe_3$); ^{13}C NMR (75 MHz, $CDCl_3$): δ = 141.1, 137.4, 129.0, 125.2, 108.6, 90.3, 72.4, 64.9, 52.6, 23.6, 21.0, –0.21; GC-MS: *m/z* = 276 (absent) [M^+], 243 (2), 231 (1), 217 (100), 201 (8), 175 (5), 149 (6), 125 (8), 119 (12), 97 (5), 91 (8), 75 (8), 73 (12); anal. calcd for $C_{16}H_{24}O_2Si$ (276.45): C, 69.51; H, 8.75; Si, 10.16; found: C, 69.45; H, 8.77; Si, 10.15.

*2-Methyl-4-phenyl-6-(trimethylsilyl)hex-5-yne-2,4-diol (**1l**)*. Yield: 4.49 g, starting from 4.99 g of 3-hydroxy-3-methyl-1-phenylbutan-1-one (58%). White solid, mp 80-81 °C. IR (KBr): *ν* = 3304 (m, br), 2968 (m), 2920 (m), 2169 (m), 1448 (w), 1250 (m), 1174 (m), 1049 (m), 875 (s), 844 (s), 689 (m) cm^{-1}; ^{1}H NMR (500 MHz, $CDCl_3$): δ = 7.67-7.61 (m, 2 H, aromatic), 7.37-7.31 (m, 2 H, aromatic), 7.29-7.23 (m, 1 H, aromatic), 4.61 (s, br, 1 H, OH), 3.41 (s, br, 1 H, OH), 2.12-1.99 (m, 2 H, CH_2), 1.56 (s, 3 H, Me), 1.21 (s, 3 H, Me), 0.19 (s, 9 H, $SiMe_3$); ^{13}C NMR (126 MHz, $CDCl_3$): δ = 146.1, 128.2, 127.4, 125.2, 109.0, 91.5, 72.6, 72.5, 55.2, 32.2, 29.7, –0.3; GC-MS: *m/z* = 276 (absent) [M^+], 258 (1), 243 (25), 203 (100), 187 (14), 185 (30), 161 (11), 159 (14), 135 (12), 125 (9), 105 (21), 99 (8), 77 (14), 75 (17), 73 (31); anal. calc for $C_{16}H_{24}O_2Si$ (276.45): C, 69.51; H, 8.75; Si, 10.16; found: C, 69.54; H, 8.77; Si, 10.13.

*1-(2-Hydroxy-2-phenyl-4-(trimethylsilyl)but-3-yn-1-yl)cyclohexan-1-ol (**1m**)*. Yield: 5.5 g, starting from 6.11 g of 2-(1-hydroxycyclohexyl)-1-phenylethan-1-one (62%). White solid, mp = 67-68 °C. IR (KBr): *ν* = 3228 (m, br), 2933 (s), 2861 (m), 2167 (m), 1458 (m), 1249 (m), 1163 (m), 1074 (w), 1031 (w), 982 (w), 972 (s), 842 (m), 700 (m) cm^{-1}; ^{1}H NMR (300 MHz, $CDCl_3$): δ = 7.69-7.62 (m, 2 H, aromatic), 7.40-7.30 (m, 2 H, aromatic), 7.30-7.20 (m, 1 H, aromatic), 4.78 (s, br, 1 H, OH), 2.94 (s, 1 H, OH), 2.21-1.82 (m, 4 H, CH_2COH + 2 H on cyclohexane ring), 1.70-1.29 (m, 8 H on cyclohexane ring) 0.19 (s, 9 H, $SiMe_3$); ^{13}C NMR (75 MHz, $CDCl_3$): δ = 146.2, 128.2, 127.4, 125.2, 109.2, 91.1, 73.8, 72.3, 53.5, 40.5, 37.7, 25.5, 22.6, 22.3, –0.3; GC-MS: *m/z* = 316 (absent) [M^+], 298 (3), 283 (4), 255 (5), 203 (100), 185 (30), 161 (5), 159 (7), 135 (6), 105 (9), 73 (14); anal. calc for $C_{19}H_{28}O_2Si$ (316.51): C, 72.10; H, 8.92; Si, 8.87; found: C, 72.25; H, 8.90; Si, 8.84.

General procedure for the palladium-catalyzed carbonylative double cyclization leading to dihydrofurofuranones 2

A 250 mL stainless steel autoclave was charged in the presence of air with PdI_2 (5.0 mg, 1.39 × 10^{-2} mmol), KI (11.5 mg, 6.95 × 10^{-2} mmol) and a solution of **1** (0.7 mmol; **1a**, 119.2 mg; **1b**, 138.8 mg; **1c**, 138.8 mg; **1d**, 152.8 mg; **1e**, 130.4 mg; **1f**, 150.1 mg; **1g**, 150.1 mg; **1h**, 169.7 mg; **1i**, 183.7 mg; **1j**, 207.8 mg; **1k**, 193.5 mg; **1l**, 193.5 mg; **1m**, 221.6 mg) in MeOH (14 mL). The autoclave was sealed and, while the mixture was stirred, the autoclave was pressurized with CO (32 atm) and air (up to 40 atm). After being stirred at 100°C for the required time (3 h for **1e**, **1f**, **1g**, **1h**, **1l**, and **1m**; 5 h for **1k**; 15 h for **1a**, **1b**, **1c**, **1d**, **1i**, and **1j**) the autoclave was cooled, degassed and opened. The solvent was evaporated and the products were purified by column chromatography on neutral alumina using as eluent hexane to hexane/EtOAc 9:1.

3-Butyl-6*a*-methyl-6,6*a*-dihydrofuro[3,2-*b*]furan-2(5*H*)-one (2a). Yield: 41.2 mg, starting from 119.2 mg of 3-methylnon-4-yne-1,3-diol **1a** (30%) (Scheme 2). Colorless oil. IR (film): *ν* = 2967 (m), 2941 (m), 2864 (w), 1754 (s), 1698 (s), 1463 (w), 1402 (m), 1279 (m), 1223 (m), 1135 (w), 1069 (m), 987 (m), 864 (w) cm^{-1}; ^{1}H NMR (300 MHz, $CDCl_3$): 4.82-4.60 (m, 2 H, CH_2O), 2.27-2.02 (m, 4 H, CH_2CH_2O + $CH_2CH_2CH_2CH_3$), 1.60-1.43 (m, 2 H, $CH_2CH_2CH_3$), 1.54 (s, 3 H, Me), 1.40-1.22 (m, 2 H, CH_2CH_3), 0.91 (t, J = 7.2, 3 H, CH_2CH_3); ^{13}C NMR (75 MHz, $CDCl_3$): δ = 182.9, 175.1, 98.7, 82.2, 77.8, 34.8, 29.6, 23.5, 22.4, 21.8, 13.8; GC-MS: *m/z* = 196 (4) [M^+], 181 (28), 165 (40), 154 (28), 153 (28), 151 (61), 136 (8), 125 (100), 108 (18), 99 (17), 79 (7), 69 (8), 57 (42); anal. calcd for $C_{11}H_{16}O_3$ (196,24): C, 67.32; H, 8.22; found: C, 67.29; H, 8.24.

3-Butyl-5,5,6*a*-trimethyl-6,6*a*-dihydrofuro[3,2-*b*]furan-2(5*H*)-one (2b). Yield: 72.2 mg, starting from 138.8 mg of 2,4-dimethyldec-5-yne-2,4-diol **1b** (46%) (Scheme 2). Yellow oil. IR (film): *ν* = 2959 (m), 2933 (m), 2873 (w), 1761 (s), 1695 (s), 1456 (m), 1384 (m), 1372 (w), 1286 (w), 1262 (w), 1225 (w), 1110 (m), 1070 (w), 838 (w), 773 (m), cm^{-1}; ^{1}H NMR (300 MHz, $CDCl_3$): δ = 2.20-2.10 (m, 3 H, CHH+ $CH_2CH_2CH_2CH_3$), 1.98 (dist d, J = 12.5, 1 H, CH*H*), 1.62 (s, 6 H, CH_3CCH_3), 1.56-1.44 (m, 2 H, $CH_2CH_2CH_3$), 1.48 (s, 3 H, Me), 1.37-1.24 (m, 2 H, CH_2CH_3), 0.91 (t, J = 7.3, 3 H, CH_2CH_3); ^{13}C NMR (75 MHz, $CDCl_3$): δ = 181.7, 175.2, 100.0, 97.5, 83.6, 45.5, 31.5, 29.7, 28.0, 27.2, 22.4, 21.7, 13.8; GC-MS: *m/z* = 224 (2) [M^+], 209 (3), 196 (16), 181 (3), 169 (72), 125 (100), 99 (7), 83 (6), 69 (3); anal. calcd for $C_{13}H_{20}O_3$ (224.30): C, 69.61; H, 8.99; found: C, 69.64; H, 8.97.

3-(*tert*-Butyl)-5,5,6*a*-trimethyl-6,6*a*-dihydrofuro[3,2-*b*]furan-2(5*H*)-one (2c). Yield: 62.8 mg, starting from 138.8 mg of 2,4,7,7-tetramethyloct-5-yne-2,4-diol **1c** (40%) (Scheme 2). White solid, mp= 65-66 °C. IR (KBr): *ν* = 2976 (m), 2870 (w), 1753 (s), 1680 (s), 1456 (m), 1351 (s), 1298 (m), 1261 (m), 1091 (m), 991 (m), 843 (w), 777 (w), cm^{-1}; ^1H NMR (300 MHz, $CDCl_3$): δ = 2.10 (dist d, *J* = 12.5, 1 H, C*H*H), 1.95 (dist d, *J* = 12.5, 1 H, CH*H*), 1.61 (s, 3 H, Me), 1.60 (s, 3 H, Me), 1.47 (s, 3 H, Me), 1.25 (s, 9 H, *t*-Bu); ^{13}C NMR (75 MHz, $CDCl_3$): δ = 179.9, 173.5, 108.2, 96.8, 82.9, 45.2, 31.4, 30.7, 28.7, 28.0, 27.4; GC-MS: *m/z* = 224 (4) [M^+], 209 (10), 196 (3), 169 (25), 168 (14), 153 (54), 125 (30), 113 (7), 99 (5), 83 (10), 57 (100); anal. calcd for $C_{13}H_{20}O_3$ (224.30): C, 69.61; H, 8.99; found: C, 69.58; H, 9.01.

5,5,6*a*-Trimethyl-3-phenyl-6,6*a*-dihydrofuro[3,2-*b*]furan-2(5*H*)-one (2d). Yield: 56.4 mg, starting from 152.8 mg of 2,4-dimethyl-6-phenylhex-5-yne-2,4-diol **1d** (33%) (Scheme 2). White solid, mp= 94-95 °C. IR (KBr): *ν* = 2979 (m), 2929 (w), 1746 (s), 1667 (s), 1449 (m), 1388 (m), 1368 (m), 1268 (m), 1200 (w), 1185 (m), 1134 (w), 1091 (m), 1071 (m), 939 (m), 781 (m), 694 (m), cm^{-1}; ^1H NMR (300 MHz, $CDCl_3$): δ = 7.98-7.90 (m, 2 H, aromatic), 7.43-7.34 (m, 2 H, aromatic), 7.31-7.21 (m, 2 H, aromatic), 2.24 (d, *J* = 12.5, 1 H, C*H*H), 2.10 (d, *J* = 12.5, 1 H, CH*H*), 1.74 (s, 3 H, Me), 1.73 (s, 3 H, Me), 1.53 (s, 3 H, Me); ^{13}C NMR (75 MHz, $CDCl_3$): δ = 182.0, 172.4, 129.3, 128.4, 127.3, 126.8, 99.6, 99.2, 83.6, 45.4, 31.9, 28.0, 27.6; GC-MS: *m/z* = 244 (23) [M^+], 189 (31), 188 (62), 145 (100), 133 (4), 117 (11), 89 (27), 63 (6); anal. calcd for $C_{15}H_{16}O_3$ (244.29): C, 73.75; H, 6.60; found: C, 73.81; H, 6.63.

6*a*-Methyl-3-(trimethylsilyl)-6,6*a*-dihydrofuro[3,2-*b*]furan-2(5*H*)-one (2e). Yield: 107.0 mg, starting from 130.4 mg of 3-methyl-5-(trimethylsilyl)pent-4-yne-1,3-diol **1e** (72%) (Figure 1). White solid, mp = 71-72. °C. IR (KBr): *ν* = 2961 (w), 1741 (s), 1636 (s), 1446 (w), 1390 (m), 1302 (m), 1279 (m), 1238 (s), 1181 (m), 1141 (w), 977 (w), 845 (s), 780 (m) cm^{-1}; ^1H NMR (500 MHz, $CDCl_3$): δ = 4.82-4.74 (m, 1H, OC*H*H), 4.73-4.64 (m, 1H, OCH*H*), 2.28-2.19 (m, 2 H, CH_2CH$_2$O), 1.53 (s, 3 H, Me), 0.22 (s, 9 H, $SiMe_3$); ^{13}C NMR (126 MHz, $CDCl_3$): δ = 198.2, 178.4, 95.3, 85.3, 79.4, 36.3, 25.1, –0.02; GC-MS: *m/z* = 212 (7) [M^+], 197 (100), 153 (3), 141 (14), 123 (72), 105 (6), 83 (5), 75 (76), 73 (65); anal. calcd for $C_{10}H_{16}O_3Si$ (212.32): C, 56.57; H, 7.60; Si, 13.23; found: C, 56.60; H, 7.59; Si, 13.20.

6,6,6*a*-Trimethyl-3-(trimethylsilyl)-6,6*a*-dihydrofuro[3,2-*b*]furan-2(5*H*)-one (2f). Yield: 149.8 mg, starting from 150.1 mg of 2,2,3-trimethyl-5-(trimethylsilyl)pent-4-yne-1,3-diol **1f** (89%) (Figure 1). White solid, mp = 70-71 °C. IR (KBr): *ν* = 2980 (m), 1745 (s), 1638 (s), 1471 (w), 1377 (m), 1303 (m), 1241 (s), 1215 (m), 1167 (w), 1124 (m), 1091 (m), 970 (w), 898 (w), 841 (s), 779 (w) cm^{-1}; ^1H NMR (300 MHz, $CDCl_3$): δ = 4.43 (dist d, *J* = 8.9, 1 H, C*H*H), 4.29 (dist d, *J* = 8.9, CH*H*), 1.45 (s, 3 H, Me), 1.17 (s, 3 H, Me), 1.02 (s, 3 H, Me), 0.23 (s, 9 H, $SiMe_3$); ^{13}C NMR (75 MHz, $CDCl_3$): δ = 197.7, 177.3, 94.2, 89.0, 86.9, 42.3, 20.7, 20.6, 18.1, –1.64; GC-MS: *m/z* = 242 (3) [$(M+2)^+$] 240 (18) [M^+], 225 (100), 207 (7), 185 (7), 163 (4), 151 (24), 141 (97), 139 (11), 123 (4), 99 (8), 75 (54), 73 (98); anal. calcd for $C_{12}H_{20}O_3Si$ (240.37): C, 59.96; H, 8.39; Si, 11.68; found: C, 59.87; H, 8.42; Si, 11.64.

5,5,6*a*-Trimethyl-3-(trimethylsilyl)-6,6*a*-dihydrofuro[3,2-*b*]furan-2(5*H*)-one (2g). Yield: 154.8 mg, starting from 150.1 mg of 2,4-dimethyl-6-(trimethylsilyl)hex-5-yne-2,4-diol **1g** (92%) (Figure 1). White solid, mp = 45-46 °C. IR (KBr): *ν* = 2959 (w), 1736 (s), 1638 (s), 1456 (w), 1381 (m), 1342 (m), 1268 (m), 1232 (s), 1200 (m), 1123 (m), 1085 (m), 1006 (w), 961 (m), 917 (m), 848 (s), 778 (m), 731 (m); cm^{-1}; ^1H NMR (300 MHz, $CDCl_3$): δ = 2.156 (dist d, *J* = 12.5, 1 H, C*H*H), 2.00 (dist d, *J* = 12.5, 1 H, CH*H*), 1.63 (s, 3 H, Me), 1.62 (s, 3 H, Me), 1.47 (s, 3 H, Me), 0.23 (s, 9 H, $SiMe_3$); ^{13}C NMR (75 MHz, $CDCl_3$): δ = 195.4, 176.7, 97.4, 95.3, 85.1, 45.1, 31.4, 27.9, 27.4, –1.51; GC-MS: *m/z* = 240 (12) [M^+], 225 (15), 207 (20), 197 (3), 185 (14), 179 (4), 172 (4), 169 (6), 163 (7), 157 (10), 141 (42), 135 (4), 123 (3), 105 (4), 99 (29), 75 (23), 73 (100); anal. calcd for $C_{12}H_{20}O_3Si$ (240.37): C, 59.96; H, 8.39; Si, 11.68; found: C, 59.99; H, 8.37; Si, 11.71.

6a-Isopropyl-5,5-dimethyl-3-(trimethylsilyl)-6,6*a*-dihydrofuro[3,2-*b*]furan-2(5*H*)-one (2h). Yield: 176.6 mg, starting from 169.7 mg of 4-isopropyl-2-methyl-6-(trimethylsilyl)hex-5-yne-2,4-diol **1h** (94%) (Figure 1). White solid, mp = 78-79 °C. IR (KBr): *ν* = 2973 (m), 1735 (s), 1626 (s), 1458 (w), 1391 (w), 1374 (w), 1333 (m), 1270 (m), 1244 (m), 1214 (m), 1144 (m), 1112 (m), 1020 (w), 919 (w), 846 (s), 774 (w), 709 (m) cm^{-1}; ^1H NMR (300 MHz, $CDCl_3$): δ = 2.26 (dist d, *J* = 12.8, 1 H, C*H*H), 1.95 (heptuplet, *J* = 6.7, 1 H, C*H*Me_2), 1.88 (dist d, *J* = 12.8, 1 H, CH*H*), 1.60 (s, 3 H, Me), 1.46 (s, 3 H, Me), 1.14 (d, *J* = 6.7, 3 H, CH_3CHCH_3), 0.84 (d, *J* = 6.7, 3 H, CH_3CHCH_3), 0.23 (s, 9 H, $SiMe_3$); ^{13}C NMR (75 MHz, $CDCl_3$): δ = 194.0, 178.2, 99.4, 97.7, 91.2, 43.7, 35.8, 32.5, 29.4, 18.1, 16.8, –0.4; GC-MS: *m/z* = 268 (2) [M^+], 253 (7), 235 (4), 225 (38), 213 (4), 197 (1), 181 (1), 167 (1), 141 (39), 135 (14), 127 (22), 99 (4), 83 (10), 75 (28), 73 (100), 71 (31); anal. calcd for $C_{14}H_{24}O_3Si$ (268.42): C, 62.64; H, 9.01; Si, 10.46; found: C, 62.77; H, 9.04; Si, 10.51.

5-Methyl-6*a*-phenyl-3-(trimethylsilyl)-6,6*a*-dihydrofuro[3,2-*b*]furan-2(5*H*)-one (2i). Mixture of diastereomers, (5*RS*,6*aSR*)/(5*RS*,6*aRS*) DR ca. 1.9, determined by ^1H NMR. Yield: 125.2 mg, starting from 183.7 mg of 4-phenyl-6-(trimethylsilyl)hex-5-yne-2,4-diol **1i** (62%) (Figure 1). Single diastereomers were formed starting from the corresponding substrate diastereomers, as reported in Table 1, entries 1 and 2.

(5RS,6aSR) Diastereomer. Yield: 37.2 mg, starting from 1.8 mg of PdI_2 (5.0×10^{-3} mmol), 4.1 mg of KI (2.5×10^{-2} mmol), 5.0 mL of MeOH, and 65.2 mg (0.25 mmol) of (2*RS*,4*SR*)-**1i** (52%) (Table 1, entry 1). Colorless oil. IR (film): ν = 2957 (m), 1748 (s), 1637 (s), 1449 (w), 1385 (w), 1359 (m), 1237 (s), 1193 (w), 1019 (m), 924 (m), 845 (s), 770 (m), 701 (m), 626 (w) cm^{-1}; ^{1}H NMR (300 MHz, $CDCl_3$): δ = 7.36 (s, 5 H, aromatic), 4.89-4.74 (m, 1 H, C*H*CH_3), 2.73 (ddd, *J* = 11.8, 4.0, 0.8, 1 H, C*H*H), 2.10 (td, *J* = 11.8, 0.8, 1 H, CH*H*), 1.51 (dd, *J* = 6.2, 0.8, 3 H, CHCH_3), 0.28 (s, 9 H, $SiMe_3$); ^{13}C NMR (75 MHz, $CDCl_3$): δ = 193.0, 176.0, 138.7, 129.0, 125.9, 96.4, 88.1, 87.2, 44.0, 20.7, –1.5 ; GC-MS: *m/z* = 290 (2) [$(M+2)^+$], 288 (26) [M^+], 273 (1), 229 (18), 220 (13), 219 (11), 201 (5), 185 (5), 178 (9), 155 (21), 141 (47), 129 (5), 115 (5), 105 (17), 77 (23), 75 (24), 73 (100); anal. calcd for $C_{16}H_{20}O_3Si$ (288.41): C, 66.63; H, 6.99; Si, 9.74; found: C, 66.66; H, 7.01; Si, 9.77.

(5RS,6aRS) Diastereomer. Yield: 86.9 mg, starting from 3.5 mg of PdI_2 (9.7×10^{-3} mmol), 8.1 mg of KI (4.9×10^{-2} mmol), 9.8 mL of MeOH, and 129.4 mg (0.49 mmol) of (2*RS*,4*RS*)-**1i** (61%) Table 1, entry 2). White solid, mp = 87-88°C. IR (KBr): ν = 2957 (m), 1747 (s), 1637 (s), 1450 (w), 1366 (m), 1275 (m), 1247 (m), 1184 (m), 1090 (w), 1017 (w), 922 (m), 845 (s), 713 (m) cm^{-1}; ^{1}H NMR (300 MHz, $CDCl_3$): δ = 7.44-7.30 (m, 5 H, Ph), 5.31-5.15 (m, 1 H, C*H*CH_3), 2.74-2.61 (m, 1 H, C*H*H), 2.49-2.59 (m, 1 H, CH*H*), 1.06 (d, *J* = 6.9, 3 H, Me), 0.30 (s, 9 H, $SiMe_3$); ^{13}C NMR (75 MHz, $CDCl_3$): δ = 194.5, 177.5, 142.5, 130.4, 127.9, 99.4, 90.0, 88.5, 40.7, 22.1, 0.0; GC-MS: *m/z* = 290 (1) [$(M+2)^+$], 288 (20) [M^+], 273 (1), 229 (9), 220 (27), 219 (20), 214 (7), 201 (4), 185 (5), 178 (6), 155 (17), 141 (54), 129 (5), 115 (5), 105 (15), 77 (19), 75 (19) 73 (100); anal. calcd for $C_{16}H_{20}O_3Si$ (288.42): C, 66.63; H, 6.99; Si, 9.74; found: C, 66.70; H, 6.95; Si, 9.77.

6*a*-(4-Chlorophenyl)-5-methyl-3-(trimethylsilyl)-6,6*a*-dihydrofuro[3,2-*b*]furan-2(5*H*)-one (2j). Mixture of diastereomers, (5*RS*,6*aSR*)/(5*RS*,6*aRS*) DR ca. 1.8, determined by ^{1}H NMR. Yield: 131.1 mg, starting from 207.8 mg of 4-(4-chlorophenyl)-6-(trimethylsilyl)hex-5-yne-2,4-diol **1j** (58%) (Figure 1). Single diastereomers were formed starting from the corresponding substrate diastereomers, as reported in Table 1, entries 3 and 4.

(5RS,6aSR) Diastereomer. Yield: 82.1 mg, starting from 2.7 mg of PdI_2 (7.5×10^{-3} mmol), 6.2 mg of KI (3.7×10^{-2} mmol), 7.6 mL of MeOH, and 110.4 mg (0.38 mmol) of (2*RS*,4*SR*)-**1j** (68%) (Table 1, entry 3). White solid, mp = 84-85 °C; IR (KBr): ν = 2957 (m), 1748 (s), 1638 (s), 1493 (w), 1357 (w), 1237

(m), 1190 (w), 1098 (w), 1014 (w), 922 (w), 845 (s), 771 (w) cm^{-1}; ^{1}H NMR (300 MHz, $CDCl_3$): δ = 7.39-7.25 (m, 4 H, aromatic), 4.87-4.74 (m, 1 H, C*H*CH_3), 2.69 (dd, *J* = 11.8, 4.0, 1 H, C*H*H), 2.16 (dist dd, *J* = 11.8, 10.7, 1 H, CH*H*), 1.52 (d, *J* = 6.2, 3 H, Me), 0.28 (s, 9 H, $SiMe_3$); ^{13}C NMR (75 MHz, $CDCl_3$): δ = 192.6, 176.2, 136.8, 134.9, 129.1, 127.3, 95.9, 87.4, 87.3, 43.6, 20.7, –1.6; GC-MS: *m/z* = 322 (26) [M^+], 263 (14), 253 (5), 228 (19), 219 (11),189 (6), 177 (2), 169 (2), 154 (4), 141 (73), 111 (11), 93 (5), 75 (23), 73 (100); anal. calcd for $C_{16}H_{19}ClO_3Si$ (322.86): C, 59.52; H, 5.93; Cl, 10.98; Si, 8.70; found: C, 59.66; H, 5.95; Cl, 11.05; Si, 8.63.

(5RS,6aRS) Diastereomer. Yield: 58.4 mg, starting from 2.5 mg of PdI_2 (6.9×10^{-3} mmol), 5.7 mg of KI (3.4×10^{-2} mmol), 7.0 mL of MeOH, and 102.5 mg (0.35 mmol) of (2*RS*,4*RS*)-**1j** (52%), (Table 1, entry 4). White solid, mp = 84-85 °C. IR (KBr): *v* = 2957 (m), 1747 (s), 1638 (s), 1493 (w), 1243 (m), 1180 (w), 1097 (w), 1015 (w), 920 (w), 844 (s), 772 (w) cm^{-1}; ^{1}H NMR (300 MHz, $CDCl_3$): δ = 7.41-7.22 (m, 4 H, aromatic), 5.31-5.14 (m, 1 H, C*H*CH_3), 2.74-2.60 (m, 1 H, C*H*H), 2.51-2.41 (m, 1 H, CH*H*), 1.11 (dist d, *J* = 6.9, 3 H, Me), 0.29 (s, 9 H, $SiMe_3$); ^{13}C NMR (75 MHz, $CDCl_3$): δ = 192.6, 176.2, 139.2, 134.9, 129.1, 127.8, 97.7, 88.6, 86.4, 38.9, 20.7, –1.52; GC-MS: *m/z* = 324 (5) [$(M+2)^+$], 322 (12) [M^+], 263 (4), 253 (5), 228 (9), 219 (11), 189 (3), 154 (2), 141 (69), 128 (2), 111 (8), 75 (17), 73 (100); anal. calcd for $C_{16}H_{19}ClO_3Si$ (322.86): C, 59.52; H, 5.93; Cl, 10.98; Si, 8.70; found: C, 59.66; H, 5.96; Cl, 11.03; Si, 8.76.

5-Methyl-6*a*-(*p*-tolyl)-3-(trimethylsilyl)-6,6*a*-dihydrofuro[3,2-*b*]furan-2(5*H*)-one (2k). Mixture of diastereomers, (5*RS*,6*aSR*)/(5*RS*,6*aRS*) DR ca. 1.8, determined by ^{1}H NMR. Yield: 150.3 mg, starting from 193.5 mg of 4-(*p*-tolyl)-6-(trimethylsilyl)hex-5-yne-2,4-diol **1k** (71%) (Figure 1). Single diastereomers were formed starting from the corresponding substrate diastereomers, as reported in Table 1, entries 5 and 6.

(5RS,6aSR) Diastereomer. Yield: 43.6 mg, starting from 2.6 mg of PdI_2 (7.2×10^{-3} mmol), 6.0 mg of KI (3.6×10^{-2} mmol), 7.2 mL of MeOH, and 99.0 mg (0.36 mmol) of (2*RS*,4*SR*)-**1k** (40%) (Table 1, entry 5). Colorless oil. IR (film): *v* = 2958 (m), 1747 (s), 1638 (s), 1513 (w), 1446 (w), 1358 (w), 1237 (m), 1193 (w), 1173 (w), 1068 (w), 1017 (m), 925 (m), 846 (s), 768 (m) cm^{-1}; ^{1}H NMR (300 MHz, $CDCl_3$): δ = 7.26-7.14 (m, 4 H, aromatic), 4.88-4.74 (m, 1 H, C*H*CH_3), 2.73 (dd, *J* = 11.8, 4.0, 1 H, C*H*H), 2.34 (s, 3 H, $CH_3C_6H_4$), 2.09 (dist dd, *J* = 11.8, 10.6, 1 H, CH*H*), 1.51 (d, *J* = 6.3, 3 H, $CHCH_3$), 0.28 (s, 9 H, $SiMe_3$); ^{13}C NMR (75 MHz, $CDCl_3$): δ = 193.3, 176.5, 138.8, 135.2, 129.5, 125.7, 95.5, 87.9, 87.3, 43.6, 21.1, 20.6, –1.5; GC-MS: *m/z* = 304 (7), [$(M+2)^+$], 303 (26) [$(M+1)^+$], 302 (100) [M^+], 243 (29), 228 (22), 219 (48), 201 (12), 192 (20), 177 (10), 169 (18), 141 (44), 119 (38), 91 (22), 75 (13), 73 (68); anal. calcd

for $C_{17}H_{22}O_3Si$ (302.45): C, 67.51; H, 7.33; Si, 9.29; found: C, 67.54; H, 7.34; Si, 9.31.

(5RS,6aRS) Diastereomer. Yield: 91.1 mg, starting from 2.7 mg of PdI_2 (7.5×10^{-3} mmol), 6.2 mg of KI (3.7×10^{-2} mmol), 7.6 mL of MeOH, and 103.8 mg (0.38 mmol) of (2*RS*,4*RS*)-**1k** (80%) (Table 1, entry 6). White solid, mp = 76-77 °C. IR (KBr): *ν* = 2957 (m), 1744 (s), 1637 (s), 1513 (w), 1453 (w), 1365 (m), 1270 (m), 1248 (m), 1183 (m), 1089 (w), 1058 (w), 1017 (m), 920 (w), 845 (s), 698 (w), 637 (w) cm^{-1}; ^1H NMR (300 MHz, $CDCl_3$): δ = 7.30-7.10 (m, 4 H, aromatic), 5.28-5.14 (m, 1 H, C*H*CH_3), 2.65 (dist dd, *J* = 12.1, 9.1, 1 H, C*H*H), 2.53 (dist d, *J* = 12.1, 1 H, CH*H*), 2.34 (s, 3 H, $CH_3C_6H_4$), 1.09 (d, *J* = 6.9, 3 H, $CHCH_3$), 0.29 (s, 9 H, $SiMe_3$); ^{13}C NMR (75 MHz, $CDCl_3$): δ = 194.4, 177.6, 139.9, 138.8, 130.6, 127.3, 98.4, 89.7, 88.1, 40.0, 22.2, 21.7, –0.4; GC-MS: *m/z* = 304 (5), [$(M+2)^+$], 303 (66) [$(M+1)^+$], 302 (69) [M^+], 287 (2), 243 (21), 234 (19), 233 (14), 228 (21), 219 (32), 211 (8), 192 (9), 169 (15), 141 (51), 119 (27), 91 (23), 75 (16), 73 (100); anal. calcd for $C_{17}H_{22}O_3Si$ (302.45): C, 67.51; H, 7.33; Si, 9.29; found: C, 67.68; H, 7.36; Si, 9.33.

5,5-Dimethyl-6*a*-phenyl-3-(trimethylsilyl)-6,6*a*-dihydrofuro[3,2-*b*]furan-2(5*H*)-one (2l). Yield: 190.5 mg, starting from 193.5 mg of 2-methyl-4-phenyl-6-(trimethylsilyl)hex-5-yne-2,4-diol **1l** (90%) (Figure 1). White solid, mp = 77-78 °C. IR (KBr): *ν* = 2956 (m), 1741 (s), 1697 (s), 1495 (w), 1452 (m), 1390 (m), 1377 (w), 1350 (m), 1268 (m), 1250 (m), 1196 (m), 1146 (w), 1028 (m), 1077 (w), 1055 (m), 937 (w), 847 (s), 778 (w), 705 (s), 629 (w) cm^{-1}; ^1H NMR (300 MHz, $CDCl_3$): δ = 7.36 (s, 5 H, aromatic ring), 2.73 (dist d, *J* = 12.4, 1 H, C*H*H), 2.30 (dist d, *J* = 12.4, 1 H, CH*H*), 1.52 (s, 3 H, Me), 1.11 (s, 3 H, Me), 0.30 (s, 9 H, $SiMe_3$); ^{13}C NMR (75 MHz, $CDCl_3$): δ = 192.0, 176.0, 140.5, 128.9, 126.5, 98.2, 97.7, 88.5, 46.2, 31.1, 26.7, –1.4; GC-MS: *m/z* = 302 (18) [M^+], 269 (1), 247 (7), 234 (9), 219 (5), 201 (9), 185 (3), 178 (16), 169 (5), 161 (20), 141 (67), 129 (5), 115 (4), 105 (45), 77 (21), 75 (16), 73 (100); anal. calcd for $C_{17}H_{22}O_3Si$ (302.44): C, 67.51; H, 7.33; Si, 9.29; found: C, 67.54; H, 7.34; Si, 9.31.

3*a'*-Phenyl-6'-(trimethylsilyl)-3'*H*-spiro[cyclohexane-1,2'-furo[3,2-*b*]furan]-5'(3*a'H*)one (2m). Yield: 167.8 mg, starting from 221.6 mg of 1-(2-hydroxy-2-phenyl-4-(trimethylsilyl)but-3-yn-1-yl)cyclohexan-1-ol **1m** (70%) (Figure 1). White solid, mp = 102-103 °C. IR (KBr): *ν* = 2940 (m), 2861 (w), 1740 (s), 1635 (s), 1449 (w), 1372 (w), 1284 (w), 1249 (m), 1193 (w), 1057 (w), 929 (w), 840 (s), 776 (w), 702 (s), cm^{-1}; ^1H NMR (300 MHz, $CDCl_3$): δ = 7.35 (s, br, 5 H, aromatic), 2.78 (d, *J* = 12.4, 1 H, C*H*H), 2.16 (d, *J* = 12.4, 1 H, CH*H*), 1.88-1.13 (m, 10 H, cyclohexane ring), 0.31 (s, 9 H, $SiMe_3$); ^{13}C NMR (75 MHz, $CDCl_3$): δ = 192.1, 176.4, 140.4, 128.85, 129.8, 126.3, 100.1, 97.9, 87.8, 44.5, 39.9, 35.2, 24.7, 28.8, –1.4; GC-MS: *m/z* = 344 (1) [$(M+2)^+$], 342 (17) [M^+], 309 (1), 283 (6), 249 (21), 248

(100), 247 (81), 232 (10), 219 (10), 201 (47), 178 (6), 141 (31), 105 (72), 77 (23), 73 (89); anal. calcd for $C_{20}H_{26}O_3Si$ (342.5): C, 70.13; H, 7.65; Si, 8.20; found: C, 70.25; H, 7.68; Si, 8.17.

General procedure for the desilylation of crude 3-(trimethylsilyl)-6,6*a*-dihydrofuro[3,2-*b*]furan-2(5*H*)-ones 2h, 2l, and 2m leading to 6,6*a*-dihydrofuro[3,2-*b*]furan-2(5*H*)-ones 3

Substrates **1h**, **1l**, and **1m** (0.7 mmol) were allowed to react under oxidative carbonylation conditions according to the procedure described above. To the crude reaction mixture, dried under vacuum and then diluted again with THF (7 mL), was added TBAF nH_2O (201.3 mg, 0.77 mmol). The resulting mixture was allowed to stir at room temperature for 2 h. The solvent was evaporated, and the residue taken up with Et_2O (40 mL) and washed with water (40 mL). The aqueous layer was extracted with Et_2O (3 × 40 mL), and the collected organic phases were dried over $NaSO_4$. After filtration, the solvent was evaporated and the products were purified by column chromatography on neutral alumina to give pure 6,6*a*-dihydrofuro[3,2-*b*]furan-2(5*H*)-one derivatives **3h**, **3l**, and **3m** (eluent: from hexane to hexane/EtOAc 9:1).

6*a*-Isopropyl-5,5-dimethyl-6,6*a*-dihydrofuro[3,2-*b*]furan-2(5*H*)-one (3h). Yield: 116.8 mg, starting from 169.7 mg of 4-isopropyl-2-methyl-6-(trimethylsilyl)hex-5-yne-2,4-diol **1h** (85%) (Scheme 3). White solid, mp= 65-66 °C. IR (KBr): *v* = 2974 (m), 1759 (s), 1653 (s), 1455 (w), 1350 (w), 1287 (w), 1214 (m), 1138 (w), 1009 (w), 887 (m), 808 (m), 782 (w), 742 (m) cm^{-1}; ^1H NMR (300 MHz, $CDCl_3$): δ = 5.05 (s, 1H, =CH), 2.37 (dist d, *J* = 12.8, 1 H, C*H*H), 2.02 (heptuplet, *J* = 6.8, 1 H, C*H*Me_2), 1.96 (distorted d, J = 12.8, 1 H, CH*H*), 1.62 (s, 3 H, Me), 1.51 (s, 3 H, Me), 1.16 (d, *J* = 6.8, 3 H, CH_3CHCH_3), 0.89 (d, *J* = 6.7, 3 H, CH_3CHCH_3); ^{13}C NMR (75 MHz, $CDCl_3$): δ = 185.8, 174.5, 98.1, 90.7, 89.6, 42.8, 34.7, 31.6, 28.3, 17.0, 15.7; GC-MS: *m/z* = 196 (5) [M^+], 168 (6), 153 (100), 141 (10), 111 (3), 83 (60), 71 (40), 69 (53); anal. calcd for $C_{11}H_{16}O_3$: C, 67.32; H, 8.22; found: C, 67.53; H, 8.20.

5,5-Dimethyl-6*a*-phenyl-6,6*a*-dihydrofuro[3,2-*b*]furan-2(5*H*)-one (3l). Yield: 127.3 mg, starting from 193.5 mg of 2-methyl-4-phenyl-6-(trimethylsilyl)hex-5-yne-2,4-diol **1l** (79%) (Scheme 3). White solid, mp= 129-130 °C. IR (KBr): *v* = 2980 (w), 1766 (s), 1651 (s), 1451 (w), 1352 (m), 1267 (m), 1193 (w), 1128 (m), 1055 (m), 937 (m), 806 (m), 703 (s) cm^{-1};^1H NMR (300 MHz, $CDCl_3$): δ = 7.46-7.31 (m, 5 H, aromatic), 5.20 (s, 1 H, =CH), 2.79 (dist d, *J* = 12.4, 1 H, CH*H*), 2.39 (dist d, *J* = 12.4, 1 H, CH*H*), 1.57 (s, 3 H, Me), 1.11 (s, 3 H, Me); ^{13}C NMR (75 MHz, $CDCl_3$): δ = 184.9, 173.6, 139.6, 129.2, 129.0, 126.4, 99.3, 89.0, 46.0, 31.1, 26.5; GC-MS: *m/z* = 230 (5) [M^+], 215 (30), 202 (7), 175 (13), 161 (2), 147 (6), 128 (2), 105 (100), 77 (27); anal. calcd for $C_{14}H_{14}O_3$: C, 73.03; H, 6.13; found: C, 73.27; H, 6.11.

3*a'*-Phenyl-3'*H*-spiro[cyclohexane-1,2'-furo[3,2-*b*]furan]-5'(3*a'*H)-one (3m). Yield: 115.4 mg, starting from 221.6 mg of 1-(2-hydroxy-2-phenyl-4-(trimethylsilyl)but-3-yn-1-yl)cyclohexan-1-ol **1m** (61%) (Scheme 3). White solid, m.p.= 126-127 °C. IR (KBr): ν = 2937 (m), 2862 (w), 1771 (s), 1655 (s), 1498 (w), 1449 (m), 1284 (w), 1249 (m), 1214 (m), 1128 (w), 1012 (m), 881 (m), 805 (m), 767 (w), 707 (m) cm^{-1}; ^{1}H NMR (300 MHz, $CDCl_3$): δ = 7.44-7.30 (m, 5 H, Ph), 5.21 (s, 1 H, =CH), 2.85 (dist d, *J* = 12.4, 1 H, C*H*H), 2.24 (d, *J* = 12.4, 1 H, CH*H*), 1.92-1.62 (m, 3 H, cyclohexane ring), 1.62-1.10 (m, 7 H, cyclohexane ring); ^{13}C NMR (75 MHz, $CDCl_3$): δ = 185.0, 173.7, 140.0, 129.1, 128.9, 126.3, 101.8, 89.1, 88.4, 44.5, 39.9, 35.2, 24.6, 22.88, 22.82; GC-MS: *m/z* = 270 (3) [M^+], 201 (15), 176 (100), 141 (2), 120 (7), 105 (84), 95 (23), 81 (11), 77 (30); anal. calcd for $C_{17}H_{18}O_3$: C, 75.53; H, 6.71; found: C, 75.50; H, 6.72.

X-Ray crystallographic data collection and structure refinement for compounds 2g and (5*RS*,6*aRS*)-2j

Single-crystal X-ray diffraction data for compounds **2g** and (5*RS*,6*aRS*)-**2j** were collected at room temperature on a Bruker-Nonius X8APEXII CCD area detector diffractometer using graphite-monochromated Mo-K_α radiation (λ = 0.71073 Å). Suitable, irregular colorless (**2g**) and pale yellow [(5*RS*,6*aRS*)-**2j**] crystals of approximate dimensions 0.20 × 0. 14 × 0.06 and 0.23 × 0.17 × 0.10 mm^3, respectively, were selected for data collection. The data were processed through the SAINT reduction (SAINT, 2003) and SADABS multi-scan absorption (Sheldrick, 2003) software. The structures were solved with the ShelXS structure solution program. In both cases, the model was refined by using version 2013/4 of ShelXL against F^2 on all data by full-matrix least squares (Sheldrick, 2008; SHELXTL, 2013). The final geometrical calculations and the graphical manipulations were performed using the XP utility within the SHELXTL software. ORTEP drawings of **2g** and (5*RS*,6*aRS*)-**2j** are given in Figures S1 and S2 while details of the crystal data/data collection/structure refinement are listed in Tables S1 and S2. Crystallographic data (excluding structure factors) for the structures reported in this paper have been deposited within the

Cambridge Crystallographic Data Centre as supplementary publication CCDC numbers 1566032 (**2g**) and 1566033 [(5*RS*,6*aRS*)-**2j**]. Copies of the data can be obtained free of charge on application to CCDC, 12 Union Road, Cambridge CB21EZ, UK; e-mail: deposit@ccdc.cam.ac.uk.

Cell cultures, assessment of cell viability, Western blot analysis, cytochrome c detection, TUNEL assay, and statistical analyses

Cell cultures. All different cell lines were obtained from American Type Culture Collection (ATCC), Manassas, VA, USA). Human adenocarcinoma breast cells MCF-7 were maintained in DMEM-F12 (Dulbecco's Modified Eagle's Medium (DME) and Ham's F-12 Nutrient Mixture) containing 5% newborn calf serum (NCS), 1% glutamine, 1% penicillin/streptomycin, all from Sigma-Aldrich). MDA-MB-231 and MDA-MB-468 TNBC cells were cultured in DMEM-F12 (Dulbecco's Modified Eagle's Medium (DME) and Ham's F-12 Nutrient Mixture) containing 10% heat inactivated fetal bovine serum (FBS), 1% glutamine, 1% penicillin/streptomycin, all from Sigma-Aldrich (Sigma–Aldrich). Murine immortalized fibroblast 3T3L-1 cells were cultured in DMEM (Dulbecco's Modified Eagle's medium) containing 10% heat inactivated fetal bovine serum (FBS) and 1% penicillin/streptomycin, all from Sigma-Aldrich. Human mammary epithelial cells MCF-10A, were maintained in DMEM-F12 supplemented with 5% horse serum (HS), 1% glutamine, 1% penicillin/streptomycin, 5 µg/mL insulin, 0.25 mg/mL hydrocortisone, 20 ng/ml hEGF (human epidermal growth factor) and 0.05 mg/mL cholera enterotoxin (Sigma–Aldrich). All cell cultures were maintained at 37 °C in a humidified 5% CO_2 atmosphere and were screened periodically for mycoplasma contamination.

Assessment of cell viability. Cells were seeded on 48 well plates (0.25 10^5 cells/well) and grown for 72 h in complete medium before being treated for 72 h with different doses (1, 5, 10, 20, 40 µM) of dihydrofurofuranones **2d**, **2e**, **2g**, **2l**, and **3l**. The effect of the different concentrations of all different compounds was measured using 3-(4,5-dimethylthiazol-2-yl)-2,5-diphenyl tetrazolium bromide (MTT) assay as previously described (Caruso et al., 2012; Chimento et al., 2013; Chimento et al., 2014; Chimento et al., 2015a; Chimento et al., 2015b; Sala et al., 2013). Seventy two hours after treatments, fresh MTT, resuspended in phosphate-buffered saline (PBS), was added to each well (final concentration 0.33 mg/mL). After 3 h incubation, cells were lysed with 200µL of DMSO. Each experiment was performed in triplicate and the optical density was measured at 570 nm in a spectrophotometer.

Western blot analysis. Cells were cultured in complete medium for 48 h in 60 mm dishes (1×10^6 cells) before being treated for 48 h with **2l** (20 µM). Methods for protein extraction and blots preparation have been previously published (Casaburi et al., 2015). Briefly, blots were incubated over night at 4°C with (a) anti-bcl-2 (1:500), (c) anti-cytochrome c (cyt c) (1:1000), (d) anti-parp-1 (1:1000) antibodies. Membranes were incubated with horseradish peroxidase (HRP)-conjugated secondary antibodies, and immunoreactive bands were visualized with the ECL Western blotting detection system (Amersham Bioscience). To assure equal loading of proteins, membranes were stripped and incubated overnight with an anti-glyceraldehyde 3-phosphate dehydrogenase (GAPDH) antibody (1:1000).

Cytochrome c detection. Cells were treated for 48 h with **2l** (20 µM), fractioned and processed for cytochrome c detection as previously reported (Chimento et al., 2012). Briefly, cells were harvested by centrifugation at 2500 rpm for 10 min at 4°C. Pellets were resuspended in 50 µL of sucrose buffer (250 mM sucrose; 10 mM Hepes; 10 mM KCl; 1.5 mM $MgCl_2$; 1 mM EDTA; 1 mM EGTA) (all from Sigma-Aldrich, Milano, Italy) containing 20 µg/mL aprotinin, 20 µg/mL leupeptin, 1 mM PMSF and 0.05% digitonine (Sigma-Aldrich). Cells were incubated for 20 min at 4°C and then centrifuged at 13,000 rpm for 15 min at 4°C. Supernatants containing cytosolic protein fraction were transferred to new tubes. Equal amounts of proteins were resolved by 15 % SDS/polyacrylamide gel and subjected to western blot analysis.

Statistical analyses. All experiments were performed at least three times and the results were from representative experiments. Data were expressed as mean values ± standard deviation (SD), statistical significance between control (basal) and treated samples were analyzed using GraphPad Prism 5.0 (GraphPad Software, Inc.; La Jolla, CA) software. Control and treated groups were compared using the analysis of variance (ANOVA) with Bonferroni or Dunn's post hoc testing. A comparison of individual treatments was also performed, using Student's t test. Significance was defined as $p < 0.05$.

Data and software availability

The crystallography data have been deposited at the Cambridge Crystallographic Data Center (CCDC) under accession numbers CCDC: 1566032 (**2g**) and 1566033 [(5*RS*,6*aRS*)-**2j**], and can be obtained free of charge from www.ccdc.cam.ac.uk/getstructures.

SUPPLEMENTAL REFERENCES

Caruso, A., Chimento, A., El-Kashef, H., Lancelot, J.-C., Panno, A., Pezzi, V., Saturnino, C., Sinicropi, M. S., Sirianni, R., and Rault, S. (2012). Antiproliferative activity of some 1,4-dimethylcarbazoles on cells that express estrogen receptors: part I. J. Enzyme Inhib. Med. Chem. *27*, 609-613.

Casaburi, I., Avena, P., De Luca, A., Chimento, A., Sirianni, R., Malivindi, R., Rago, V., Fiorillo, M., Domanico, F., Campana, C., Cappello, A. R., Sotgia, F., Lisanti, M. P., and Pezzi, V. (2015). Estrogen related receptor α (ERRα) a promising target for the therapy of adrenocortical carcinoma (ACC). Oncotarget *6*, 25135-25148.

Chimento, A., Sirianni, R., Casaburi, I., Ruggiero, C., Maggiolini, M., Andò, S., and Pezzi, V. (2012). 17β-Estradiol activates GPER- and ESR1-dependent pathways inducing apoptosis in GC-2 cells, a mouse spermatocyte-derived cell line. Mol. Cell Endocrinol. *355*, 49-59.

Chimento, A., Sala, M., Gomez-Monterrey, I. M., Musella, S., Bertamino, A., Caruso, A., Sinicropi, M. S., Sirianni, R., Puoci, F., Parisi, O. I., Campana, C., Martire, E., Novellino, E., Saturnino, C., Campiglia, P., and Pezzi, V. (2013). Biological activity of 3-chloro-azetidin-2-one derivatives having interesting antiproliferative activity on human breast cancer cell lines. Bioorg. Med. Chem. Lett. *23*, 6401-6405.

Chimento, A., Casaburi, I., Rosano, C., Avena, P., De Luca, A., Campana, C., Martire, E., Santolla, M. F., Maggiolini, M., Pezzi, V., and Sirianni, R. (2014). Oleuropein and hydroxytyrosol activate GPER/ GPR30-dependent pathways leading to apoptosis of ER-negative SKBR3 breast cancer cells. Mol. Nutr. Food Res. *58*, 478-489.

Chimento, A., Saturnino, C., Iacopetta, D., Mazzotta, R., Caruso, A., Plutino, M. R., Mariconda, A., Ramunno, A., Sinicropi, M. S., Pezzi, V., and Longo, P. (2015a). Inhibition of human topoisomerase I and II and anti-proliferative effects on MCF-7 cells by new titanocene complexes. Bioorg. Med. Chem. *23*, 7302-7312.

Chimento, A., Sirianni, R., Casaburi, I., Zolea, F., Rizza, P., Avena, P., Malivindi, R., De Luca, A., Campana, C., Martire, E., Domanico, F., Fallo, F., Carpinelli, G., Cerquetti, L., Amendola, D., Stigliano, A., and Pezzi, V. (2015b). GPER agonist G-1 decreases adrenocortical carcinoma (ACC) cell growth in vitro and in vivo. Oncotarget. *6*, 19190-19203.

Chopade, P. R., Davis, T. A., Prasad E., and Flowers, R. A. (2004). Solvent-dependent diastereoselectivities in reductions of β-hydroxyketones by SmI_2. Org. Lett. *6*, 2685-2688.

Gabriele, B., Mancuso, R., Maltese, V., Veltri, L., and Salerno, G. (2012). Synthesis of furan-3-carboxylic and 4-methylene-4,5-dihydrofuran-3-carboxylic esters by direct palladium iodide catalyzed oxidative carbonylation of 3-yne-1,2-diol derivatives. J. Org. Chem. *77*, 8657-8668.

Ma, X., Li, Z., Liu, F., Cao, S., and Rao, H. (2014). Tetra-*n*-butylammonium bromide: a simple but efficient organocatalyst for alcohol oxidation under mild conditions. Adv. Synth. Catal. *356*, 1741-1746.

Markó, I. M., and Schevenels, F. T. (2013). Anionic cascade reactions. One-pot assembly of (*Z*)-chloro-exo-methylenetetrahydrofurans from β-hydroxyketones. Belstein J. Org. Chem. *9*, 1319-1325.

Martin, V. A., Murray, D. H., Pratt, N. E., Zao, Y. B., and Albizati, K. F. (1990). J. Am. Chem. Soc. *112*, 6965-6878.

SAINT, version 6.45, Bruker Analytical X-ray Systems, Madison, WI, 2003.

Sala, M., Chimento, A., Saturnino, C., Gomez-Monterrey, I. M., Musella, S., Bertamino, A., Milite, C., Sinicropi, M. S., Caruso, A., Sirianni, R., Tortorella, P., Novellino, E., Campiglia, P., and Pezzi, V. Synthesis and cytotoxic activity evaluation of 2,3-thiazolidin-4-one derivatives on human breast cancer cell lines (2013). Bioorg. Med. Chem. Lett. *23*, 4990-4995.

Schneider, C., Hansch M., and Weide, T. (2006). The Zirconium alkoxide-catalyzed aldol-Tishchenko reaction of ketone aldols. Chem. Eur. J. *11*, 3010-3021.

Sheldrick, G.M. (2003). SADABS Program for absorption correction, version 2.10, Analytical X-ray Systems, Madison, WI.

Sheldrick, G. M. (2008). A short history of *SHELX*. Acta Cryst. *A64*, 112-122.

SHELXTL-2013/4 (2013). Bruker Analytical X-ray Instruments, Madison, WI.

Yasuda, M., Hayashi, K., Katoh, Y., Shibata, I., and Baba, A. (1998). Highly controlled chemoselectivity of tin enolate by its hybridization state. Anionic complex of tin enolate coordinated by tetrabutylammonium bromide as halo selective reagent. J. Am. Chem. Soc. *120*, 715-721.